

CIRCULATING COPY
Sea Grant Depository

WOODS HOLE OCEANOGRAPHIC INSTITUTION

REFERENCE NO. 71-5

REPORT OF THE OCEANOGRAPHIC ENGINEERING
SUMMER PROJECT

Scott C. Daubin

A. J. Williams, III

Ronald C. Gularte and Peter F. Poranski
Daniel P. Charnews and Richard J. Jaffee
Carl S. Albro and T. Gray Curtis, Jr.

RECEIVED

APR 19 1971

**SEA GRANT
DEPOSITORY**

WOODS HOLE, MASSACHUSETTS

CIRCULATING COPY
Sea Grant Depository

WOODS HOLE OCEANOGRAPHIC INSTITUTION
Woods Hole, Massachusetts

REFERENCE NO. 71-5

REPORT OF THE OCEANOGRAPHIC ENGINEERING
SUMMER PROJECT

by

Scott C. Daubin

A. J. Williams, III

Ronald C. Gularte and Peter F. Poranski
Daniel P. Charnews and Richard J. Jaffee
Carl S. Albro and T. Gray Curtis, Jr.

January 1971

TECHNICAL REPORT

*Supported by the National Science Foundation Sea
Grant No. GH-104.*

*Reproduction in whole or in part is permitted for
any purpose of the United States Government. In
citing this manuscript in a bibliography, the
reference should be followed by the phrase:
UNPUBLISHED MANUSCRIPT.*

Approved for Distribution



Scott C. Daubin, Chairman
Department of Ocean Engineering

1970

Report of the Oceanographic Engineering
Summer Project

by

Scott C. Daubin

A. J. Williams, III

Ronald C. Gularte and Peter F. Poranski

Daniel P. Charnews and Richard J. Jaffee

Carl S. Albro and T. Gray Curtis, Jr.

Woods Hole Oceanographic Institution
Woods Hole, Massachusetts

November 2, 1970

Table of Contents

Introduction	Page 2
Syllabus of Oceanographic Systems	Page 3
Project Reports:	Page. 13
" <u>In Situ</u> Surface Film Detector"	
Ronald C. Gularte	
Peter F. Poranski	
"Water Transport Off Nobska Point by Dye Tracing"	
Daniel P. Charnews	
Richard J. Jaffee	
"Detection of Salt Fingers by Eclipsed Schlieren Technique"	
Carl S. Albro	
T. Gray Curtis Jr.	

1970

Report of the Oceanographic Engineering
Summer Project

Introduction:

This is the report of a summer program in oceanographic engineering conducted at the Woods Hole Oceanographic Institution under the sponsorship of the Sea Grant Office of the National Science Foundation¹. The activity was part of the joint graduate education program in ocean engineering between the Massachusetts Institute of Technology and the Woods Hole Oceanographic Institution. The objectives of the summer program were to expose the graduate students to the work of the Institution, to provide an insight into the field of oceanographic engineering and to offer experience in conducting such engineering both "at sea" and in the laboratory. The way in which the subject was organized to meet these objectives is described in the syllabus which follows. Two groups of students participated, those entering the joint program and those who had completed a graduate academic year in the program at M.I.T. The program thus served also to guide and orient the incoming students into the nature, purposes and procedures of the joint program in ocean engineering.

The reports of the student projects constitute the bulk of this document. Each team of two students consisted of one second year and one incoming graduate student. The projects were samples of activity from three broad areas in which ocean engineers become involved: field measurement and analysis, development and use of unattended instrumentation and laboratory experimentation and modelling of the real ocean. The reader should remember that the work reported on was accomplished in less than a ten week period.

This report is issued in the hope that it will be useful as a model for the planning and execution of such activities.


Scott C. Daubin


A. J. Williams, III

1. Sea Grant No.GH-104

Syllabus of Oceanographic Systems

W.H.O.I./M.I.T. JOINT PROGRAM IN OCEAN ENGINEERING

1970

Instructors: 13.990 Oceanographic Systems - I
Dr. S. C. Daubin 13.991 Oceanographic Systems - II
Dr. A. J. Williams, III

This subject consists of four parts which in conjunction with the seminars at the Woods Hole Oceanographic Institution and the Marine Biological Laboratory constitute a full summer program in ocean engineering.

The first part is a series of lectures and demonstrations of oceanographic instruments by their designers. These instruments represent solutions of measurement problems in the fields of oceanic dynamics at large and small scales, surface and subsurface navigation and in situ measurement of ocean parameters.

The second part of the subject consists of the creative involvement in an instrumentation project by each student, working individually or in teams. Projects will be assigned at the beginning of the term or preferably in accordance with the student's own choice. Each project will normally require a concise statement of the objective in terms of a "specification", research into the literature, consideration of available options, design, construction, and the design and conduct of a field experiment for test and evaluation.

The third part of the subject is shipboard experience; this will ideally be part of the project work.

The fourth part of this subject will consist of seminars conducted by each student. Seminar topics will be chosen during the initial phases of the subject to permit opportunity for topical research.

There will be no formal examination or quiz during this subject. Students, however, will be required to keep notebooks containing the following:

- Critiques of seminars attended
- Lecture notes
- Seminar background research notes
- Project library and laboratory notes

Students will submit a written project report in addition to their oral presentation. Grades will be based on the quality of the notebooks, the seminars, and the project solutions as communicated in the report and the presentation.

Summer 1970

13.990 Oceanographic Systems - I
13.991 Oceanographic Systems - II

LECTURE SCHEDULE

June 22	<u>Outline & Introduction:</u> Seminar Topics Projects	Williams
June 29	<u>Swallow Floats I:</u> Compressibility Fingers, Power, Turns Counting	Dorson & Williams
July 6	<u>Swallow Floats II:</u> Sofar & Vertical Current Meter Long Range Signaling and Oceanic Circulation	Webb
July 13	<u>Autoprobe:</u> Isotherm Follower Isobaric Platform	Burt
July 20	<u>Alnav:</u> Subsurface Acoustic Beacon Navigation	Marquet
July 27	<u>Surface Navigation:</u> VLF, Omega & Satellite Analog Computation	Williams
August 3	<u>Moored Current Meter:</u> Data Processing & Recording	Koehler
August 10	<u>Surface & Free-Fall Geomagnetic Electrokinetograph</u>	Drever
August 17	<u>Sensor Circuitry:</u> Pressure & Temperature Measurements <u>In Situ</u>	Burt
August 24	<u>Microstructure STD:</u> Small Scale, Ultraprecise Temperature and Conductivity Probe	Brown
August 31	<u>Optical Oceanography:</u> Surface and Subsurface Remote Sensing Salt Finger Detector	Williams

Summer 1970

13.990 Oceanographic Systems - I
13.991 Oceanographic Systems - II

Seminar Topics

Eulerian Current Measurements
Lagrangian Current Measurements
Temperature Measurement in the Ocean
Pollution Monitoring
Acoustical Telemetry
Economics of Unattended Monitoring Platforms
Submersible Research Vehicle Navigation
Surface Research Vessel Navigation
Research Aircraft Navigation
Environmental Acoustical Holography
Handling Heavy and Awkward Weights at Sea

Seminars will be researched and presented individually. Only one student will be assigned to a topic. Other topics of particular interest to the student may be substituted on the approval of the instructor.

STUDENT PROJECTS

Each student will choose projects on which he will work during the entire summer term. In general, two students will work together on a project.

The first stage will entail library research and consultation with local authorities about the measurement or instrumentation problem and previous solutions to the problem. A well-referenced report of this stage of the investigation will be required at the end of the second week of the term.

The second stage of the project will be the planning of experiments or design of instruments, for which a project proposal should be submitted at the end of the third week of the term. The next stage will require detailed planning of experiments and, design and construction of instruments. Some projects will conclude at this point, in which case, a final report will be submitted in the sixth week and a new project initiated. Other projects will require taking of samples or deployment of instruments and analysis of results. Possibly, preliminary results will require modification of initial plans and instruments, followed by further field work.

Final reports are to be submitted at the end of the summer term. Each student will also present a portion of his project as a seminar.

Monitoring of Pollution Related Parameters

	<u>Scientific Contact</u>
<u>In Situ</u> Surface Film Analyzer	Blumer
Specification of Nobska Outfall Monitor	Wright
Salinity Recorder	
Biological Sampling Problem	Sanders
Chemical Sampling In Estuaries	Zafiriou
Benthic Oxygen Demand Monitor	Teal
Deep Benthic Oxygen Demand Monitor	Teal

Instrument Evaluation

Acoustic Releases, Signal Handling <u>In Situ</u>	
Acoustic Releases, Mechanical Linkage	
Thin Film Current Detector	Nowak (NEU)

Research Projects

Salt Fingers, Mechanical and Optical Design, Equipment Testing	Williams
---	----------

Summer 1970

13.990 Oceanographic Systems - I
 13.991 Oceanographic Systems - II

	Mon.	Tues.	Wed.	Thurs.	Fri.
Morning	Lecture 0900-1100 Instr.Lab. Blake 206		Visiting Hours		
12 - 1	Chemistry Lunch	Geology & Geophysics Lunch	Biology Lunch	Peanut Butter Club	
Afternoon		2:30 Physical Oceano- graphy Seminar		1400-1600 Weekly Meeting 201 Blake	
Evening	8:00 Colloquium				

	Mon.	Tues.	Wed.	Thurs.	Fri.
6/22-26	(201 Blake) Introduction Daubin/ Williams			Weekly Meeting	Cruise
6/29-7/3	Swallow Floats I Dorson & Williams			Weekly Meeting	Project Report A
7/6-10	Swallow Floats II Webb			Weekly Meeting	Project Report B
7/13-17	Autoprobe Burt			Weekly Meeting	
7/20-24	Alnav Marquet			Weekly Meeting	Cruise
7/27-31	Surface Navigation Williams			Seminars 1 & 2	Final Report for Short Projects
8/3-7	Moored Current Meter Koehler			Seminars 3 & 4	Cruise
8/10-14	Surfaced Free Fall GEK Drever			Seminars 5 & 6	
8/17-21	Sensor Circuit Burt			Project Reports 1 & 2	Cruise
8/24-28	STD Brown			Project Reports 3 & 4	
8/31-9/3	Optical Oceano- graphy			Project Reports 5 & 6	Critique

SUPPLEMENTARY INFORMATION ABOUT PROJECTS

In Situ Surface Film Analyzer

Widespread interest in oil pollution monitoring has created a demand for an instrument to sample surface films automatically, one which might operate continuously on a Coast Guard vessel or unattended on a moored buoy. Dr. Max Blumer, who is an authority on organic material in the ocean, has suggested two approaches. The first approach is to modify a commercially available analyzer which uses a moving wire or chain to convey a hydrocarbon solution through a cleaning oven and a pyrolyzing oven. The pyrolysis product is burned with hydrogen and the ions remaining in the combustion gases are collected. The ion current is approximately proportional to the number of carbon atoms pyrolyzed in the second oven. To modify this analyzer for in situ measurement, it is necessary not only to get surface film material on the conveyor as by dipping through the surface, but to remove all salt water as salt would swamp the ion current from organic sources. Solvent extraction might bypass this difficulty, the solvent might even be adsorbed on a filament passing through the surface. Silicones adsorbed on glass give a hydrophobic, lipophilic surface which might selectively pick up hydrocarbon films. A screen has been used by Garret to collect surface films and one might convey the film to an extractor on a screen belt and proceed from the extraction to the commercial analyzer.

A second approach to analyzing the surface film for hydrocarbons is to measure ultra-violet absorption through the surface. First, the wavelength or wavelengths giving a critical determination of hydrocarbons should be selected. This work can be done on the Cary 14 Spectrophotometer in the lab. The determination should be sensitive to hydrocarbons indicative of spills but insensitive to unpolluted surface films and to seawater. These investigations can be done with hydrocarbons in solution at concentrations equivalent to the material in a surface film. It should be verified that conclusions drawn from dilute solutions carry over to films. If the approach seems promising, the development of an instrument would require work on a light source, recording or telemetering equipment, a detector, a power source, positioning equipment, and packaging.

There is now neither support for this work nor a proposal for support. However, favorable preliminary results would give impact to a proposal. This project represents a possible long-term commitment with relatively high risk. Without funding, investigation of the first approach would have to be restricted to literature search, hypothesis, and tentative experiments. The student should become acquainted with techniques of chemical analysis which are applicable. Investigation of the second approach would give a better estimate of the success of an instrument. There are fewer imponderables. Optical and spectrophotometric techniques should be mastered.

Benthic Oxygen Demand Monitor

Dr. John Teal has measured the uptake of oxygen from seawater by organisms living in the bottom. He wishes to have an instrument built to take these measurements more routinely. Eventually, he would like to deploy an instrument on the bottom by DSRV and retrieve it after several hours.

The early work will be done in marshes so parts of the instrument can be dry. A bell jar with circulating pump and oxygen sensing electrode will be put on the bottom in shallow water. An amplifier, power supply, and recorder will be on the bank.

All parts of this instrument but the oxygen electrode must be specified or designed. Funds are available to build and buy the equipment. It should be tested in available marshes.

There will be electronic work involved, however, this need not discourage a student unfamiliar with electronics from choosing this project. Operational amplifiers will be used, the principles of which each student should know. Advice will be available for specialized problems.

It is probable that this project will not consume the full term. Design of a submerged instrument for deep studies is a larger project. However, it would be reasonable to attack a portion of it for the remainder of the term.

Bottom Finding, Triggering and Signaling of Sample Bottle Closure

Dr. Werner Deuser requires a water sample to be made as near the bottom as practical without stirring up sediment. A pinger will be available to locate the bottom approximately but it would be difficult to hold the bottom of the cast just above the sediment long enough for the messenger to trigger the bottom bottle. Probably a mechanical trigger which senses the bottom and signals the pinger when the bottle inverts would best meet the demands of this problem. The other bottles on the cast would be triggered by messenger.

The design should be well thought out, allowing for improbable snarling. Funds are available for construction of the device in the instrument shop. The project must include tests off the dock and from a ship to discover shortcomings in the design. A complete, tested unit will be delivered to Deuser at the end of August.

This project will not require much formal research. It depends heavily on ingenious design. If the design proceeds smoothly, the project will only occupy half the term.

Specification of Monitor for Nobska Outfall

A sewer outfall for the town of Falmouth may be installed 3/8 mile off Nobska Point in 90 feet of water in the next few years. This presents a local opportunity to study a problem about which there is insufficient information but much concern. From studies by Dean Bumpus and W. Redwood Wright last summer, it appears that the effluent will be sufficiently diluted to change the character of the Sound water less than occurs naturally. But it is possible that under unusual conditions, either in the sewage treatment plant or in the Sound, changes disruptive to the ecology may occur.

A two-phase program to study this location would be informative. The first phase would detect unusual conditions in the Sound before installation of the outfall. These conditions might be wind induced or of biological origin again possibly weather induced. What parameters should be monitored to detect these conditions? Offhand, one thinks of particle trajectories, turbidity, oxygen, and temperature. The spacing of samples in time and position must be specified too. And it is necessary to consider how the acquired data can be analyzed to disclose the critical conditions sought. This information would aid the town of Falmouth in deciding whether to install the outfall or use some other disposal system. Similar analyses would aid

other towns facing a similar choice.

The second phase of the program would detect changes in the physical properties of the water in the Sound after installation of the outfall. Again, parameters to monitor, frequency of sampling, and a program to acquire and process the data must all be specified. The results obtained would be valuable for a variety of reasons. Ecological changes could be related to physical property changes, before and after outfall information could be made available, and a warning system to detect malfunctions could be established.

There is now neither support nor a proposal for support for this kind of program at the Oceanographic. But several groups are concerned with measuring parameters of interest and might legitimately work in Vineyard Sound. Bumpus and Wright worked in this way. The specification of a monitor may lead to a proposal to build one later, although it would be good to start monitoring as early as possible.

Acoustic Releases

Acoustic releases form a vital component of subsurface moorings and are attractive devices for remote control of many functions on other instruments. Five or more companies manufacture them and three have been used at Woods Hole Oceanographic Institution with poor success in some cases. A.M.F. has proved the most dependable for us with Inter-Oceanic (Remaco) and O.R.E. releases unsatisfactory. At other facilities, other releases have been used successfully.

It is worth investigating causes of failure with different releases. Two areas should be investigated, acoustic signal processing and mechanical details of the release hook. To investigate the former, a release should be wired to monitor each stage of processing from the deck with the release submerged. False triggering might be investigated near the canal where ship traffic is heavy.

A report of detailed behavior of several acoustic releases would be a valuable contribution to several projects here. These projects might bear the cost of minor equipment.

Salt Fingers

It is assumed by many oceanographers that salt fingers - microstructure convection cells - occur at discontinuities in the thermocline in many areas of the ocean. Yet no one has directly observed salt fingers outside the laboratory. It remains an instrumental challenge to detect them in situ.

The problems of detection are the remoteness of the discontinuity, the smallness of the convecting cells, and the similarity of physical properties of the counter-flowing fluids. Considering the last problem, there are several physical properties which could be used to distinguish the counter-flowing fluids; as the salinity and temperature, speed of sound, and optical index of refraction would all be indicators. And the velocity of the fluid itself is another indicator of salt fingers. The choice of parameters to measure and the technique of measurement is central to the instrumental problem.

I have support to study this problem and field an instrument to try to detect salt fingers optically. A student choosing this project would work with me, first accumulating information about expected parameter fluctuations and measurement limits, then testing optical systems on artificially generated salt fingers, and finally constructing an instrument to detect salt fingers in situ. If the results of this study are promising, I will seek continuing support and the project may be expanded to a thesis.

PROJECT REPORTS

IN SITU SURFACE FILM DETECTOR

By

Ronald C. Gularte

Peter F. Poranski

Ocean Engineering

W.H.O.I./M.I.T. Joint Program

Woods Hole Oceanographic Institution
Woods Hole, Massachusetts
August 20, 1970

Woods Hole,
Massachusetts

August 20, 1970

Dr. Scott C. Daubin
Ocean Engineering Department
Woods Hole Oceanographic Institution
Woods Hole, Massachusetts

Dear Dr. Daubin:

The accompanying report, "In Situ Surface Film Detector", is submitted in compliance with the course outline for Oceanographic Systems I, II that you gave to us at the beginning of the current semester.

This report has given us a much deeper insight into the problems of detecting hydrocarbon films on the water's surface. We thoroughly enjoyed the experience of doing it and we hope that it will meet with your approval.

Yours very truly,

Ronald C. Gúlarde

Ronald C. Gúlarde

Peter F. Poranski

Peter F. Poranski^{com}

ACKNOWLEDGEMENTS

The successful completion of the studies herein reported was made possible by the cooperation of many individuals. To all those who in any manner aided in the work, the authors express their sincere thanks. They are especially grateful to Albert J. Williams, III, Postdoctoral Investigator, Woods Hole Oceanographic Institution, for his time and advice throughout the duration of the project; William S. Shultz, Manager, Woods Hole Ocean Engineering Model Shop, for his knowledge and aid in the fabrication of the instrument; James R. Sullivan for his moral guidance.

TABLE OF CONTENTS

List of Illustrations	18
Abstract	20
Introduction	21
Project Description	21
Detection Element	22
Fabrication	23
Electronics	23
Calibration	24
Analysis of Data	24
Recommendations	25
Selected References	26

LIST OF ILLUSTRATIONS

Illustration	Page
1. Project Schedule	22a
2. Installation Site	22b
3. Schematic of Detection Element	22c
4. System Installation	23a
5. System Installation - Housing Removed	23b
6. Flotation Platform	23c
7. Schematic of Circulation System	23d
8. Rear View of Instrumentation Package	23e
9. Instrumentation Package Console	23f
10. Temperature - Resistance Curve for Sensor	24a
11. Electronic Schematic of the Sensor	24b
12. Gasoline Calibration Data	24c
13. Diesel Calibration Data	24d
14. Diesel Equivalent Calibration Curve	24e
15. Straight Line Background Response	25a
16. Straight Line Background Response - Noise	25b
17. Response - Type 1A	25c
18. Response - Type 1B	25d
19. Response - Type 1C	25e
20. Response - Type 2A	25f
21. Response - Type 2B	25g
22. Response - Type 2C	25h
23. Response - Type 3A	25i

Illustration	Page
24. Response - Type 3B	25j
25. Response - Type 3C	25k
26. Response - Type 4A	25l
27. Response - Type 4B	25m
28. Percent Occurrence - Each Test Day	25n
29. Percent Occurrence - Six Day Total	25o
30. Percent Occurrence - Tide Cycle	25p

ABSTRACT

We are well aware of the deleterious influence that oil pollution has on the ocean. It is interesting to note that the major oil spills get the most publicity such as Union Oil's platform A in Santa Barbara Channel and the Torrey Canyon incident, etc., and that with these major spills a considerable amount of effort is put forth in attempting to correct the situation. It is believed that the lesser more frequent, less dramatic and usually undetected spills in which no correction measures are taken probably do greater harm to the ocean in the long run.

As it is known that oil on the surface of the ocean breaks down with the more volatile hydrocarbons escaping into the atmosphere and the more soluble ones dissolving into the water column it is imperative that the early detection system be devised.

What is contained herein is a description of the design, calibration and testing of an in situ surface film detector for continuously monitoring the surface of the sea for presence of hydrocarbons.

INTRODUCTION

A literature search was performed in which only one instrument was found that continuously monitored oil pollution. This instrument is being developed by I.I.T. Research Institute and is described as an infrared olemeter that continuously monitors and permanently records contamination. Field tests were supposed to have been completed by the end of 1967 but due to difficulties are still in progress at the present time.

There are many "remote" sensor systems, most of them using multispectral methods, that is advantage is taken of the changes in emissivity, reflectivity, etc., with wave-length. The most noteworthy has been developed by the University of Michigan. This optical-mechanical scanner has the ability to record both reflected and emitted radiation, and it allows object comparisons to be made between widely separated portions of the electromagnetic spectrum. This unit can be used at night through the use of thermal infrared detection. Through the use of electronic blocking a greater flexibility in choice of specific bandwidths is obtained. Careful densitometric measurements provide a reflectance spectrum which has the "potential" of being identified as that of oil.

At the present time the methods described above can only detect the presence of oil. Through color enhanced infrared photographs and uncertain assumptions of the thickness of the oil slick, quantitative measurements of the amount of oil can be obtained.

In order to obtain a positive identification of the oil pollution at present, a sample must be returned to the laboratory where gas chromatography and infrared spectroscopy are helpful in identifying the petroleum product. It is interesting to note that the Gulf Research Laboratory, Pittsburg, Pennsylvania, is developing a shipboard system which, using a gas chromatograph, can obtain chromatograms (at five minute intervals) of the lower boiling point hydrocarbons. The instrument was developed primarily for offshore exploration of natural gas.

Gas chromatography is one of the most efficient and widely used methods for separating components of oil pollutant. If the gas chromatogram of an unknown shows a qualitative and quantitative match with the reference sample, except for peaks which represent compounds of high volatility or solubility in water which would be lost from the in situ sample, the two products can be judged as being from the same source.

Thus to summarize, the remote sensing methods available will detect the presence and possibly the amount of oil on the surface. In order to obtain a positive identification, a sample must be returned to the laboratory and a gas chromatogram obtained.

PROJECT DESCRIPTION

The remote sensing and laboratory methods presented in the introduction could most probably be applied to an in situ continuous oil pollution monitoring system, but the time and budgetary constraints placed upon the project would not allow their consideration.

What has been developed and is reported herein is a self contained in situ system for continuously monitoring the ocean surface for the presence of hydrocarbon pollution.

The system collects hydrocarbon vapors just above the sea surface and passes them over a sensor which changes resistance in the presence of hydrocarbons. The change in resistance, and thus the presence or absence of hydrocarbons, is recorded.

The project started on July 13, 1970 with completion scheduled on or about August 27, 1970. The anticipated schedule is shown in Figure 1. The unit was installed next to the draw bridge on Eel Pond (see Figure 2) on August 11, 1970 and continuously monitored the surface until August 18, 1970.

On August 18, 1970 a seminar was given in the Laboratory of Oceanography at Woods Hole Oceanographic Institution in which the system was described and the results of the Eel Pond investigation presented.

DETECTION ELEMENT

A commercially available sensor was used in which, as mentioned above, the electrical resistance changes in the presence of hydrocarbons.

The sensing element was obtained from Danforth, a division of the Eastern Company, who are licenced under patent no. 3,045,198, which is held by James P. Dolan and William M. Jordan of Seattle, Washington.

The element consists of exposed electrically conductive discrete adsorbent particles (such as silver, gold carbon, etc.) anchored in an electrically non-conductive resilient matrix as shown in Figure 3.

The electrical path is formed by contact between the discrete conductive particles. The change in resistance is attributed by the inventors to the adsorption of the hydrocarbon vapors onto the conductive particles as well as the absorption of the vapor within these particles. The adsorption is the adhesion of an extremely thin layer of hydrocarbons to the surface of the conductive particles and absorption the actual penetration of the hydrocarbons into the interstices between the conductive particles.

As mentioned above, the particles are anchored in a resilient material which allows them to move apart when exposed to hydrocarbon vapor and to return to their previous position upon dissipation or departure of the adsorbate.

Thus the particles in the presence of air are closely spaced, as shown at A in Figure 3, and the electrical resistance would be low. Typical values would be around 100 ohms. In the presence of hydrocarbons the vapors would be absorbed between the particles as shown at B in Figure 3. Resistance changes from 100 ohms in air to 5 megohms in carbon tetrachloride have been reported.

It should be noted that the resilient matrix into which the particles are embedded is reportedly fabricated from material such as natural rubber, synthetic rubber or polyethylene. But no mention is made of the fact that some of these materials change dimensionally when exposed to hydrocarbon vapors, and that this in part might be responsible for such large changes in resistance.

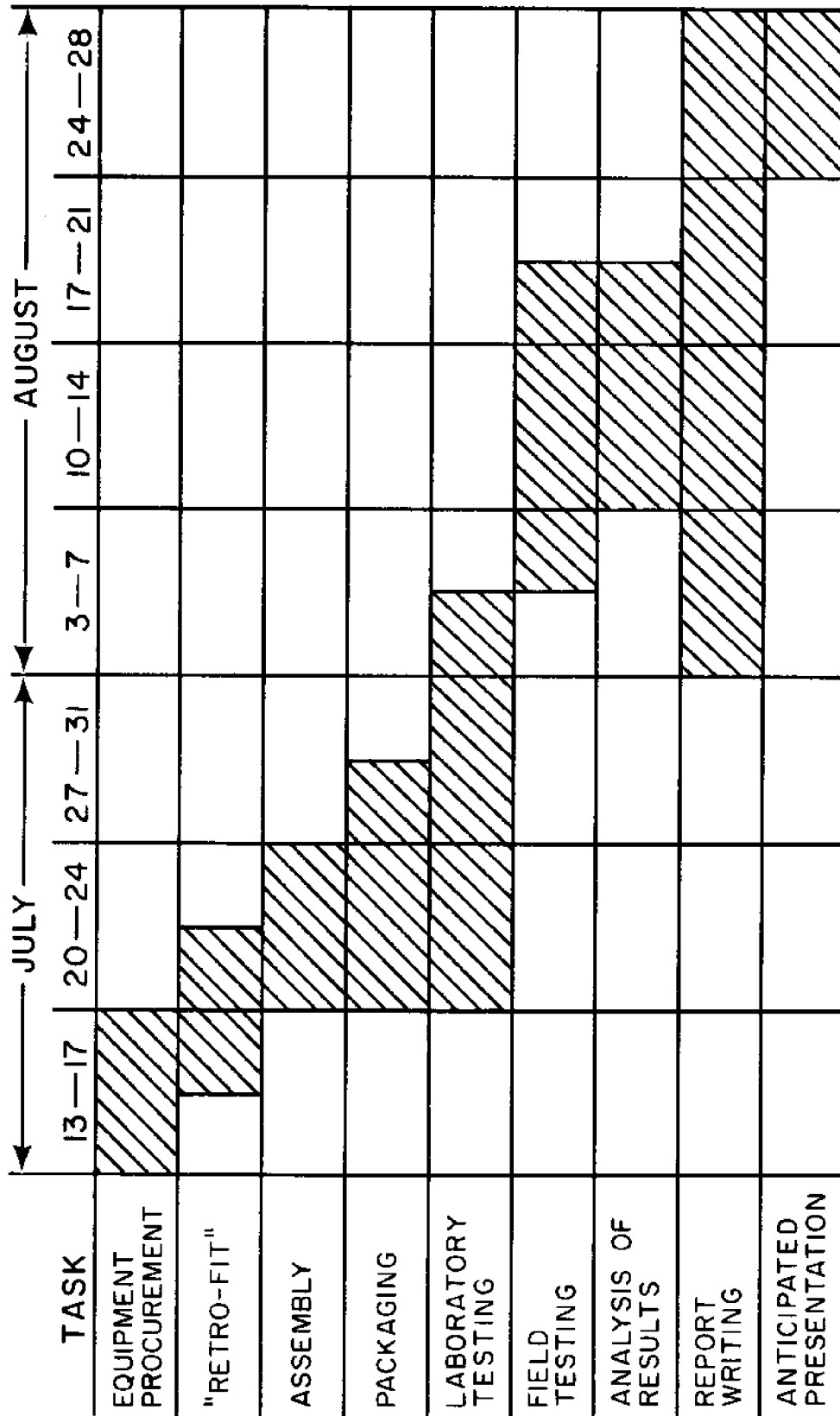


Figure 1. Project Schedule

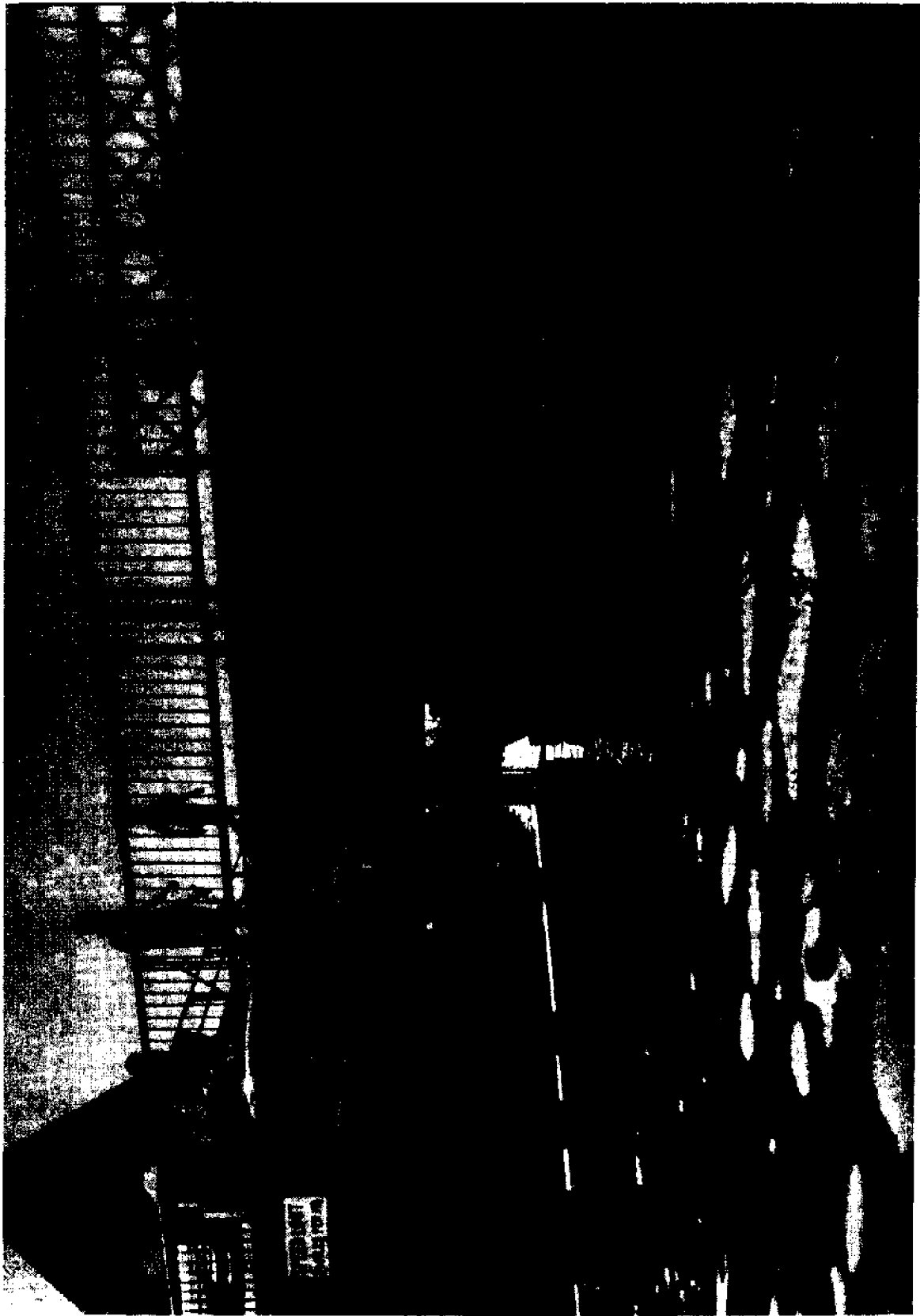


Figure 2. Installation Site

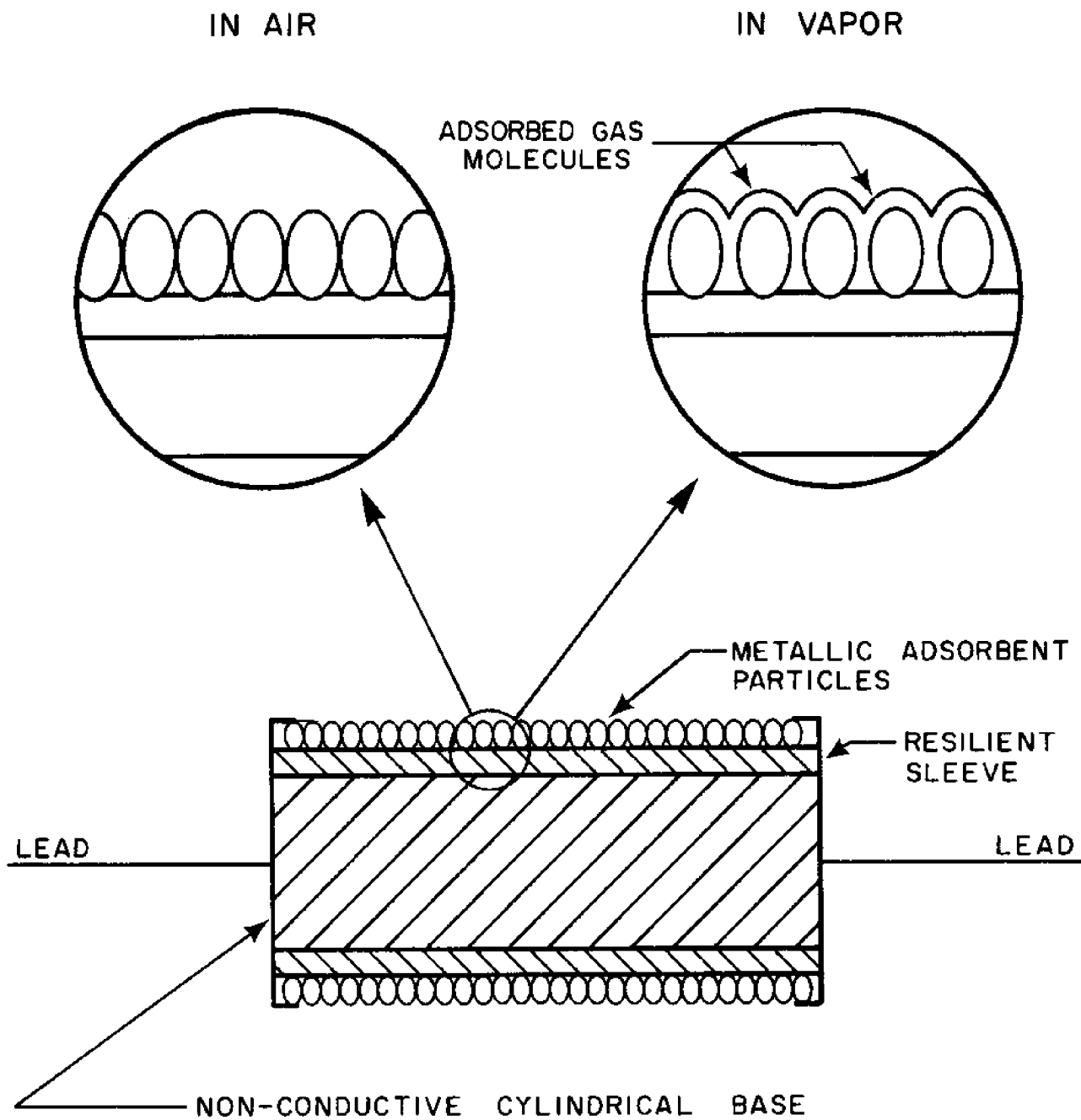


Figure 3. Schematic of Detection Element

FABRICATION

The system was designed with the power supply, electronics and recorder in one unit as shown at A in Figure 4 and the sensors, fan and circulation system mounted on a platform as shown at B in the photograph. This type of construction allowed the instrumentation to be mounted stationary on the dock while the flotation platform maintained the vapor intake (shown at C) just above the water surface with changing tides. That is with tidal variation the flotation platform is free to raise or lower on the guides shown at D in the Figure. Another view of the system with the cover removed from the instrumentation package is shown in Figure 5. Also in this photograph the three five gallon containers which were used for the flotation platform can be seen at A. The automotive type 12 volt battery which was used as a power supply is shown at B.

An enlarged view of the flotation platform is shown in Figure 6. Mounted on this platform is a circulation system. Visible in the photograph is the plumbing necessary to pass vapors past the detecting sensor (shown at A) and fresh air past the compensating sensor (shown at B). Also shown in this photograph is the fan housing (shown at C) and the deflector (shown at D). The deflector is designed with a baffle system to prevent both wind and water from gusting into the vapor system.

The circulation system was incorporated into the design for two reasons: 1) to cool the sensors, 2) to draw the hydrocarbon vapors past the sensors to decrease the response time of the instrument. A schematic of the circulation system is shown in Figure 7. In this figure it can be seen that the fan draws vapor past the detecting sensor as well as fresh air across the compensating sensor. The ducting in this system was designed in an attempt to obtain the same flow resistance in the vapor and fresh air systems. This was done in order to get the same flow across both sensors and thus achieving the same cooling rate on each sensor.

A closeup view of the instrument platform is shown in Figure 8. In this photograph the temperature compensating bridge network is shown at A. This network converts the changes in resistance of the sensors into a 0 to 1 milliamp signal which is recorded on a "Rustrak" recorder, the housing of which is shown at B. A 12 volt d.c. fan is used in the circulation system and the bank of resistors shown at C as well as the rheostat at D are used to control the fan speed.

A view of the console of the instrument package is shown in Figure 9. The "Rustrak" recorder is shown at A. Just below the recorder is a port (shown at B) for adjusting the trim potentiometer in the bridge network. Also shown is a power switch at C and the control for the fan speed rheostat at D.

ELECTRONICS

The Danforth vapor alarm, that was originally used, consisted of a three transistor oscillator network that operated the unit's audible alarm and a bridge network for the sensor. For full scale deflection on the unit's meter, a change in resistance from 800 to 3000 ohms, or 2200 ohms, was needed. This bridge network, after laboratory tests, was found not to be sensitive enough to pick up small scale hydrocarbon changes and, because of this, it was rejected.

The first bridge network that we designed was a single sensor bridge similar to the one incorporated by Danforth, but more sensitive. For a full scale deflection

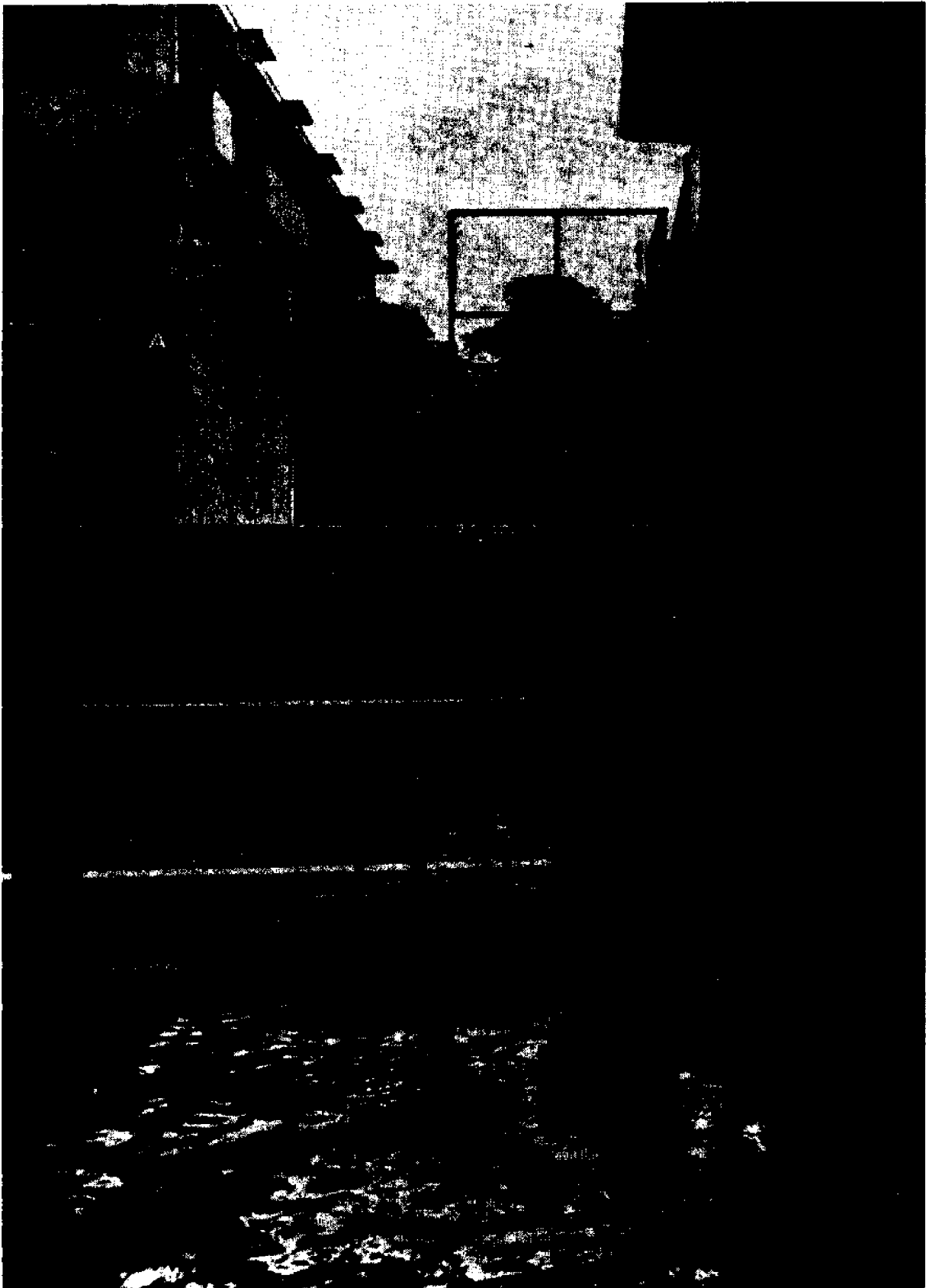


Figure 4. System Installation



Figure 5. System Installation - Housing Removed



Figure 6. Flotation Platform

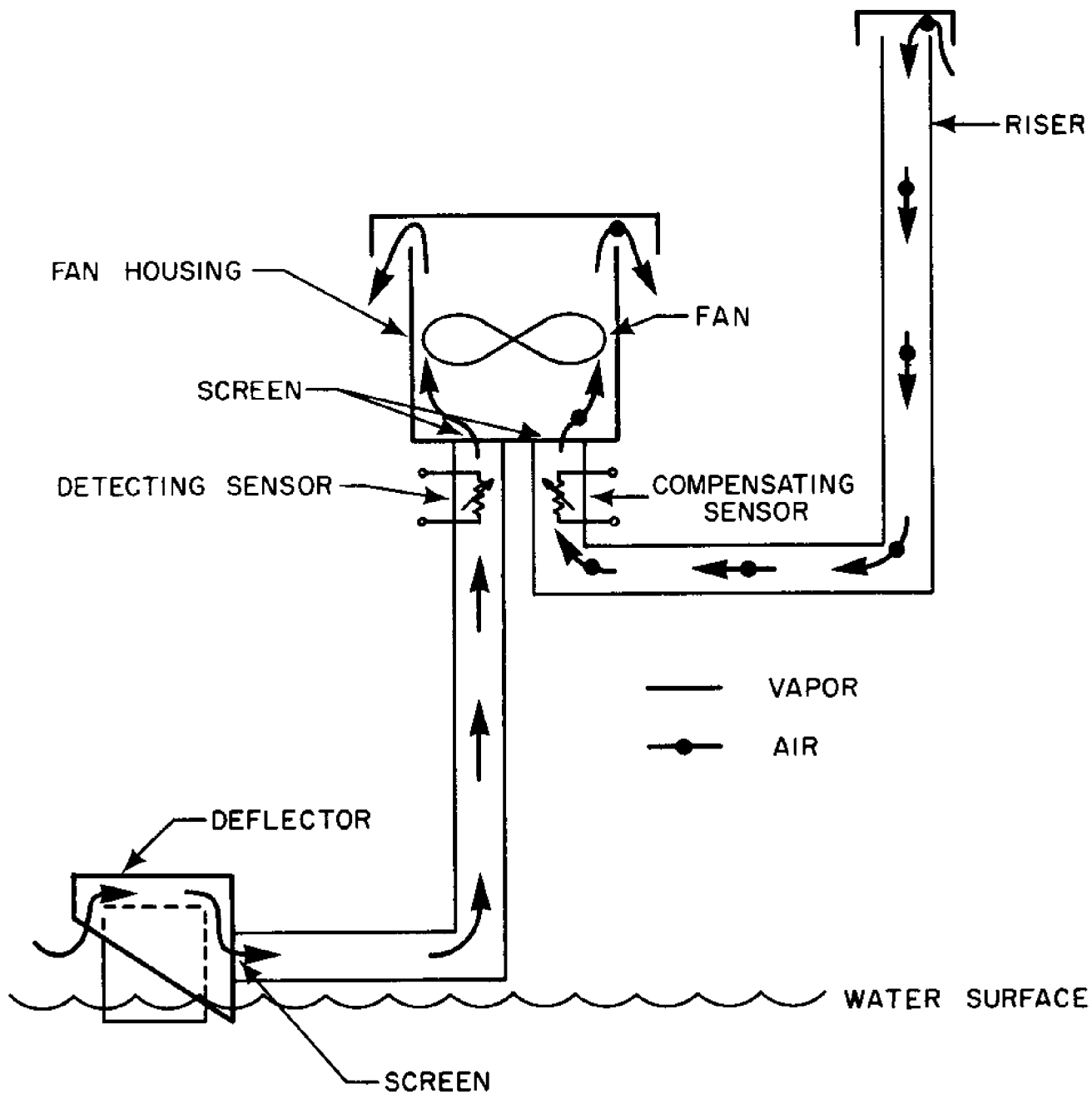


Figure 7. Schematic of Circulation System

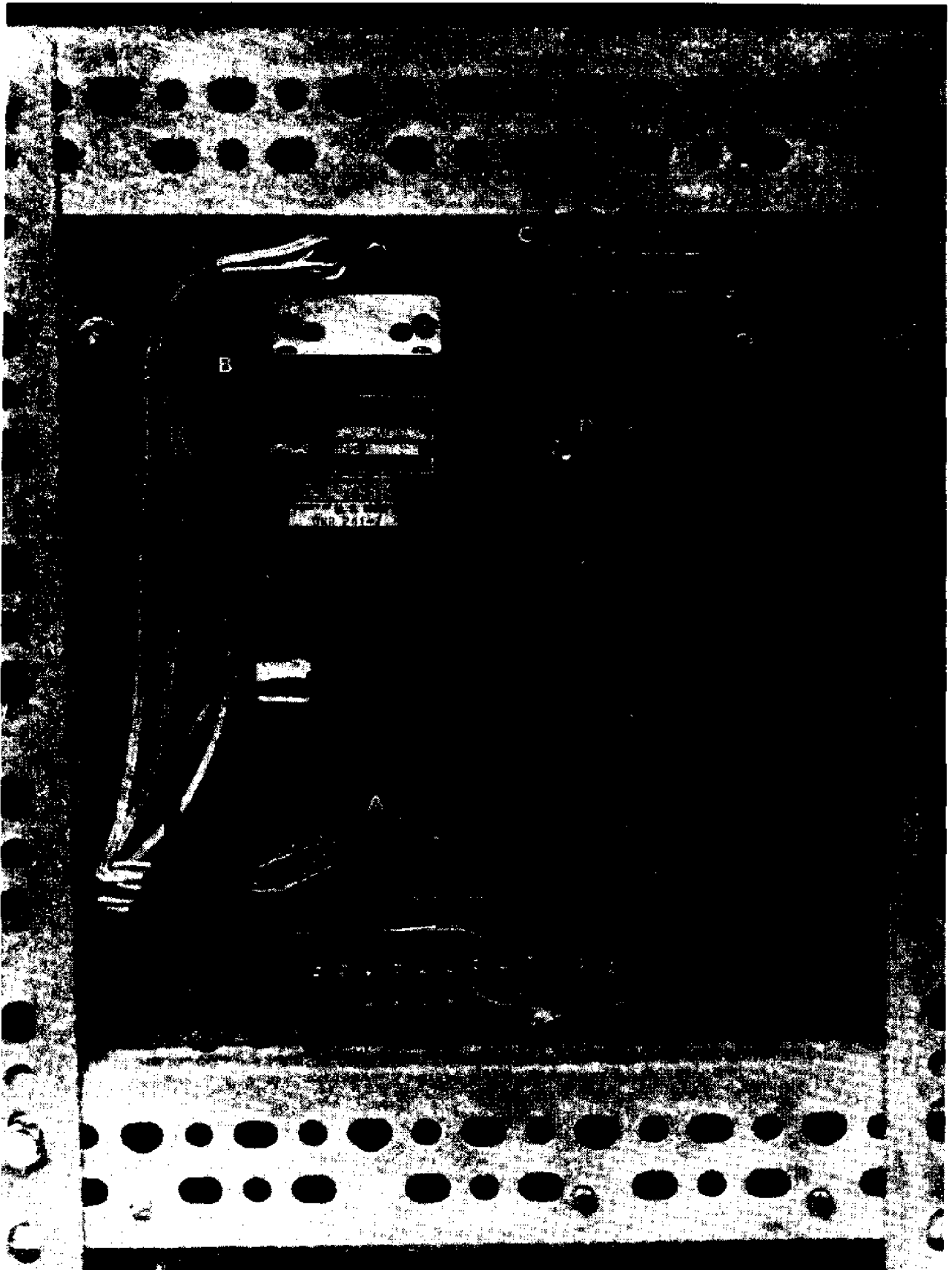


Figure 8. Rear View of Instrumentation Package

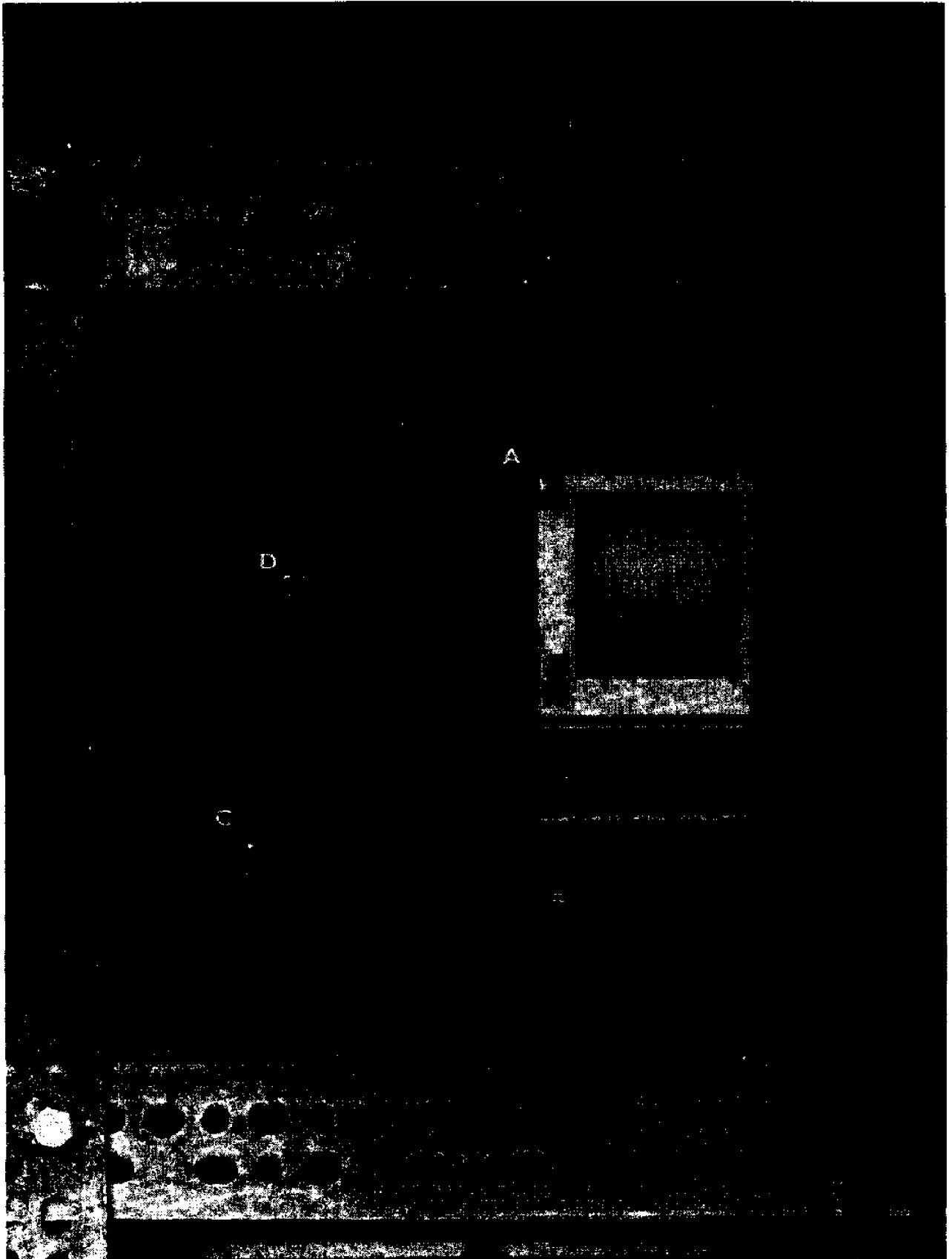


Figure 9. Instrumentation Package Console

on a one millamp meter a change in resistance from 800 to 1200 ohms, or 400 ohms was necessary. Thus, this bridge network was approximately four times as sensitive as the original Danforth unit. The network was tested thoroughly in the lab and was found to be sensitive to a small change in hydrocarbon levels. When the unit was tested out of doors it proved to be unsatisfactory because it was found to be sensitive to temperature as well as hydrocarbons. The sensor was then tested in an environmental chamber to determine its temperature sensitivity. Its temperature sensitivity was found to be excessive (see Figure 10) and because of this the single sensor bridge was also rejected.

In order to overcome the temperature problem a dual sensor bridge was designed and ultimately used (see Figure 11). Both sensors are exposed to the same temperature variations thereby nulling out its effect. Only one of the sensors is exposed to the presence of hydrocarbons.

Besides being temperature compensated, this network is also more sensitive. For a full scale deflection on a one milliamp meter a change in resistance from 825 to 1010 ohms, or 185 ohms is necessary. Thus, this bridge network is approximately twelve times as sensitive as the original Danforth unit.

The output of the bridge network is recorded on a "Rustrak" recorder, and the whole unit is supplied by a twelve volt, standard, car battery. The maximum current drawn by the bridge network is approximately 17 milliamps. The "Rustrak's" current requirement is 20 milliamps, nominal. The fan originally drew 2 amps of current but was modified by series resistance so that it has a current drain of 690 milliamps. Therefore the total current drain of the system is virtually that of the fan. Because of this large current drain the unit is self-sufficient for only seven days and then the battery must be changed. The battery was, in actuality, changed every three days.

CALIBRATION

The system was calibrated "on site" in Eel Pond by placing known quantities of hydrocarbons in a specific area under the sensing element of the unit. A barrier, toroidal in shape with a diameter of $\frac{1}{2}$ meter, was placed around the sensing unit. This barrier, floating at the surface, confined a surface area of approximately .2 square meters. Known quantities of hydrocarbons were introduced into this area with a calibrated syringe.

Gasoline was first used but did not produce repeatable results (see Figure 12). Fresh diesel fuel proved to be much better for the calibration of the unit and satisfactory results were obtained for 1, 3, 5, $7\frac{1}{2}$, and 10 cubic centimeters (see Figure 13). The results obtained from the calibration data were converted into cubic centimeters per square meter and plotted against the total number of units deflected with 5 units equaling .1 milliamp output. For example, the 5 cubic centimeter test caused a 5 unit amplitude rise which is equivalent to .1 milliamp. Therefore, this is equal to 25 cubic centimeters per square meter - $5\text{cc}/0.2\text{m}^2 = 25\text{cc}/\text{m}^2$ (see Figure 14).

The calibration was done in order to give some meaning to the magnitudes of hydrocarbon presence obtained while monitoring Eel Pond; the amplitudes obtained can be equated to an equivalent amount of fresh diesel. Thus, a "diesel equivalent" is defined as the amplitude recorded by the instrument when sensing 1 cubic centimeter of fresh diesel on a surface of 1 square meter.

ANALYSIS OF DATA

The unit was placed in Eel Pond on August 11, 1970, and data was recorded

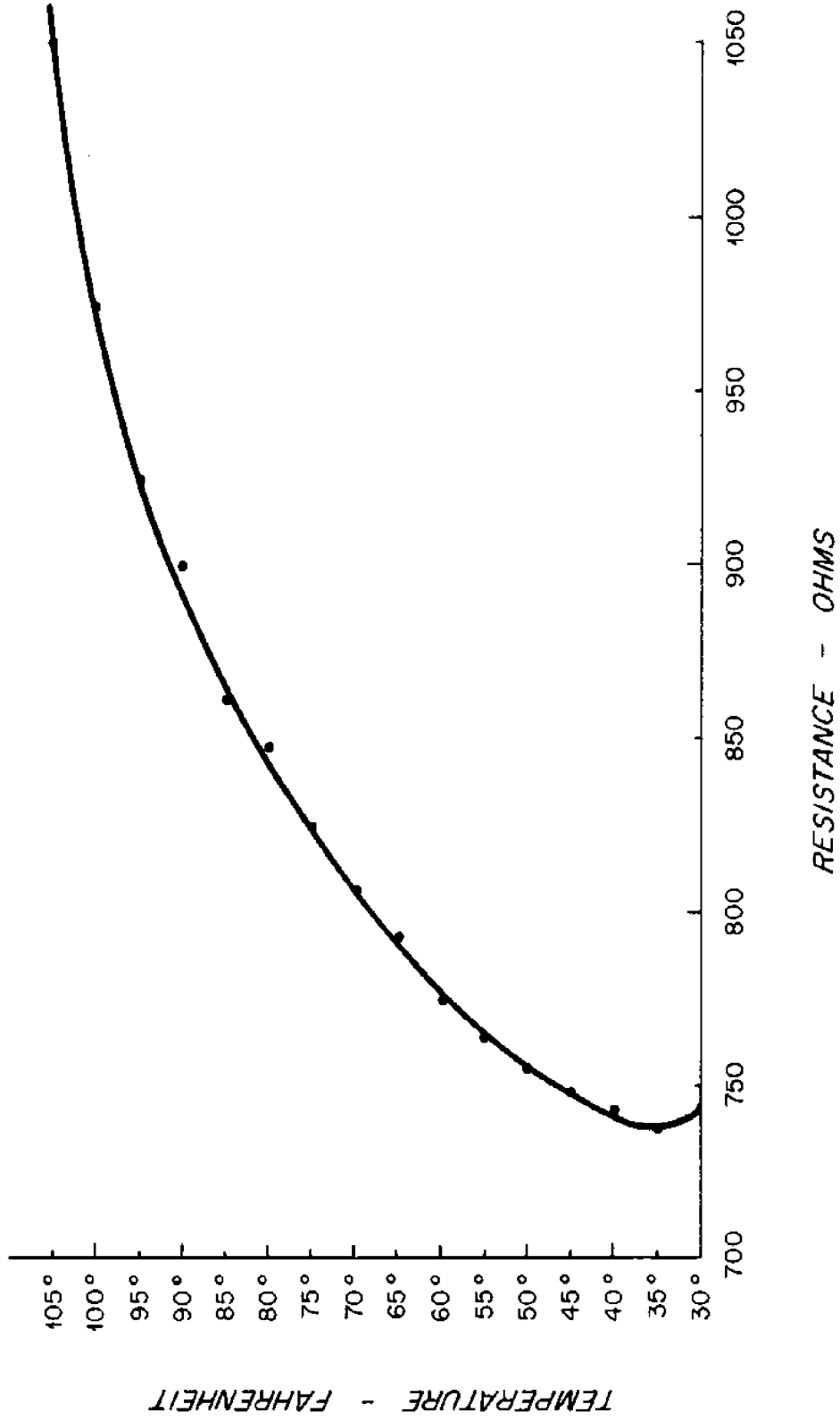


Figure 10. Temperature - Resistance Curve for Sensor

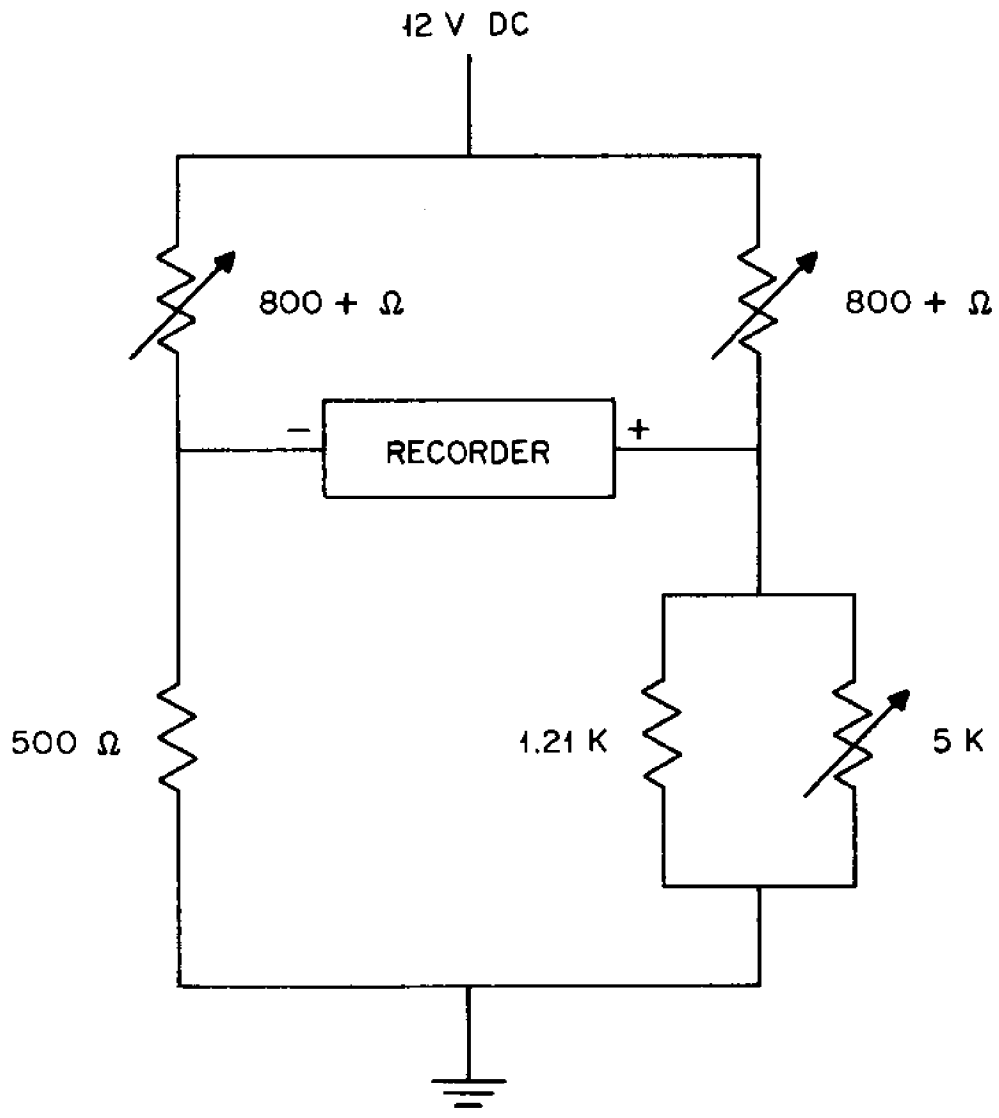


Figure 11. Electronic Schematic of the Sensor

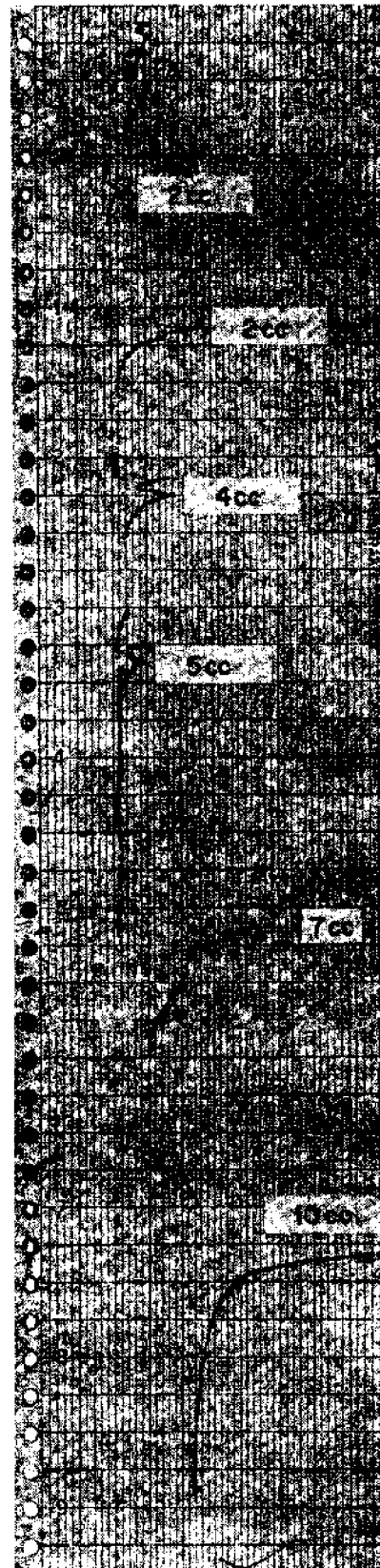
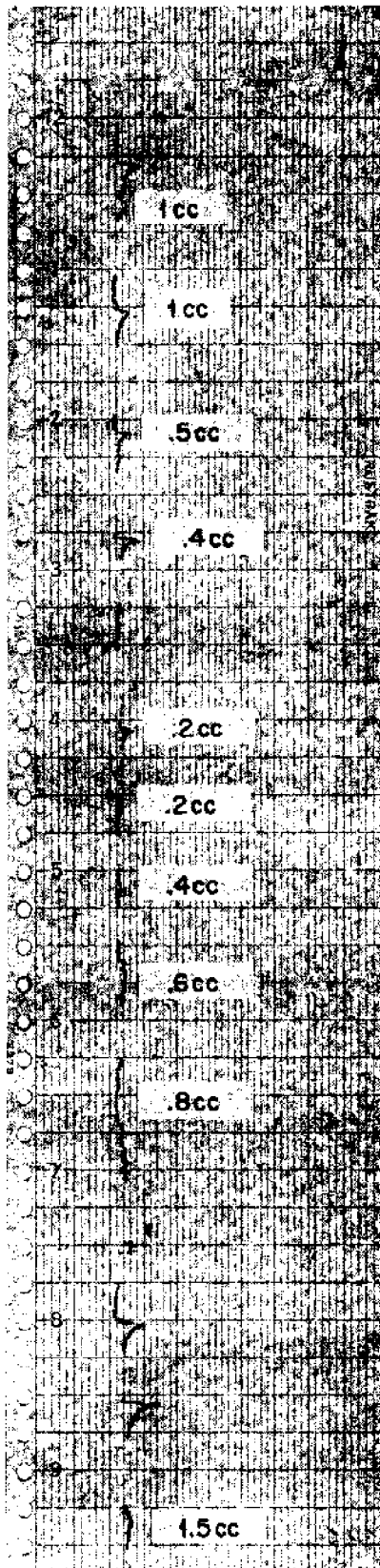


Figure 12. Gasoline Calibration Data

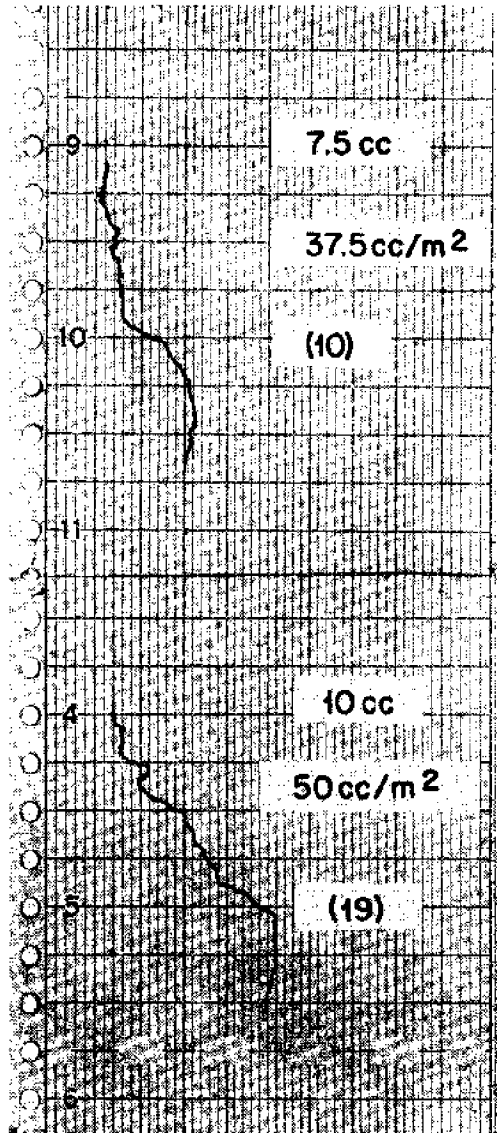
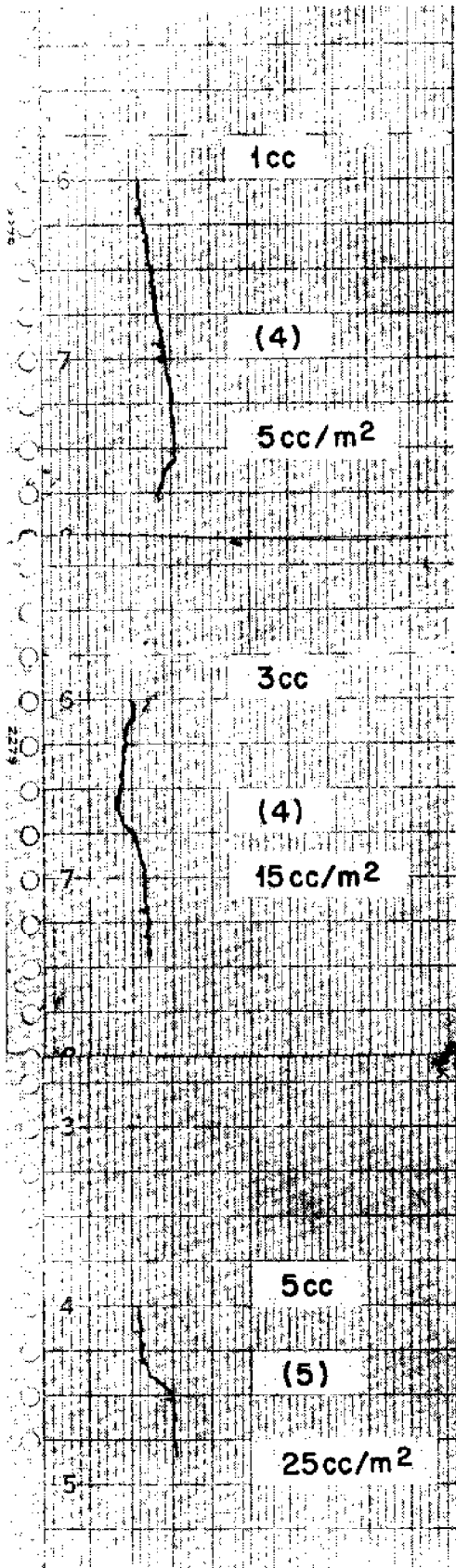


Figure 13. Diesel Calibration Data

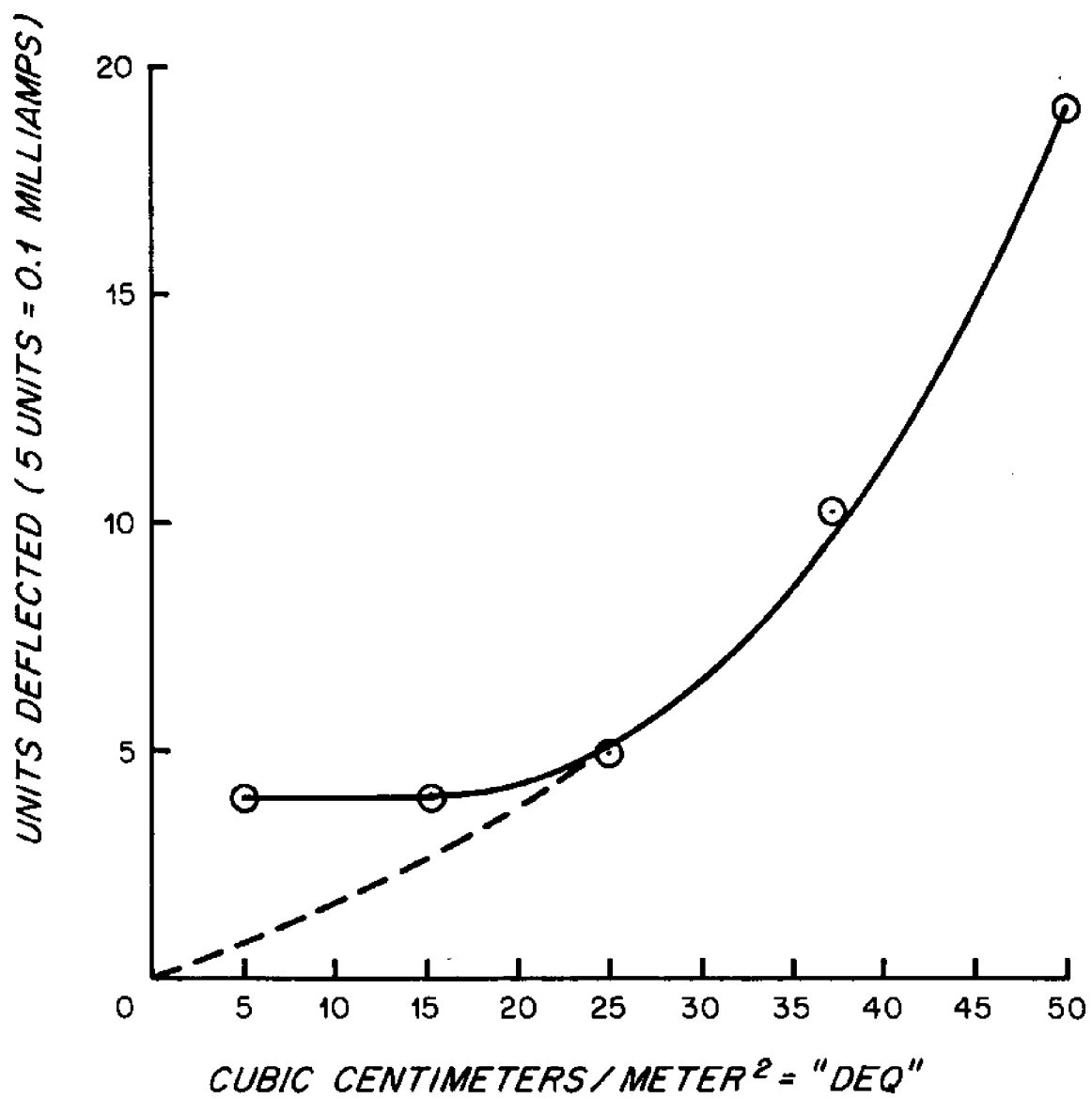


Figure 14. Diesel Equivalent Calibration Curve

essentially over a six day period of time from 1100, August 12 to 1000, August 18. The majority of the trace recorded on the "Rustrak" was a straight line graph (see Figure 15). One variation of this basic straight line was a series that contained small fluctuations (see Figure 16). This does not appear to indicate hydrocarbon presence but rather system noise, possibly arising from small wind currents passing over the sensor.

The signals that were recorded can be grouped into four basic categories. The first group (Type 1) is characterized by a fairly quick rise, then a level period followed by an exponential fall (see Figures 17, 18 and 19). Figure 17 shows a maximum diesel equivalent of 15cc/m^2 and has a time duration of 2.5 minutes. The "Rustrak" records at a rate of 6 inches per hour, $\pm 5\%$. Figure 18 shows two separate indications of hydrocarbons. The first has a maximum diesel equivalent of 17cc/m^2 with a time duration of 6 minutes, and the second, 15cc/m^2 over a 2.5 minute period of time. Figure 19 shows two indications, both with a diesel equivalent of 17cc/m^2 .

The second group (Type 2) is characterized by a slower, more erratic, rise time; and does not necessarily have a level intermediate period, but rather a build up to a peak, and the standard exponential decay (see Figures 20, 21 and 22). Figure 20 shows two traces, both with a diesel equivalent of 12cc/m^2 . The first has an approximate time duration of 10 minutes, the second, 2 minutes. Figure 21 also shows traces. The first is a Type 2 indication that reaches a maximum of 35cc/m^2 for its diesel equivalent and the second is a Type 1 which shows a good comparison between the two types. Figure 22 shows a longer duration trace, approximately 25 minutes.

The third group (Type 3) is characterized by a linear rise with an extremely rapid fall off (see Figures 23, 24, and 25). This type is also characterized by a longer time duration and also reaches higher diesel equivalents. For example, Figure 25 reaches a maximum of 41cc/m^2 and has a time duration in excess of one hour. The fourth group (Type 4) shows characteristics of all of the preceding groups combined into one trace (see Figures 26 and 27).

All of the signal recorded during the six day test period was plotted and analyzed in the following manner. The percent occurrence of hydrocarbon presence during each half hour time period was computed and plotted against time. This does not give the amount of hydrocarbons present but rather the amount of time that hydrocarbons were present during any one half hour period of time (see Figure 28). The tidal cycle is also plotted on this graph. This graph shows us that the presence of hydrocarbon appears to be correlated to some extent with high tide. This appears to be true with the exception of August 15, which showed no hydrocarbon presence, and August 16, which showed an overabundance of hydrocarbons.

The data were then analyzed by computing the percent occurrence of hydrocarbon presence during each half hour time period over the whole six day test period. This is just a summing up of the occurrences appearing in Figure 28 (see Figure 29).

The data were also plotted using the tidal cycle as a reference (see Figure 30). This graph shows the percent occurrence of hydrocarbon presence during the time periods before and after high tide.

RECOMMENDATIONS

The sensitivity of the system could be improved in at least two ways. The first would be to incorporate an active circuit, using operational amplifiers, etc., in the temperature compensating bridge network. A second consideration would be the

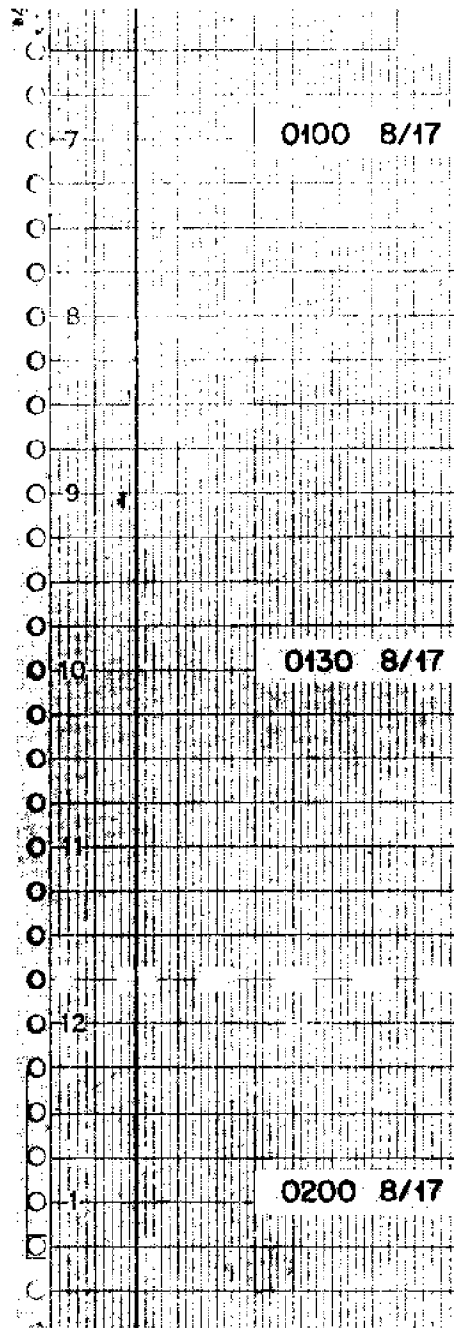


Figure 15. Straight Line Background Response

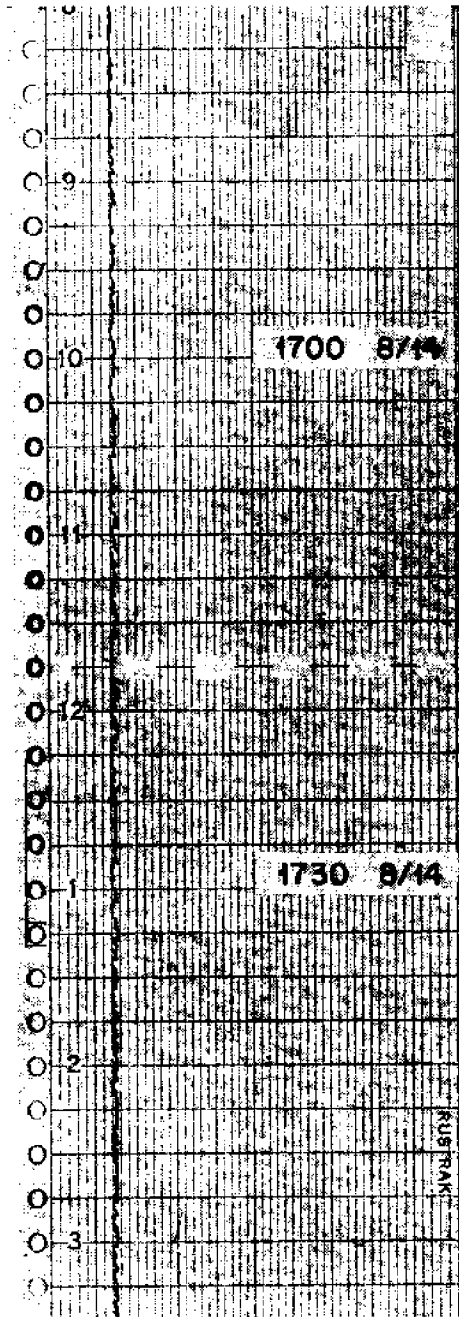


Figure 16. Straight line Background Response - Noise

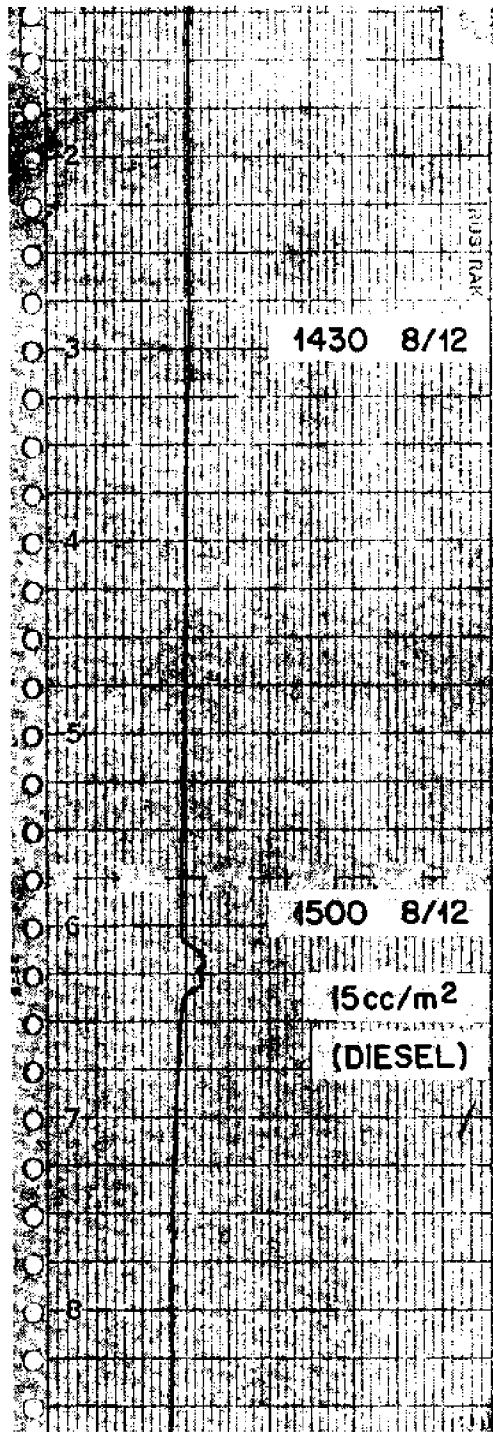


Figure 17. Response - Type 1A

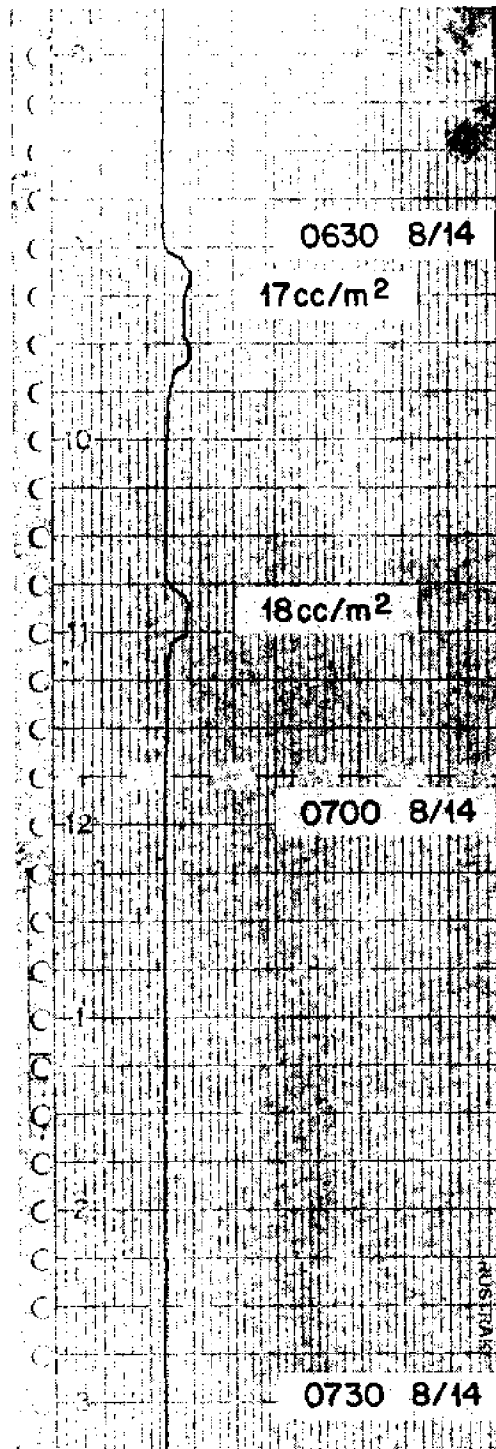


Figure 18. Response - Type 1B

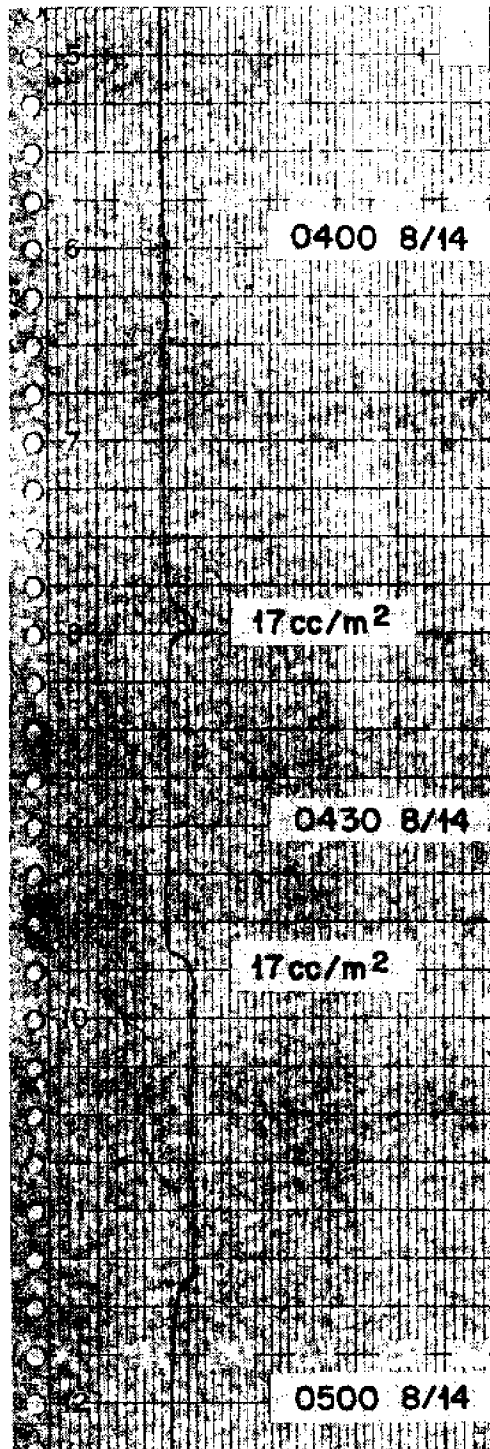


Figure 19. Response - Type 1C

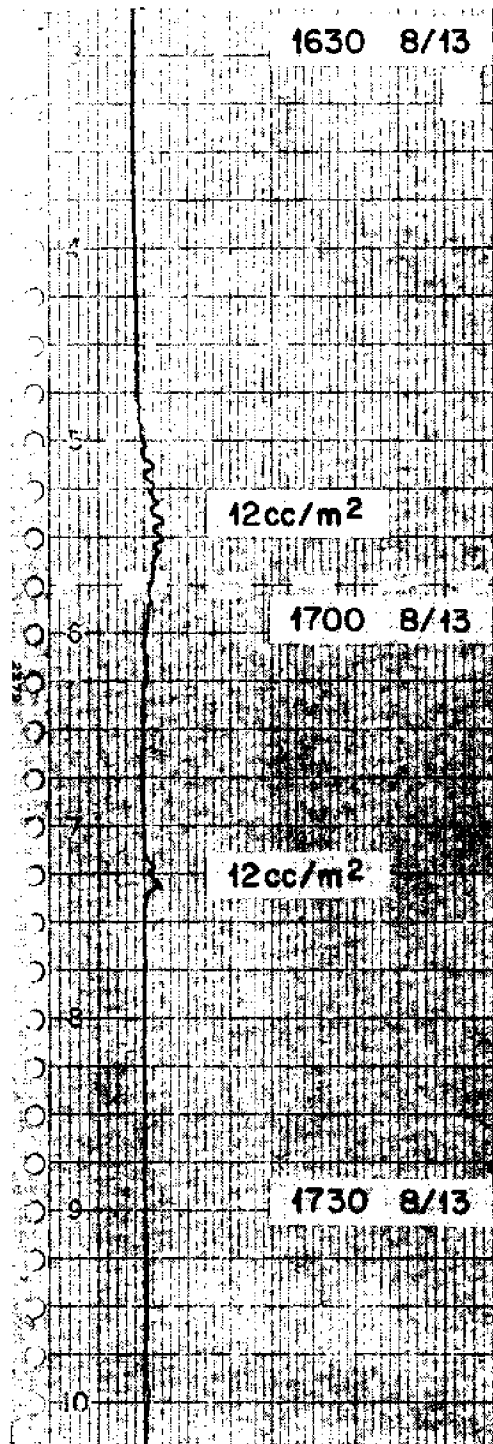


Figure 20. Response - Type 2A

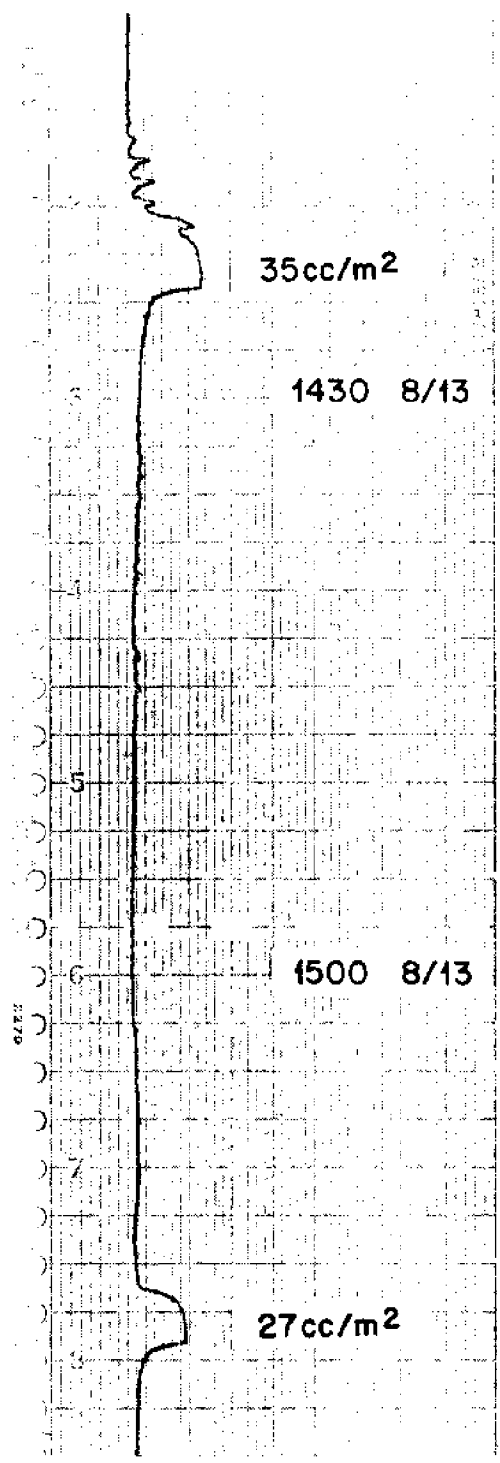


Figure 21. Response - Type 2B

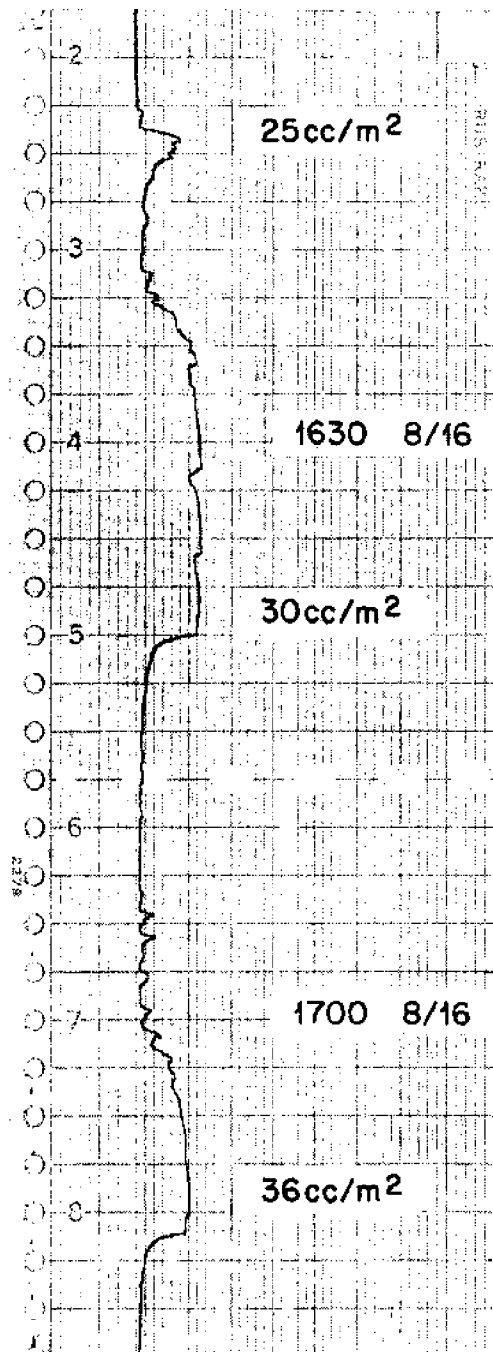


Figure 22. Response - Type 2C

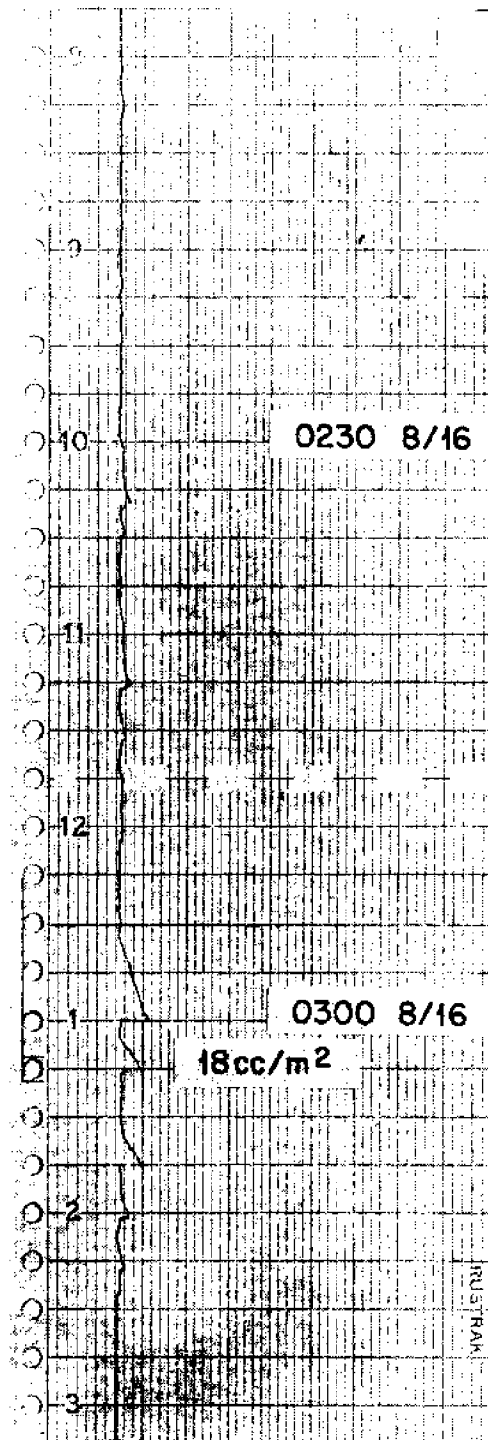


Figure 23. Response - Type 3A

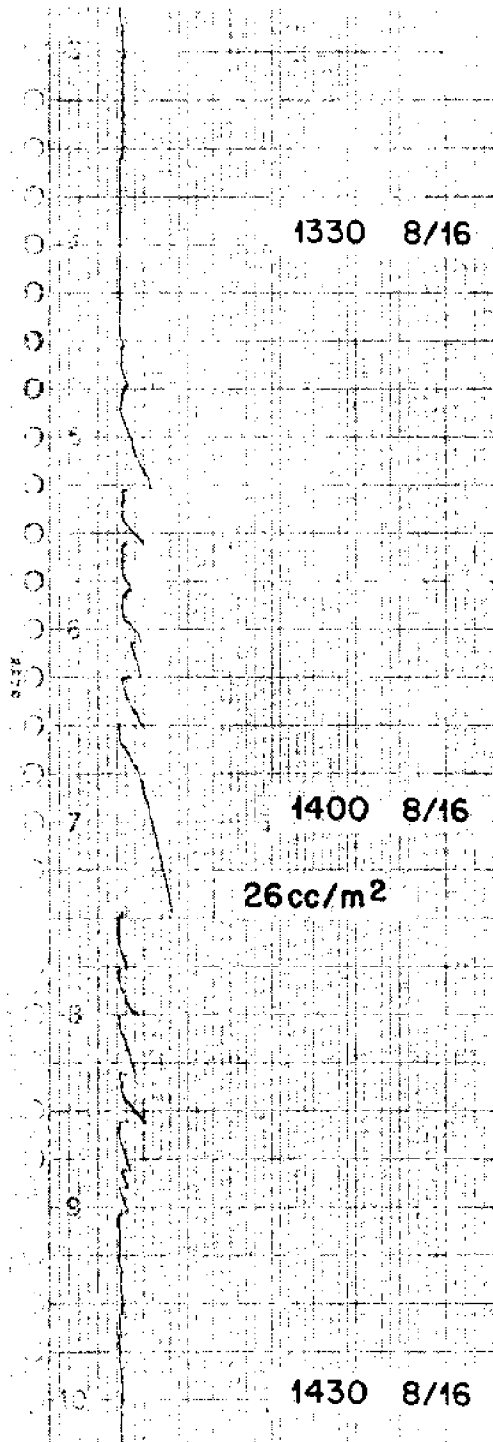


Figure 24. Response - Type 3B

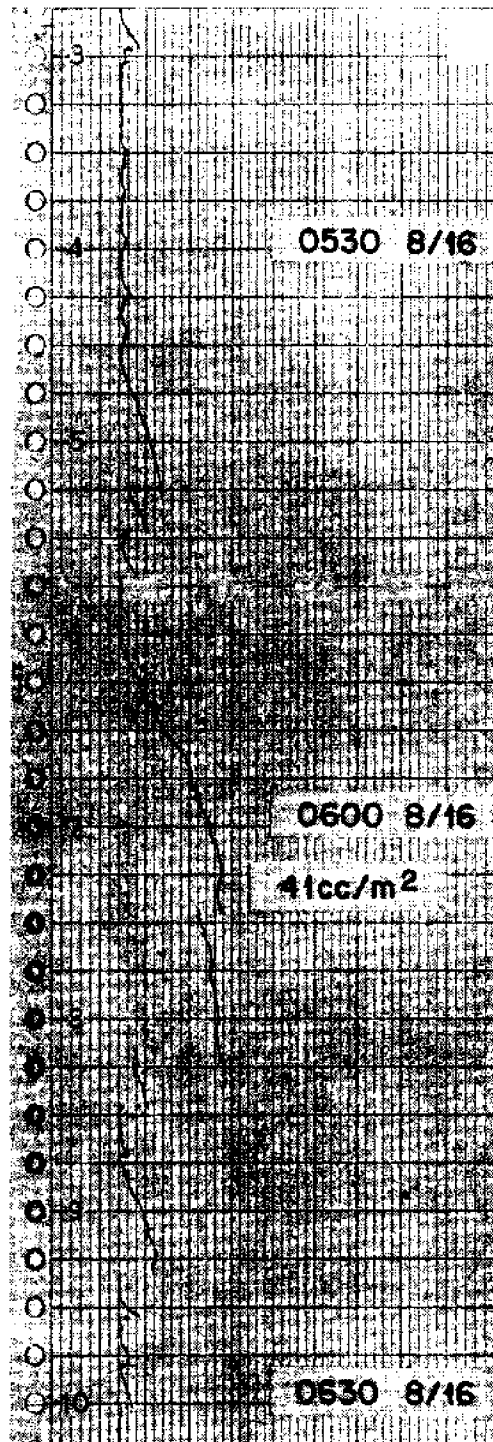


Figure 25. Response - Type 3C

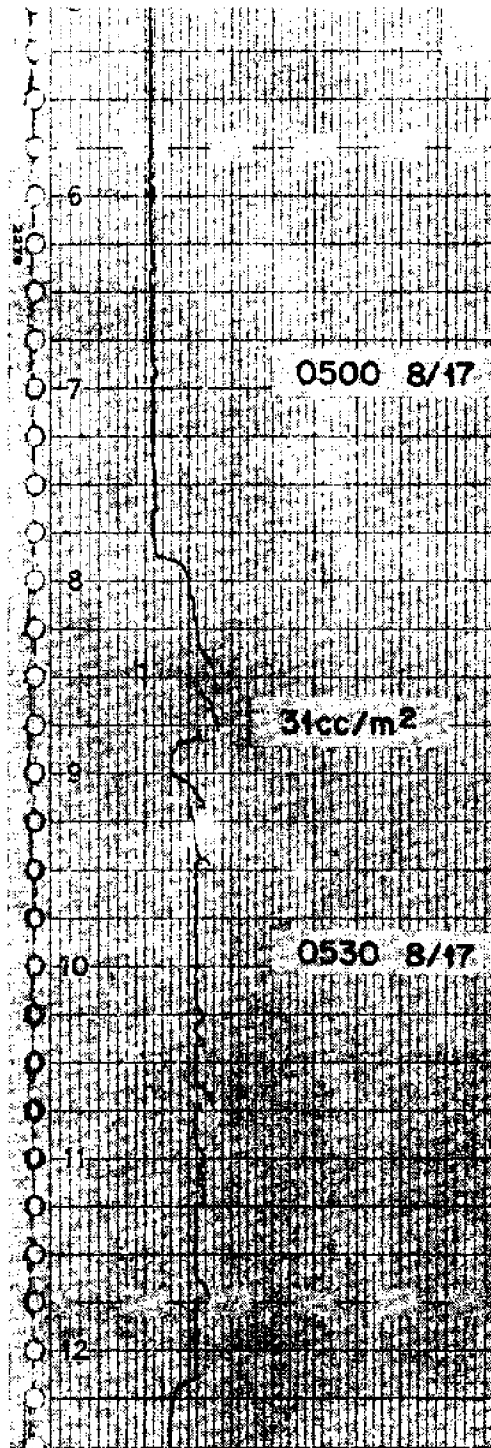


Figure 26. Response - Type 4A

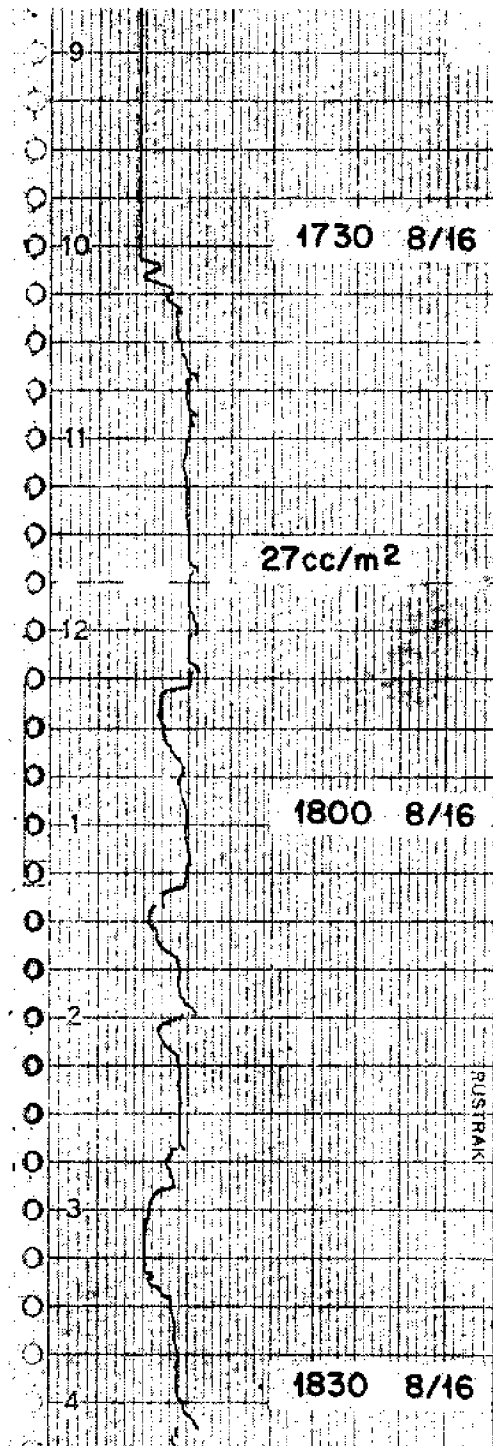


Figure 27. Response - Type 4B

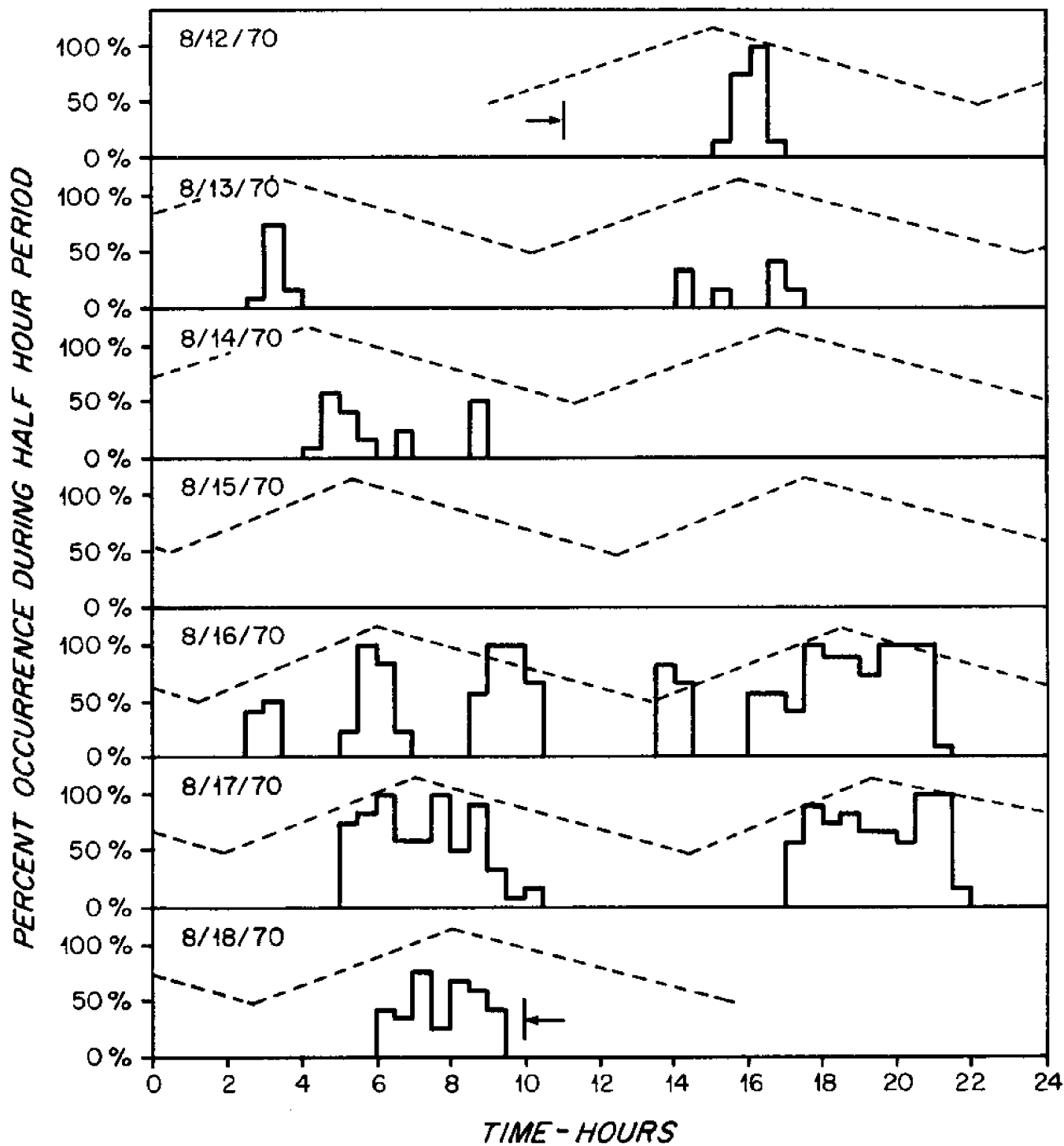


Figure 28. Percent Occurrence - Each Test Day

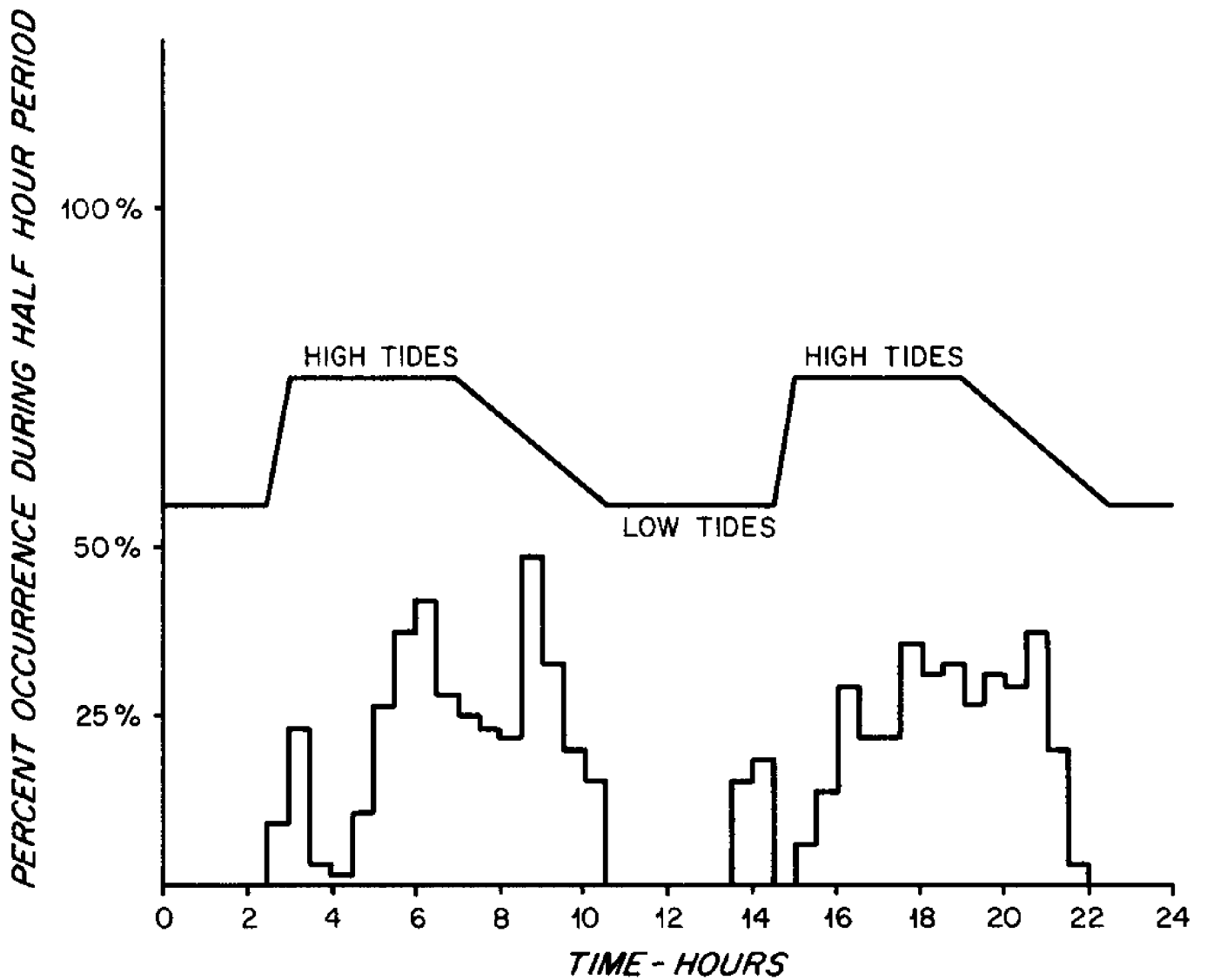


Figure 29. Percent Occurrence - Six Day Total

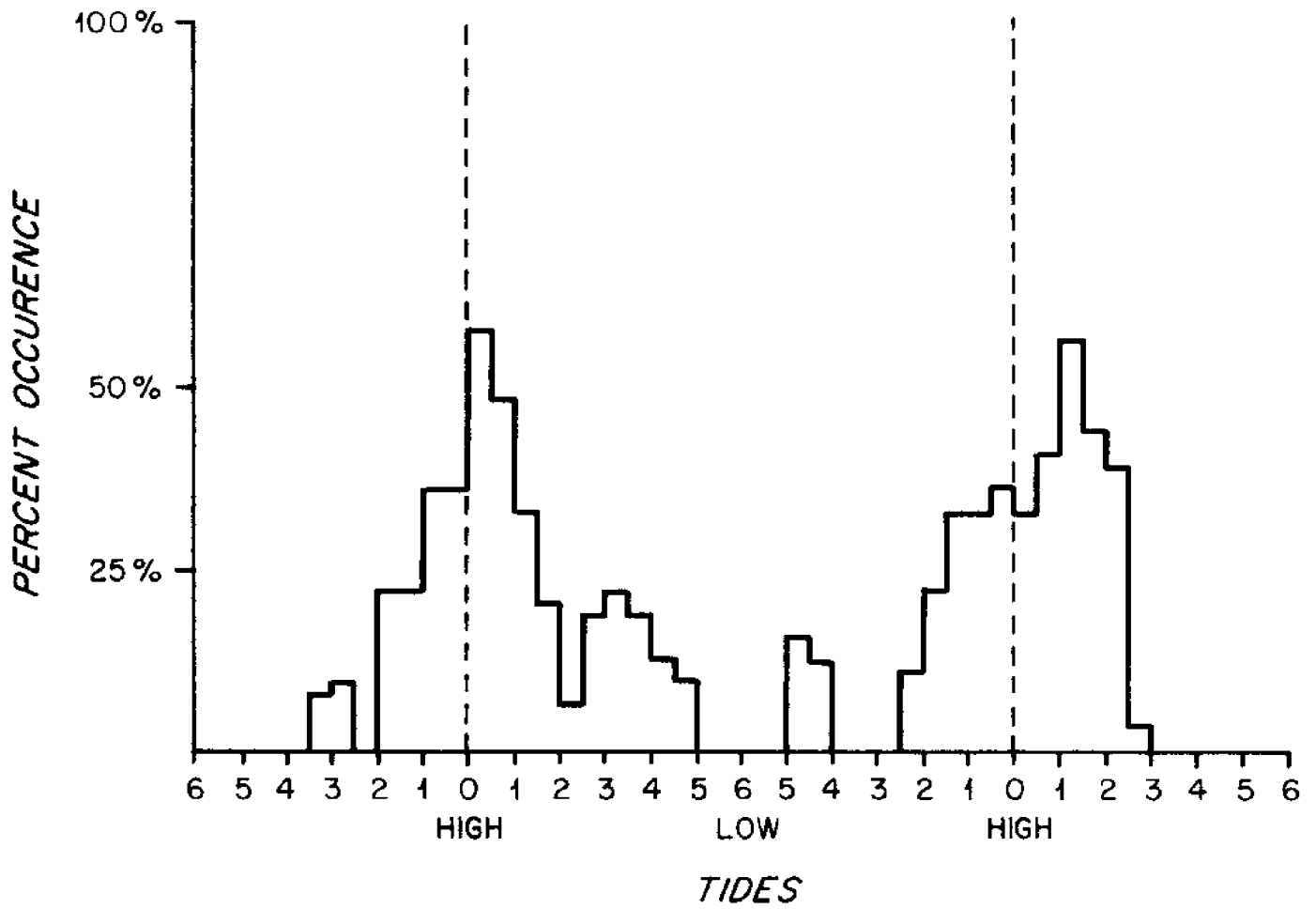


Figure 30. Percent Occurrence - Tide Cycle

re-design of the sensing element based on the principles outlined by the inventors, that is using a different sensor configuration, or based on the mechanism of the expanding resilient base material as discussed above. In either case it is highly probably that a sensor configuration which is less temperature sensitive could be designed.

A second area for improvement would be packaging. If a unit of this type were to be installed on a ship or buoy it would be desirable to have the system more compact. This unit described in this report was a prototype and was designed to allow ease of access to the components. Therefore an operational system would be greatly condensed with respect to the overall size of this unit. Also consideration would have to be given to other design parameters such as shock loading, corrosion, etc., if the unit were to be produced in quantities.

By far the largest power drain on the system was the circulation fan. If the unit is to operate for extended periods of time with a reasonable power requirement a more efficient fan would have to be incorporated.

The flotation platform was designed essentially to allow for tidal variations. That is for installation on Eel Pond, wave action was considered to be small. For areas with significant waves the platform design could be refined for better wave response.

The sampling technique used was to collect vapors just above the sea surface and draw them past the sensor using a circulation system. Each installation will most probably require a unique collection scheme at the sea surface. That is, a buoy system obviously need not compensate for tidal variation. Also some means could be incorporated into the system for removing the film from the surface for more complete laboratory analysis in the event that hydrocarbon vapors are detected by the present system.

SELECTED REFERENCES

1. Estes, John E., Golomb, Berl, "Monitoring Environmental Pollution", Journal of Remote Sensing, 2, vol. 1, no. 2, March/April 1970.
2. Berridge, S., Dean, R., Fallows, R., Fish, A., "The Properties of Persistent Oils at Sea", Journal of the Institute of Petroleum, vol. 54, no. 2, Nov., 1968, pp. 300-309.
3. Blumer, M., "Oil Pollution of the Oceans", Oceanus, vol. XV, no. 2, Oct. 1969, pp. 3-7.
4. Brunnock, J., Duckworth, D., and Stephens, G., "Analysis of Beach Pollutants", Journal of the Institute of Petroleum, vol. 54, no. 539, Nov. 1968, pp. 310-325.
5. Garrett, W., Collection of Slick-Forming Materials From the Sea, Washington, D.C., U.S. Naval Research Laboratory, March 1962.
6. Kawahara, Fred., Laboratory Guide for the Identification of Petroleum Products, U.S. Department of the Interior, Jan. 1969.

7. "Oil Spills: An Environmental Threat", Environmental Science & Technology, vol. 4, no. 2, Feb. 1970, p. 67.
8. Ramsdale, S. and Wilkinson, R., "Identification of Petroleum Sources of Beach Pollution by Gas - Liquid Chromatography", Journal of the Institute of Petroleum, vol. 54, no. 539, Nov. 1968, pp. 326-332.
9. "Remote Sensors Map Barrier to Oil Slick", Oceanology International, vol. 5, no. 4, April 1970, p. 9.
10. Salkowski, Martin, Detection of Oil Contamination in Sea Water, Vol. I, Experimental Investigations, April 19, 1965 through December 31, 1966, Chicago, I.I.T. Research Institute, Feb. 1966.
11. -----, Detection of Oil Contamination in Sea Water, Vol. II, Detailed Data, April 19, 1965, through December 31, 1966, Chicago, I.I.T. Research Institute, Jan. 1967.
12. Swaby, L., and Forziati, A., Remote Sensing of Oil Slicks, Washington, D. C., Federal Water Pollution Control Administration, April 1970.
13. Zachariasen, Fredrik, Oil Pollution in the Sea: Problems for Future Work, Arlington, Va., Institute for Defense Analysis, June 1968.

WATER TRANSPORT OFF NOBSKA POINT BY DYE TRACING

By

Daniel P. Charnews

Richard J. Jaffee

Ocean Engineering

W.H.O.I./M.I.T. Joint Program

Woods Hole Oceanographic Institution
Woods Hole, Massachusetts
August 27, 1970

ABSTRACT

Water transport in Vineyard Sound off Nobska Point of east and west tidal current flows was examined on August 4 and August 7, 1970. Surface water flow was studied by the introduction of 22 gallons of Rhodamine B dye - acetic acid - ethanol solution in the water on each day. The movement and dispersion of the dye patch was analyzed by aerial photographs and fluorometer samples. A comparison of surface water flow and deeper water flow (down to 20 feet) was accomplished by a simultaneous release of drogues.

On the eastward flow, it was found that surface water moves closer to shore than deeper water, with the closest approach to land under the action of westerly and southwesterly winds being approximately 0.7 nautical miles. On the westward flow, it was again found that surface water moves closer to land than deeper waters. Under the influence of a southeasterly wind, part of the dye patch washes ashore at Nonamesset Island. Also, close to Nonamesset Island an eddy current exists drawing water back into Great Harbor.

ACKNOWLEDGEMENTS

The field program upon which this study is based represents the combined efforts of many of the W.H.O.I. staff. Also the advice and assistance of many people contributed greatly to the project. The authors especially wish to thank Mr. Dean F. Bumpus for his helpful advice and his generous offer of his time and the use of his boat, the "Huckleberry". The many excellent photographs contained within this report are the work of Mr. F. Claude Ronne. The skill and expertise of the work of Mr. Robert G. Weeks, the pilot of the airplane, and Mr. Arthur D. Colburn, the captain of the ASTERIAS, is acknowledged by the authors.

We sincerely appreciate the unselfishness of every person who offered their time to the actual field program. We also wish to thank numerous people for their advice and encouragement, especially Dr. Albert J. Williams, 3rd and Dr. Scott C. Daubin of the Ocean Engineering Department of W.H.O.I.

TABLE OF CONTENTS

	Page
I. Introduction	34
II. Field Methods	34
A. Logistics	34
B. Experimental Procedures	35
C. Aerial Photography	36
III. Experiments	36
A. July 29, 1970	36
B. August 4, 1970	37
C. August 7, 1970	37
IV. Data Analysis	37
A. Eastward Flow Photographs	37
B. Westward Flow Photographs	38
C. Drogues and Water Samples	39
V. Results	44
VI. Recommendations	44
References	45

LIST OF ILLUSTRATIONS

		Page
Figure 1	Eastward Flow; 2 minutes after dye release	37a
Figure 2	Eastward Flow; 18 minutes after dye release	37b
Figure 3	Eastward Flow; 24 minutes after dye release	38a
Figure 4	Eastward Flow Distribution; 24 minutes after dye release	38b
Figure 5	Eastward Flow; 49 minutes after dye release	38c
Figure 6	Eastward Flow; 66 minutes after dye release	38d
Figure 7	Eastward Flow Distribution; 66 minutes after dye release	38e
Figure 8	Overall Eastward Flow Distribution	38f
Figure 9	Eastward Flow Beach Sampling Points and NOBSKA Sampling Points	38g
Figure 10	Eastward Flow Dye and Drogues	38h
Figure 11	Eastward Flow ASTERIAS Water Sampling Points	38i
Figure 12	Westward Flow; 1 minute after dye release	38j
Figure 13	Westward Flow; 15 minutes after dye release	38k
Figure 14	Westward Flow; 39 minutes after dye release	39a
Figure 15	Westward Flow; 54 minutes after dye release	39b
Figure 16	Westward Flow Distribution; 54 minutes after dye release	39c
Figure 17	Westward Flow; 61 minutes after dye release	39d
Figure 18	Westward Flow; 69 minutes after dye release	39e
Figure 19	Westward Flow Distribution; 69 minutes after dye release	39f
Figure 20	Westward Flow; 85 minutes after dye release	39g
Figure 21	Westward Flow; 88 minutes after dye release	39h
Figure 22	Overall Westward Flow Distribution	39i
Figure 23	Westward Flow Dye and Drogues	40a
Figure 24	Westward Flow ASTERIAS Water Sampling Points	43a
Figure 25	Dye Concentration vs Distance Along Run	43b

Illustration	Page
Figure 26 Dye Concentration vs Distance from Nobska Point	43c

Tables

Table 1	Readings Obtained from Water Samples Taken by ASTERIAS on Eastward Flow	41
Table 2	Readings Obtained from Water Samples Taken by NOBSKA on Eastward Flow	41
Table 3	Readings Obtained from Water Samples Taken by ASTERIAS on the Westward Flow	43

I. INTRODUCTION

The town of Falmouth, Massachusetts, has been considering a sewer system and treatment plant to take care of its growing population. One plan has been to take the effluent from the proposed plant and dispose of it through an outfall at Nobska Point on Vineyard Sound, see U.S. Coast and Geodetic Survey charts 259 and 260. This site was chosen on the basis of work done by Bumpus, Wright and Vaccaro (1969) using current meter observations, salt bridge readings, drogue experiments, drift bottle experiments, sea bed drifter experiments, and chemical analysis of the water. From their observations, they concluded that if the outfall were located 700 yards off Nobska Point at 141 degrees T in 90 feet of water, the effluent would run parallel to the shore and have a final dilution of 1700-2800 parts of sea water to each part of effluent. From the dilution factors and the estimates supplied by the engineers of nitrogen, phosphorus, and B.O.D. in the effluent, it was concluded that the extra organic matter would not seriously deplete the oxygen content of the water.

The site was chosen not only for keeping the effluent off shore, but because of the 90 foot depth. The effluent will be warm and less saline than the surrounding water, it will thus rise toward the surface. The diffuser should be designed to mix most of the effluent before it reaches the surface. Bumpus, Wright, and Vaccaro used basically subsurface experiments in determining the tidal currents. Should, however, the effluent reach the surface, these experiments may not give the behavior of the complete surface layer. This report involves studying the surface layer of the water driven by wind as well as tidal currents.

To track the surface layer, a dye was injected at the surface over the proposed site and tracked. This method was chosen since good results have been obtained at Lamont Geological Observatory by Costin, Davis, Gerard and Katz (1963) in their work in the New York Bight, and by many others. The dye was introduced at slack water to see the flow patterns at the transition between flows as well as when the tide was fully developed. Due to the 10 week time limit for the project, this also seemed the fastest way to get a qualitative idea of the surface flow patterns in the area off Nobska Point. To compare this with the data Bumpus, Wright, and Vaccaro obtained, drogues were also launched just before the dye was injected.

II. FIELD METHODS

A. Logistics

The following equipment was procured before the week of the experiments.

Boats:

1. ASTERIAS
2. NOBSKA
3. Huckleberry

Plane: Cessna 172

- Dye:
1. Loaded Dye Barrel - 22 gallons ethanol, Rhodamine B., acetic acid solution
 2. Barrel
 3. Barrel Stand
 4. Pipe Fittings and Valve

Charts:

1. ASTERIAS - #259 and #260
2. Huckleberry - #259 and #260
3. NOBSKA - Xerox copy of #259 and #260
4. Cessna 172 - Xerox copy of #259 and #260

Stationery:

1. 3 notebooks with gummed stickers
2. 3 waterproof pens

Navigating Instruments:

1. 3 sextants
2. 1 three-arm protractor
3. Dividers
4. Parallel Rule

Sample Collecting Equipment:

1. 210 collecting bottles - 15 ml.
2. 3 bottle holders
3. 1 bucket thermometer
4. 1 anemometer

Drogues: 4

Communication:

3 Walkie Talkies Call letters IW9789

B. Experimental Procedures

Before each experiment a 40% solution by weight of Rhodamine B dye and acetic acid was diluted with ethanol to a specific gravity of 0.965 in order to insure it remained near the surface for photographic purposes. Approximately 22 gallons of this solution was used on each day. This solution was mixed in a 50 gallon drum which was then lashed with a barrel stand to the stern of the NOBSKA. With the equipment loaded on the boats and plane, the NOBSKA was positioned over the proposed outfall site, the position being verified by sextant, 3 arm-protractor, navigational chart #260, and depth sounder. When the plane was circling above the NOBSKA, four drogues set at 5, 10, 15 and 20 feet were released. Then the valve on the dye barrel was opened and the dye flowed out for approximately 1.25 hours.

For the remainder of the experiment the ASTERIAS took water samples, horizontal sights on known landmarks, wind velocity readings, and temperature readings. The "Huckleberry" tracked the drogues taking horizontal sights on known landmarks. The plane took aerial photographs and directed the ASTERIAS to interesting areas to take water samples. The experiment ran approximately three hours, limited by the range of the airplane and the change in light conditions. At the end of the three hours, the drogues were picked up and the experiment terminated.

In order to coordinate the boats and the plane, short wave radio was used. The ASTERIAS was made the command boat and communicated with the "Huckleberry" and the plane by Citizen Band walkie-talkie. The ASTERIAS and the NOBSKA used their marine radios.

Below is the schedule each experiment followed:

August 4, Eastward Flow		August 7, Westward Flow
Beginning at 0750		Beginning at 1552
0755	- on site with boats and plane - drogues released	1535
0800	- dye released - tracking drogues water sampling wind readings temperature measurements photographs taken	1540
1200	- Termination of experiment -	1900

C. AERIAL PHOTOGRAPHY

A Cessna 172 aircraft was used to obtain aerial photographs of the movement and dispersion of the dye patch. Only oblique photographs could be taken because of the lack of a port hole in the bottom of the plane. A Hasselblad camera was used with a Corning filter 3-66 to obtain black and white photographs, and a Mamiya Sekor 35 mm camera was used to take infrared color photographs. Unfortunately, the general quality of the infrared color photographs was poor and none are included in this report.

The fluorescent spectrum of Rhodamine B has a maximum at 5800 angstroms. The Corning filter 3-66 cuts off all light below 5600 angstroms and has 75% transmission at 5800 angstroms. Thus, prints show a white dye patch on a black sea for the filtered black and white photographs.

Since sun reflection off the water between 1100 and 1400 would have caused poor photographic conditions, dye releases were planned either early in the morning or late in the afternoon depending upon currents off Nobska Point.

III. EXPERIMENTS

A. July 29, 1970

During the week of July 27, 1970, a large high pressure system centered near Bermuda and a cold front along the Canadian border caused a prolonged period of temperature inversion and stagnant air throughout the Northeast. A typical day off Nobska Point was characterized by fog and haze with a partial clearing in the afternoon as the sun rose higher in the sky. During the afternoon of July 28, the sun completely burned off the haze in the afternoon. During July 29, the tidal currents off Nobska Point shifted to the east at approximately 1530, so that dye release was planned at this time, weather permitting. On July 29, partial clearing began at about 1400, but by 1530 fog and haze had returned to

the area, so operations had to be postponed. Nevertheless, valuable experience in logistics, navigation, and communications was obtained before postponement.

B. August 4, 1970

On August 4, currents off Nobska Point turned to the east at approximately 0750. A cold front, causing widespread showers, passed through the area during the early morning hours of August 4. Partial clearing began at 0630, and by 0800 only scattered clouds were visible in the area. Photographic conditions were not ideal, however, with some haze still present.

The four drogues were released at 0755 and dye release commenced at 0800. Dye release continued for 1½ hours. Because of a delay caused by the uncertain weather, the period of slack water was missed by approximately 15 minutes. Photographs were taken of the dye patch until approximately 1030 at which time fuel requirements necessitated leaving the area. Water samples were taken and the drogues were followed until approximately 1230.

Wind direction shifted from westerly to southwesterly during the course of the morning, and wind speed increased to 11.5 knots by 1135.

<u>Time</u>	<u>Direction</u>	<u>Speed</u>
0855	265°T	6 knots
0945	265°T	8 knots
1025	230°T	9 knots
1135	225°T	11.5 knots

C. August 7, 1970

On August 7, the current off Nobska Point turned to the west at approximately 1552. Weather and photographic conditions were ideal with unlimited visibility.

The four drogues were released at 1535 and the dye release commenced at 1540. Dye release from the NOBSKA continued for 1½ hours. Photographs were taken of the dye patch until approximately 1730. Water samples were taken and the drogues were followed until approximately 1845. Throughout the afternoon, wind direction and speed remained constant at 130°T and 8 knots.

While locating the outfall site and anchoring position, the NOBSKA underwent engine failure, with the result that she had to be towed by the ASTERIAS to the outfall site. After the completion of the dye release, she then had to be towed back to W.H.O.I.

IV. DATA ANALYSIS

A. Eastward Flow Photographs

Figure 1 was taken at 0802, two minutes after dye release and approximately 12 minutes after the current had shifted to the east. The NOBSKA is anchored over the outfall site and the dye is moving at a direction of 70°T. The length of the dye patch is approximately 35 yards.

Figure 2 was taken at 0818, 18 minutes after dye release. Dye is still streaming out from the NOBSKA and the ASTERIAS can be seen at the forward edge of the dye patch. The dispersion of the dye can be noticed and a zig-zag pattern in the dye is evident as it approaches the first shoal to the northeast of the outfall site.



Figure 1. Eastward Flow; 2 minutes after dye release

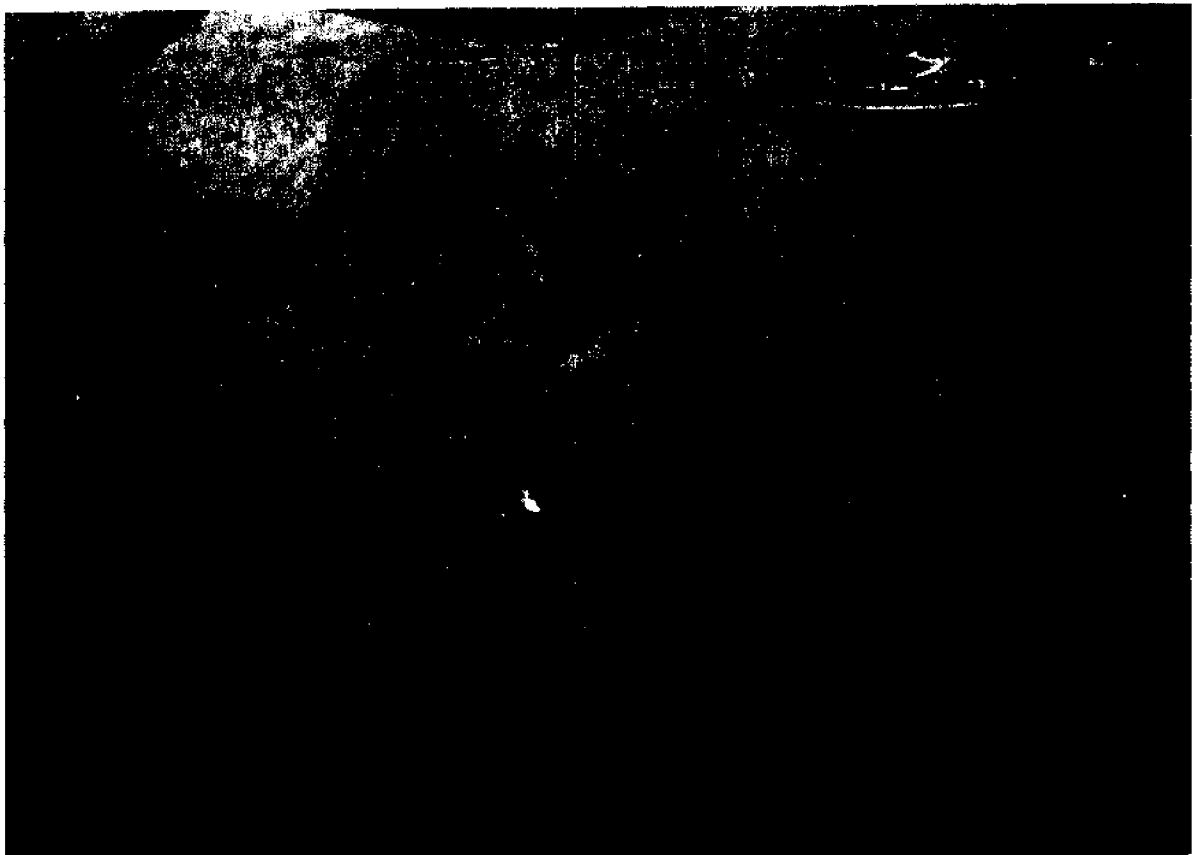


Figure 2. Eastward Flow; 18 minutes after dye release

Figure 3 was taken at 0824, 24 minutes after dye release. Dye is still streaming out from the NOBSKA, the ASTERIAS is again at the forward edge of the dye patch, and the "Huckleberry" can be seen closer to shore. From the location of the "Huckleberry" and the dye patch, it can be seen that the drogues (tracked by the "Huckleberry" are ahead of the dye and closer to shore. Later in the morning it was observed that part of the dye patch moved closer to shore than the drogues. From the photograph, the dye underwent a significant change in direction approximately 1000 yards from the outfall site. Figure 4 shows the geographical distribution of the dye patch as photographed in Figure 3. As the dye approached the first shoal, it was diverted to the southeast before coming back to the northeast. At this time, 24 minutes after dye release, the dye patch has covered an area of approximately 300,000 square yards (0.75 square nautical miles). This area was determined by planimeter measurements.

Figure 5 was taken at 0849, 49 minutes after dye release. Dispersion and dilution of the dye patch is quite evident. The cloud-like appearance of the dye is due to its being drawn below the surface and the resulting change in visual reflectance. This feature of Rhodamine B has been widely observed in aerial photography by others (3, 4, and 5). In this photograph, the diverting effect of the shoal has diminished and the dye is moving toward the east-northeast again.

Figure 6 was taken at 0906, 66 minutes after dye release. Dispersion of the dye is evident, but now (and in later observations) the dye has split into two paths with most of the dye taking the path further away from shore. Figure 7 shows the geographical distribution of the dye photographed in Figure 6. The dye has now covered an area of 660,000 square yards (1.65 square nautical miles). Figures 4 and 7 thus give a dispersion rate of 470,000 square yards per hour (1.2 square nautical miles per hour).

As time progressed, the quality of the photographs became poorer because of decreasing dye concentrations, so quantitative analyses became quite difficult. However, from visual observations, the overall dispersion of the dye patch could be plotted (Figure 8). Figure 8 shows the dye patch passing between the two shoals to the east of the outfall site and then splitting into two sections with the major part staying further out into Vineyard Sound. It was also noted that the drogues remained approximately in the middle of the major part of the dye patch.

B. Westward Flow Photographs

Figure 12 was taken at 1541, one minute after dye release and 11 minutes before the current shifted to the west. The NOBSKA is anchored over the outfall site, the ASTERIAS is near the dye patch, and the "Huckleberry" is in the foreground of the photograph. The dye patch is moving toward the south at $170^{\circ}T$ and its length is about 15 yards. The period of slack water was evident at this time with a net velocity of 0.2 knots at $170^{\circ}T$. This southerly flow continued for approximately 11 minutes.

Figure 13 was taken at 1555, 15 minutes after dye release and three minutes after the current had shifted to the west. The dye that had been moving in a southerly direction is beginning to move toward the west. The location of the "Huckleberry" to the south of the NOBSKA indicates that the drogues are lagging behind the dye patch which has begun a westward movement.



Figure 3. Eastward Flow; 24 minutes after dye release

70° 40' W

35'

30'

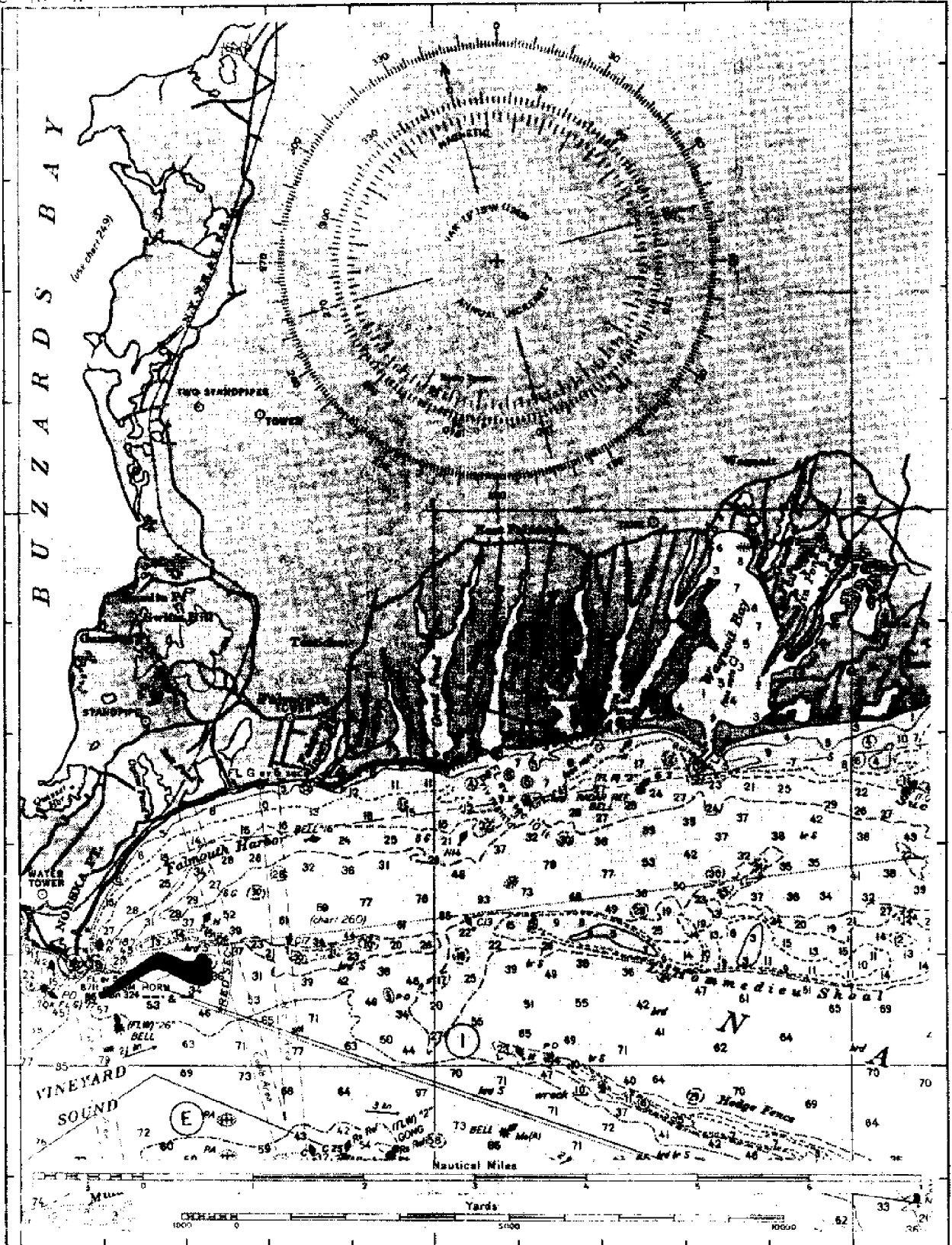


Figure 4. Eastward Flow Distribution; 24 minutes after dye release



Figure 5. Eastward Flow; 49 minutes after dye release

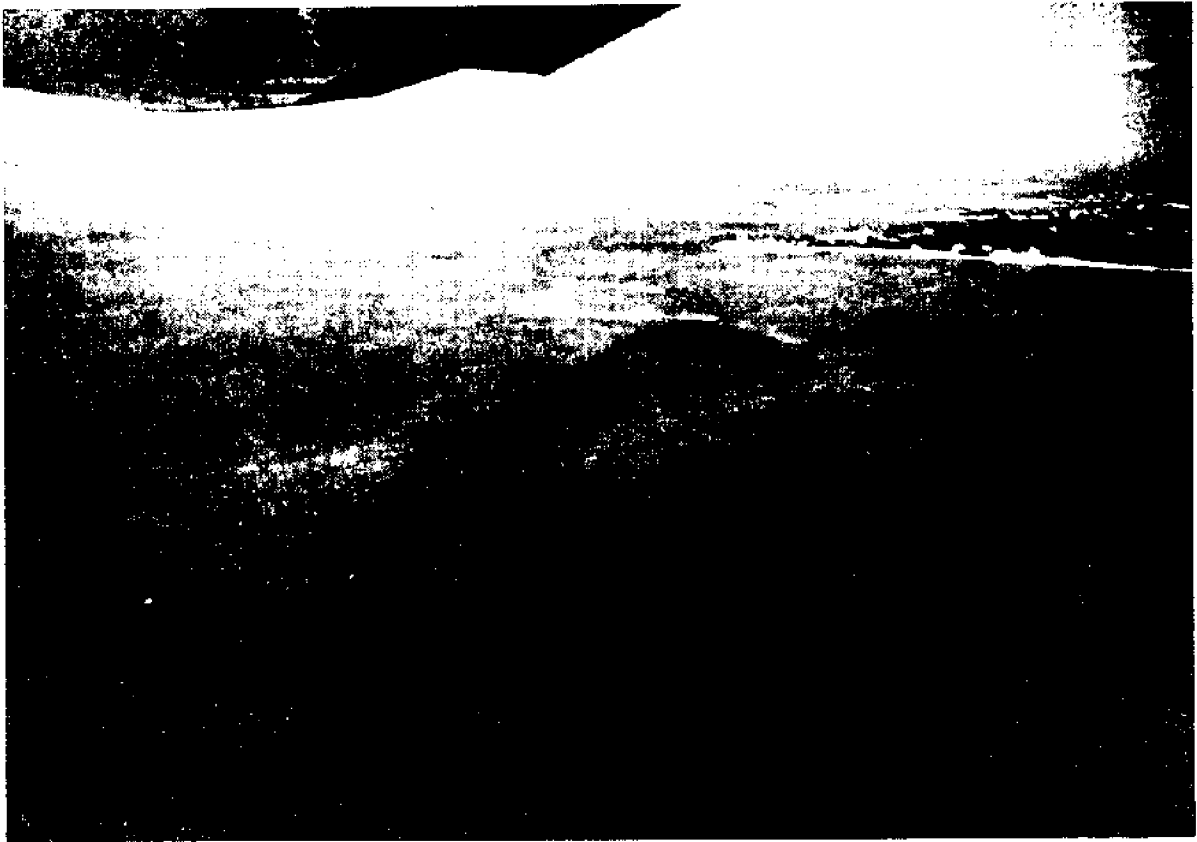
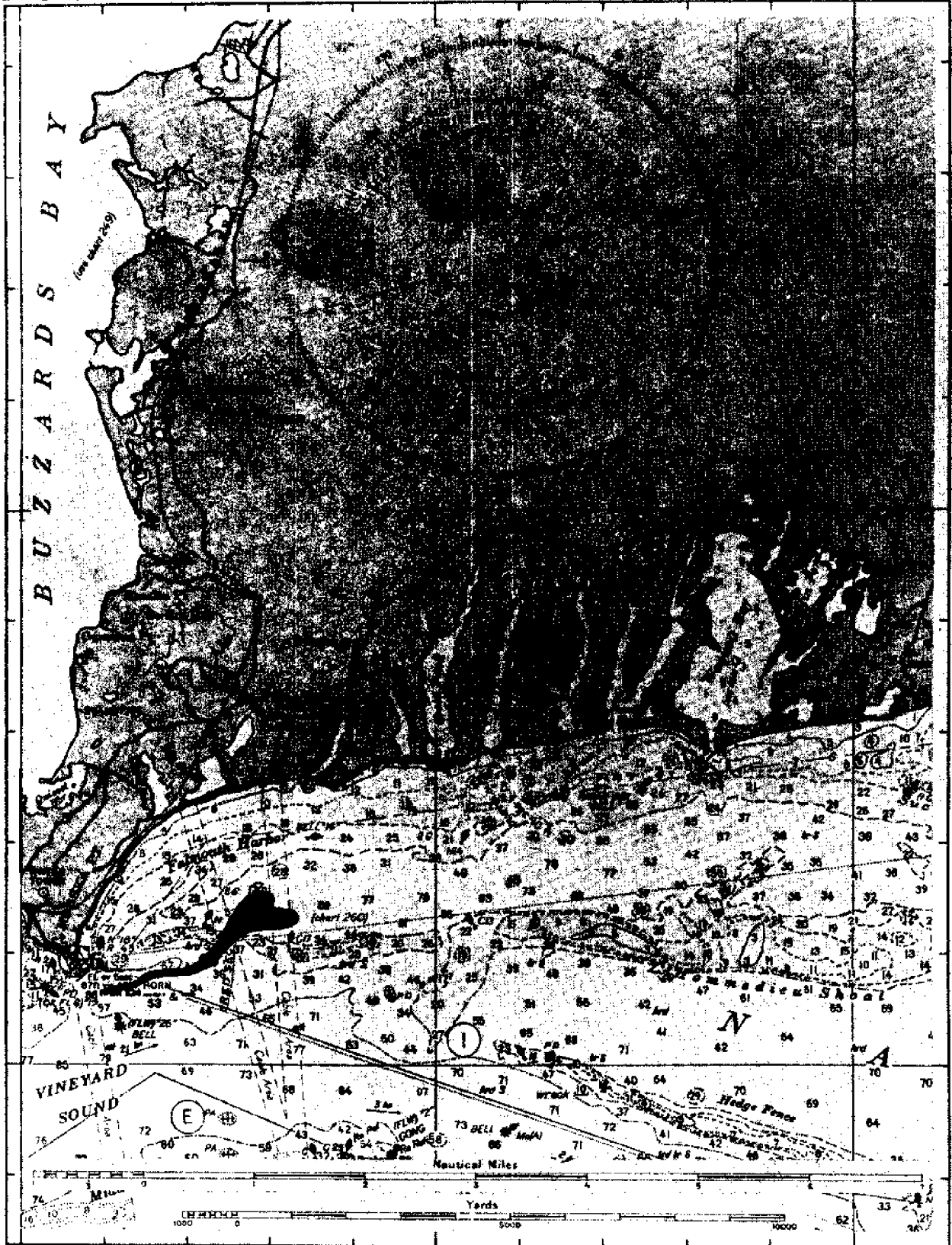


Figure 6. Eastward Flow; 66 minutes after dye release

70° 40' W

35'

30'



35'

41° 30' N

Figure 7. Eastward Flow Distribution; 66 minutes after dye release

70° 40' W

35'

30'

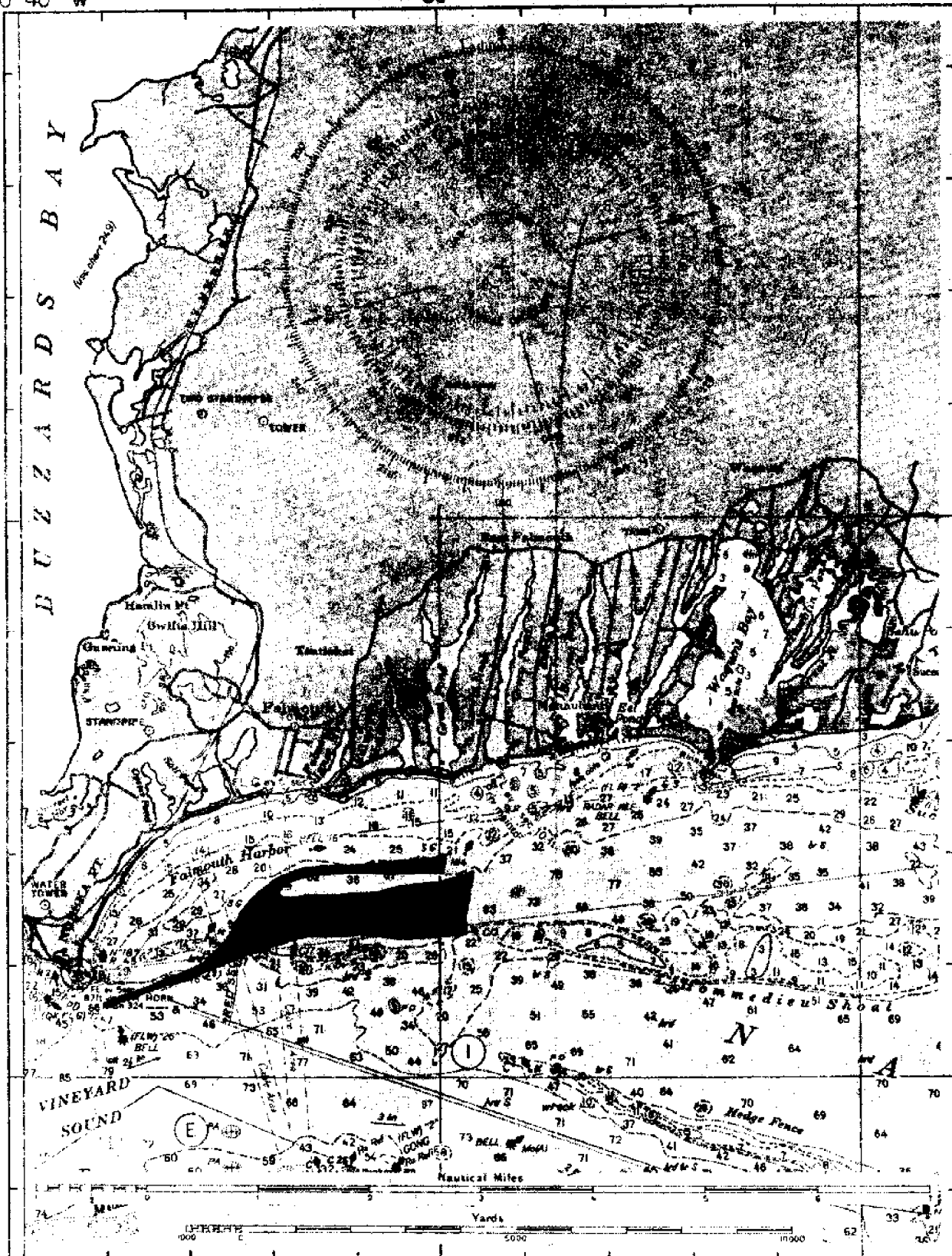
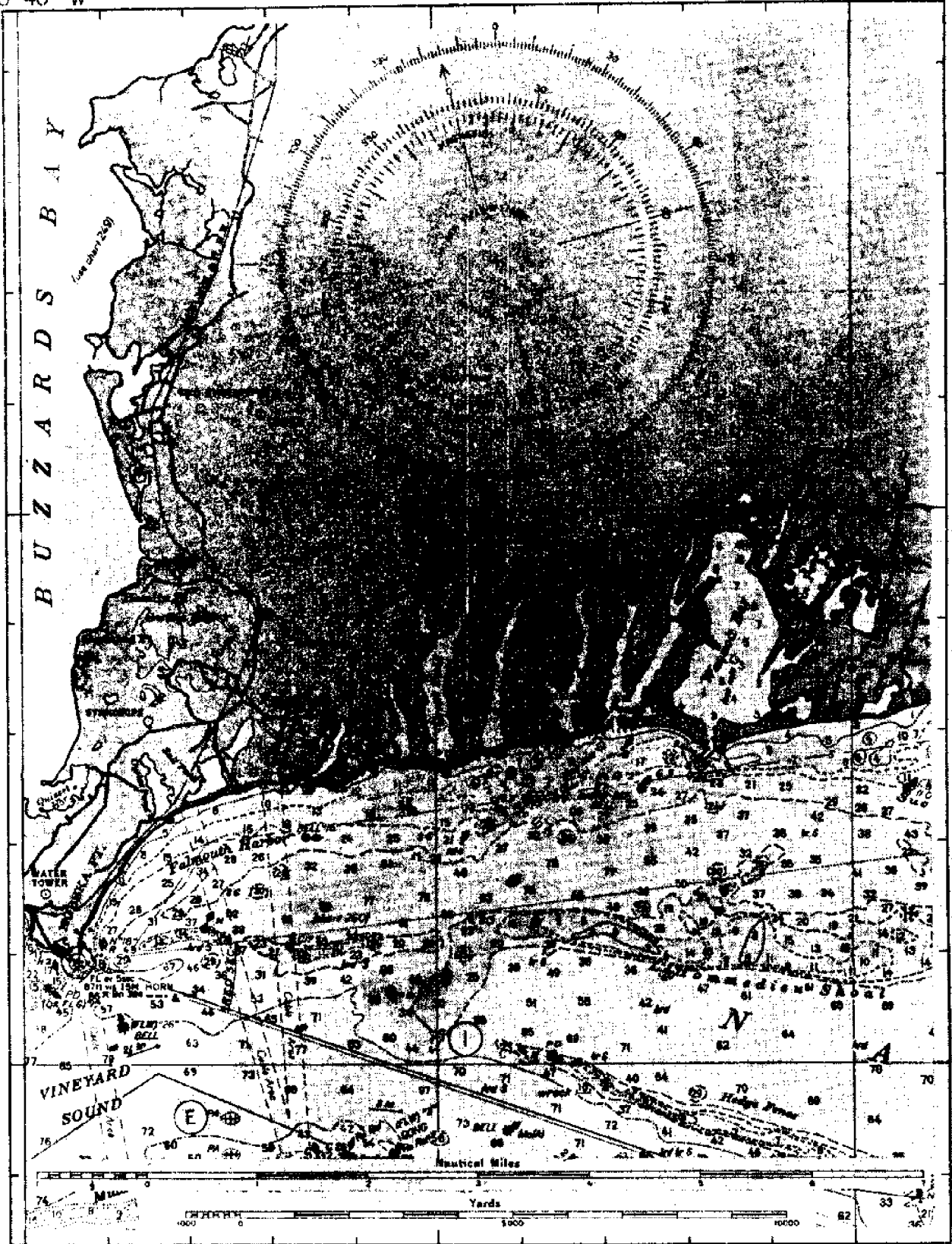


Figure 8. Overall Eastward Flow Distribution

70° 40' W

35'

30'



35'

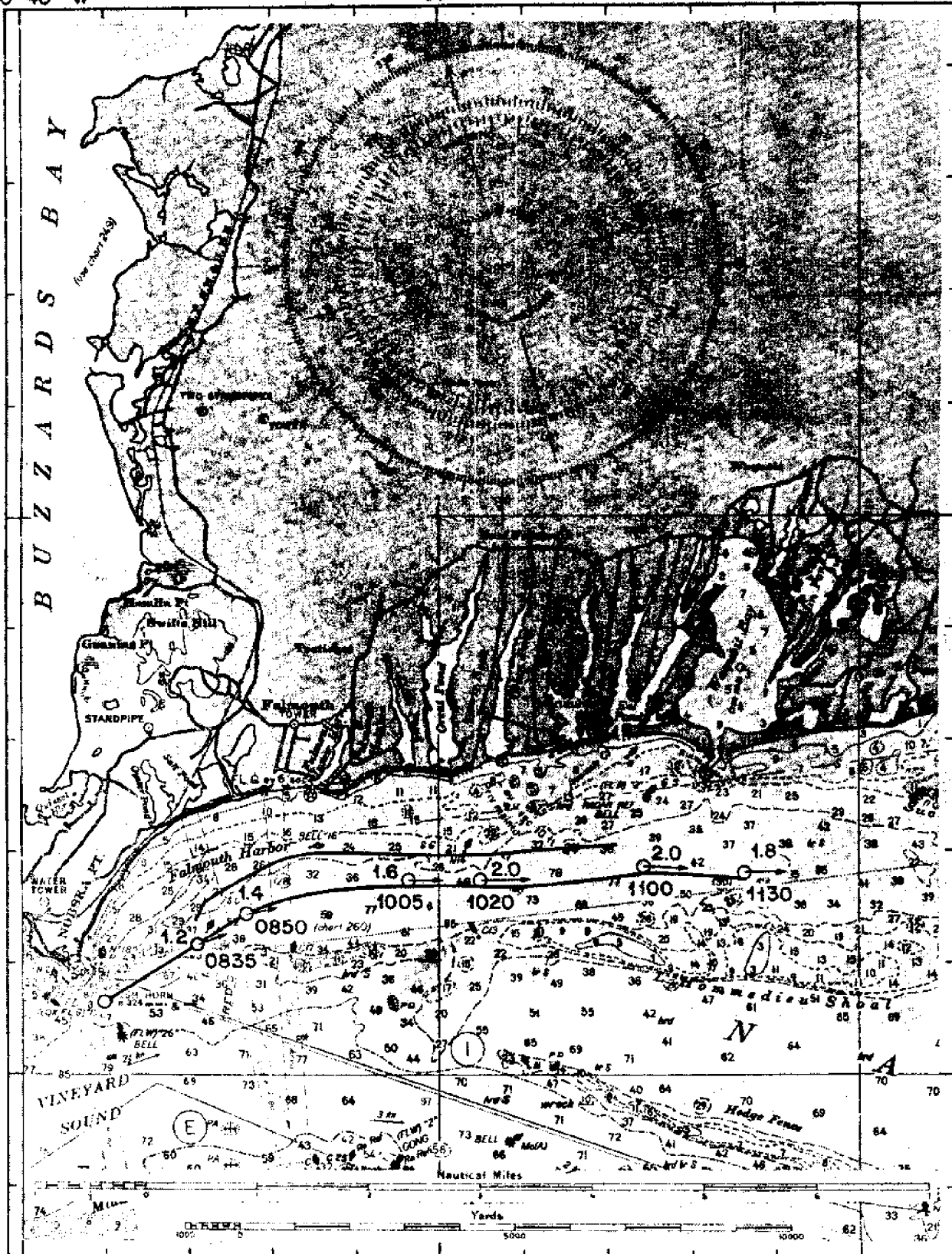
41° 30' N

Figure 9. Beach Sampling Points & "Nobska" Sampling Points East Flow ●

70° 40' W

35'

30'



35'

41°
30'
N

Figure 10. Eastward Flow Dye

Kts.

Drogues

⊙ →

Time

-38h-

70° 40' W

35'

30'

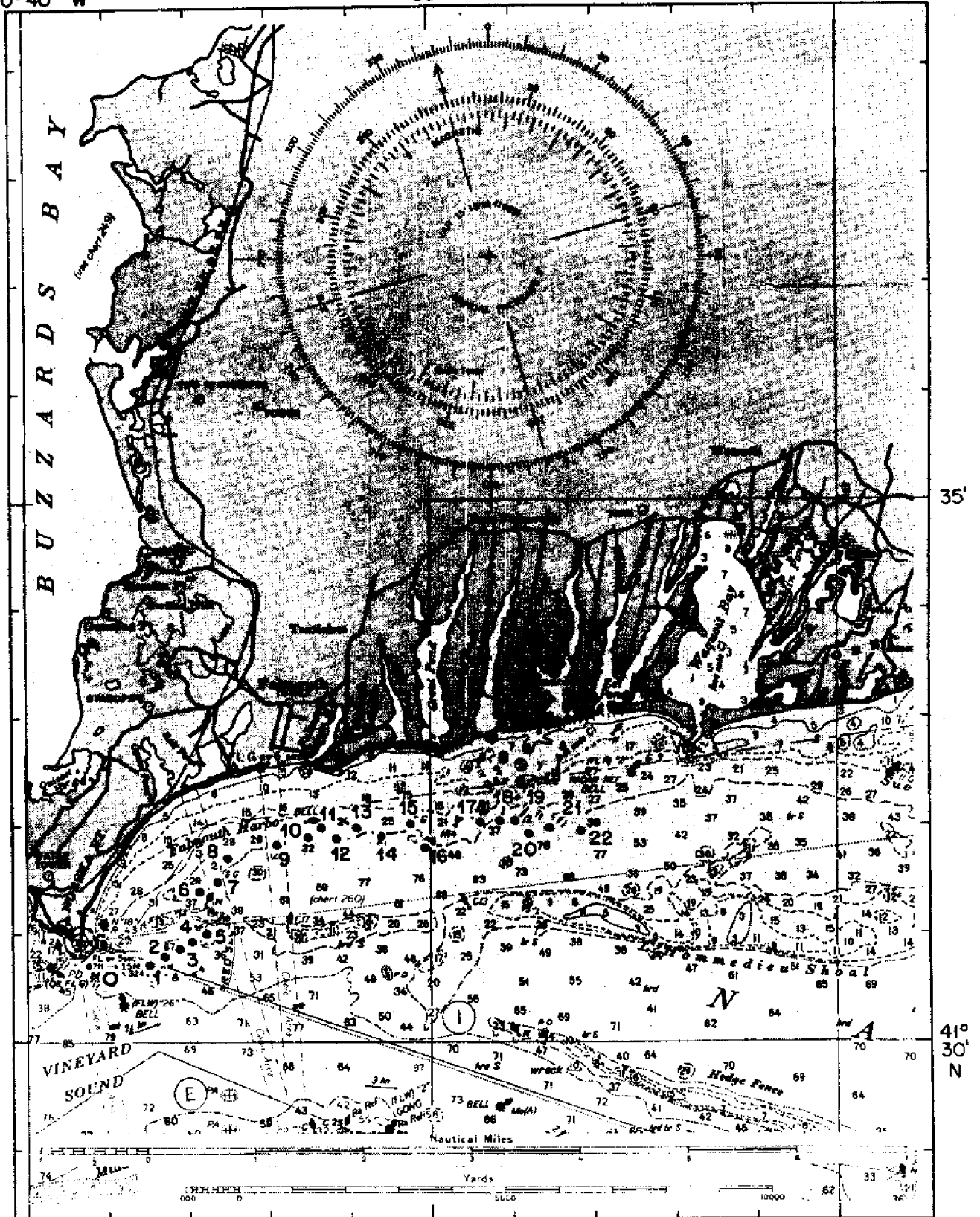


Figure 11. Eastward Flow "Asterias" Water Sampling Points

Bottle No. ●

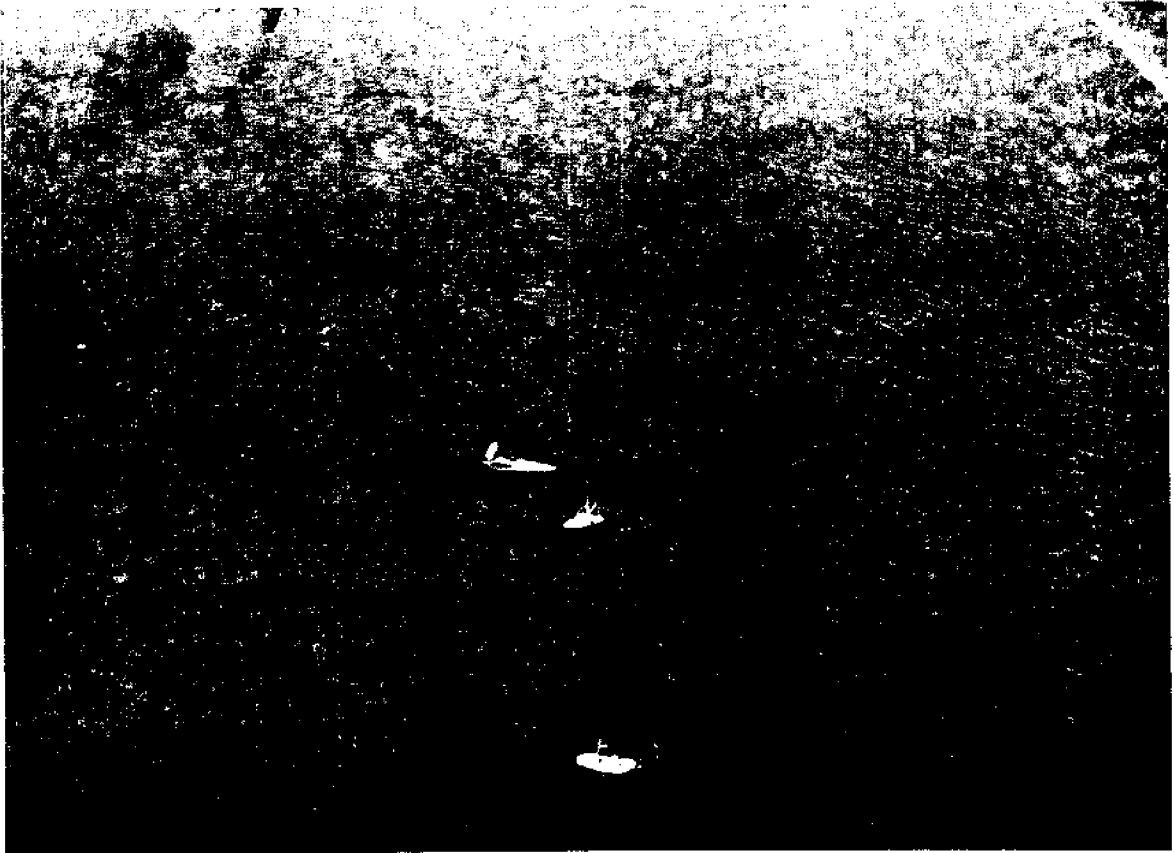


Figure 12. Westward Flow; 1 minute after dye release



Figure 13. Westward Flow; 15 minutes after dye release

Figure 14 was taken at 1619, 39 minutes after dye release. The dye can be seen to be curving around Nobska Point. The ASTERIAS is seen in the foreground of the photograph making a pass across the dye patch (Run #1). The "Huckleberry" is in the middle of the dye patch tracking the drogues. From the position of the "Huckleberry" it is seen that the drogues still trail the forward edge of the dye patch. The portion of the dye that originally was to the south lags the main part of the dye and is still to the south.

Figure 15 was taken at 1634, 54 minutes after dye release. The curvature and dispersion of the dye patch is clearly evident. The forward edge of the dye patch has reached buoy Red "2", the entrance to Great Harbor (see extreme left forward edge of dye patch in photo). The second buoy marking the entrance to Great Harbor (Black Gong "1") can be seen in the foreground of the photograph. Figure 16 shows the geographical distribution of the dye patch as photographed in Figure 15. At this time, 54 minutes after dye release, the dye patch has covered an area of approximately 325,000 square yards (0.81 square nautical miles).

Figure 17 was taken at 1641, 61 minutes after dye release. The peculiar cloud formation mentioned previously is evident. The dye patch has passed buoy Red "2" and has now reached the Black Gong "2". The speed of the forward edge of the dye patch is found to be 1.1 knots by a comparison of Figures 15 and 17 and knowing that the buoys at the entrance to Great Harbor are separated by 0.125 nautical miles.

Figure 18 was taken at 1649, 69 minutes after dye release. An overall view of the dye patch from Nobska Point to Nonamesset Island is visible. Sheep Pen Harbor on Nonamesset Island is in the foreground. The ASTERIAS can be seen at the forward edge of the dye patch. At its closest approach, the dye patch is about 175 yards from Nonamesset Island. Figure 19 shows the geographical distribution of the dye patch as photographed in Figure 18. The dye patch has covered an area of approximately 430,000 square yards (1.1 square nautical miles). Figures 16 and 19 give a dispersion rate of 420,000 square yards per hour (1.05 square nautical miles per hour).

Figure 20 was taken at 1705, 85 minutes after dye release. The edge of the dye patch can be seen to be within 40 yards of Nonamesset Island.

Figure 21 was taken at 1708, 88 minutes after dye release. From this photograph, it can be seen that the dye is essentially on shore at a small section of Nonamesset Island.

From visual observations, it was noted that the major portion of the dye did not wash ashore on Nonamesset Island, but rather veered away from shore and continued down Vineyard Sound in the accompaniment of the drogues. It was also observed that an eddy current was present close to Nonamesset Island that brought part of the dye patch back around Sheep Pen Harbor and into Great Harbor.

Figure 22 shows the overall movement and dispersion of the dye patch. The point of contact of the dye patch and Nonamesset Island as well as the eddy current back into Great Harbor are noted. Also, it is seen that the major portion of the dye does not reach shore but rather continues down Vineyard Sound.

C. Drogues and Water Samples

The horizontal sights positioning the drogues were plotted on C. and G.S. chart #260 with the time of the sights. From the time between sights and the



Figure 14. Westward Flow; 39 minutes after dye release

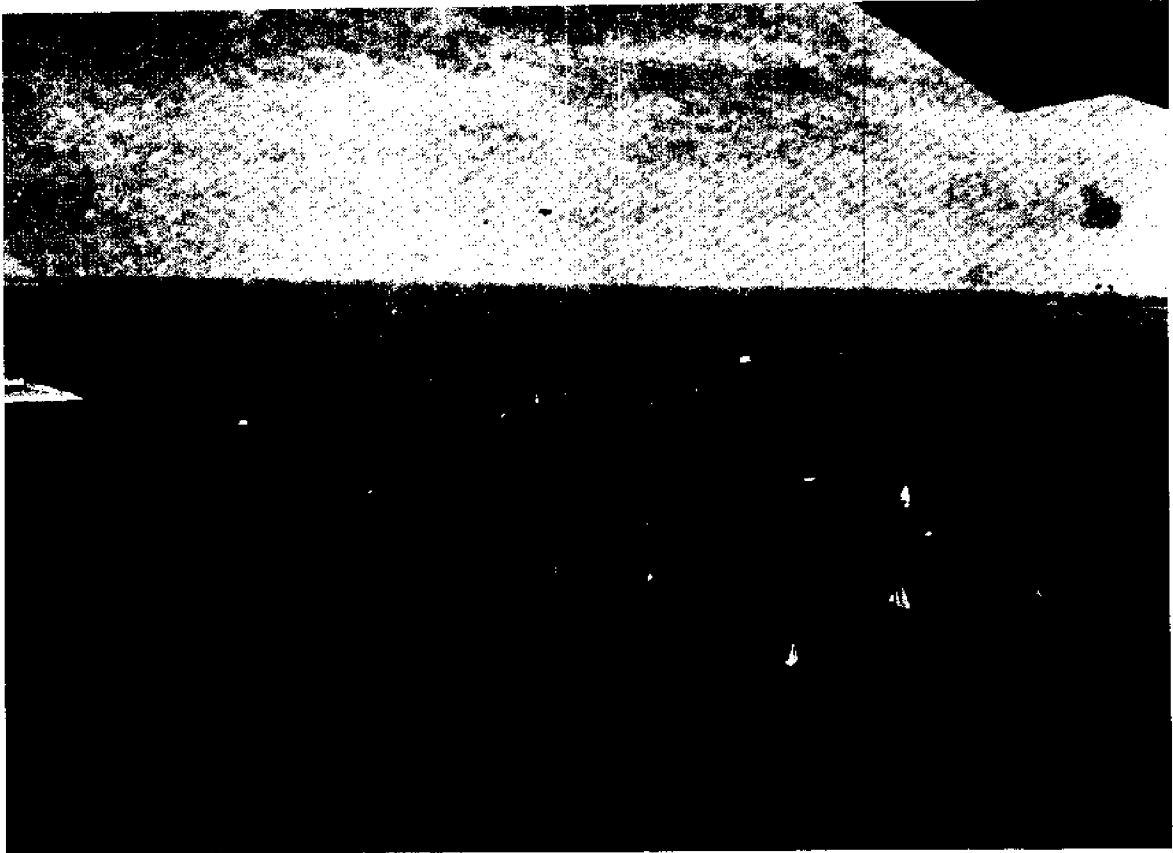


Figure 15. Westward Flow; 54 minutes after dye release

45' W

70° 40'

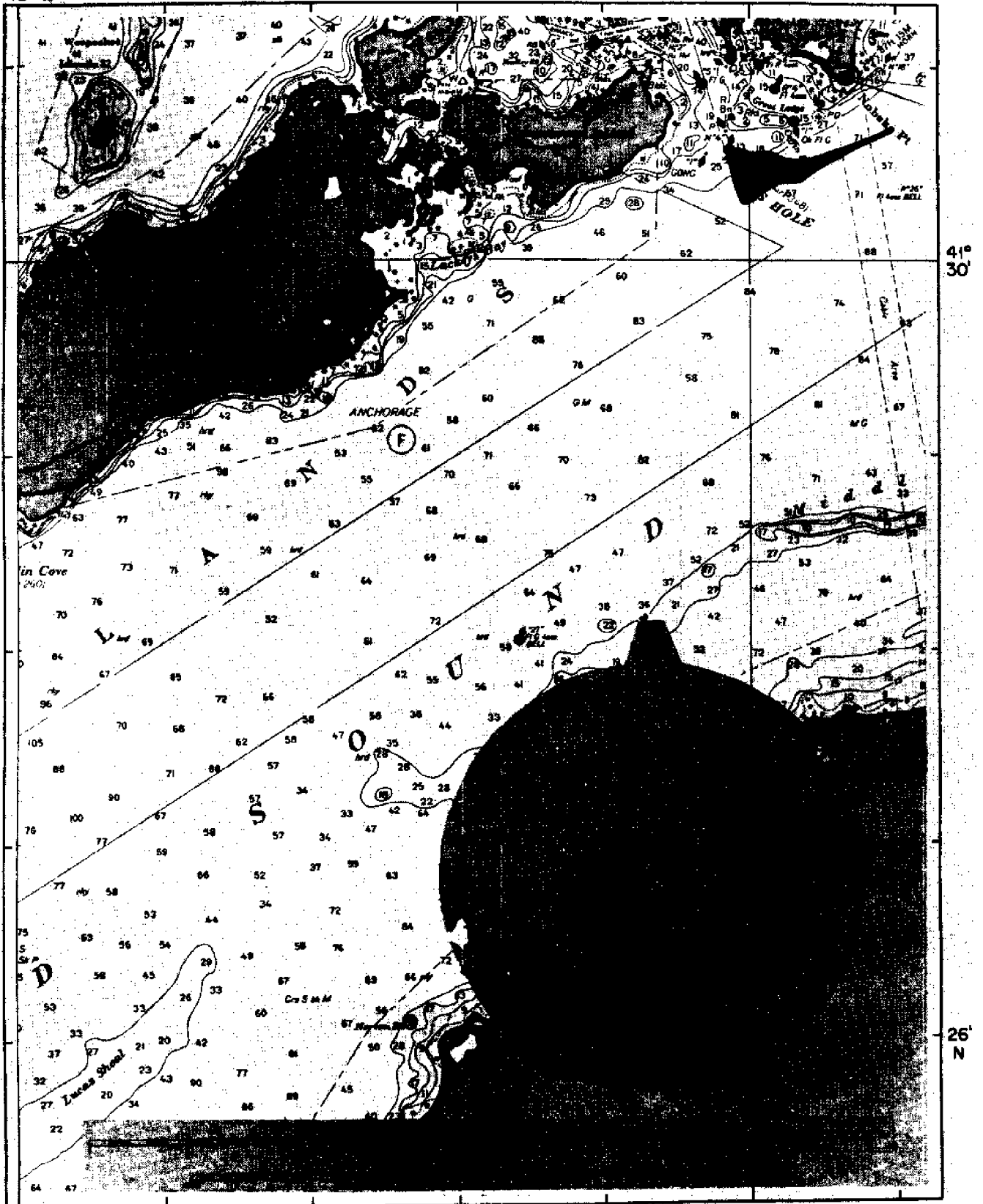


Figure 16. Westward Flow Distribution; 54 minutes after dye release

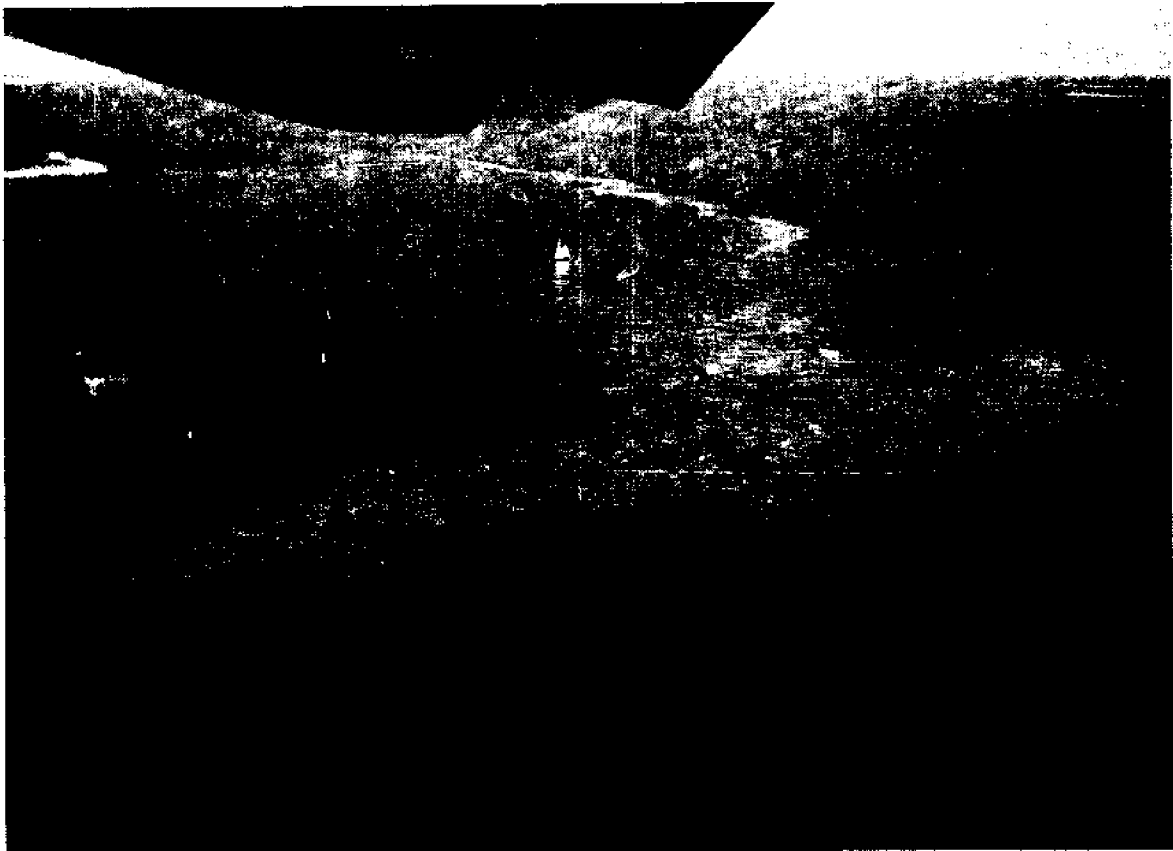


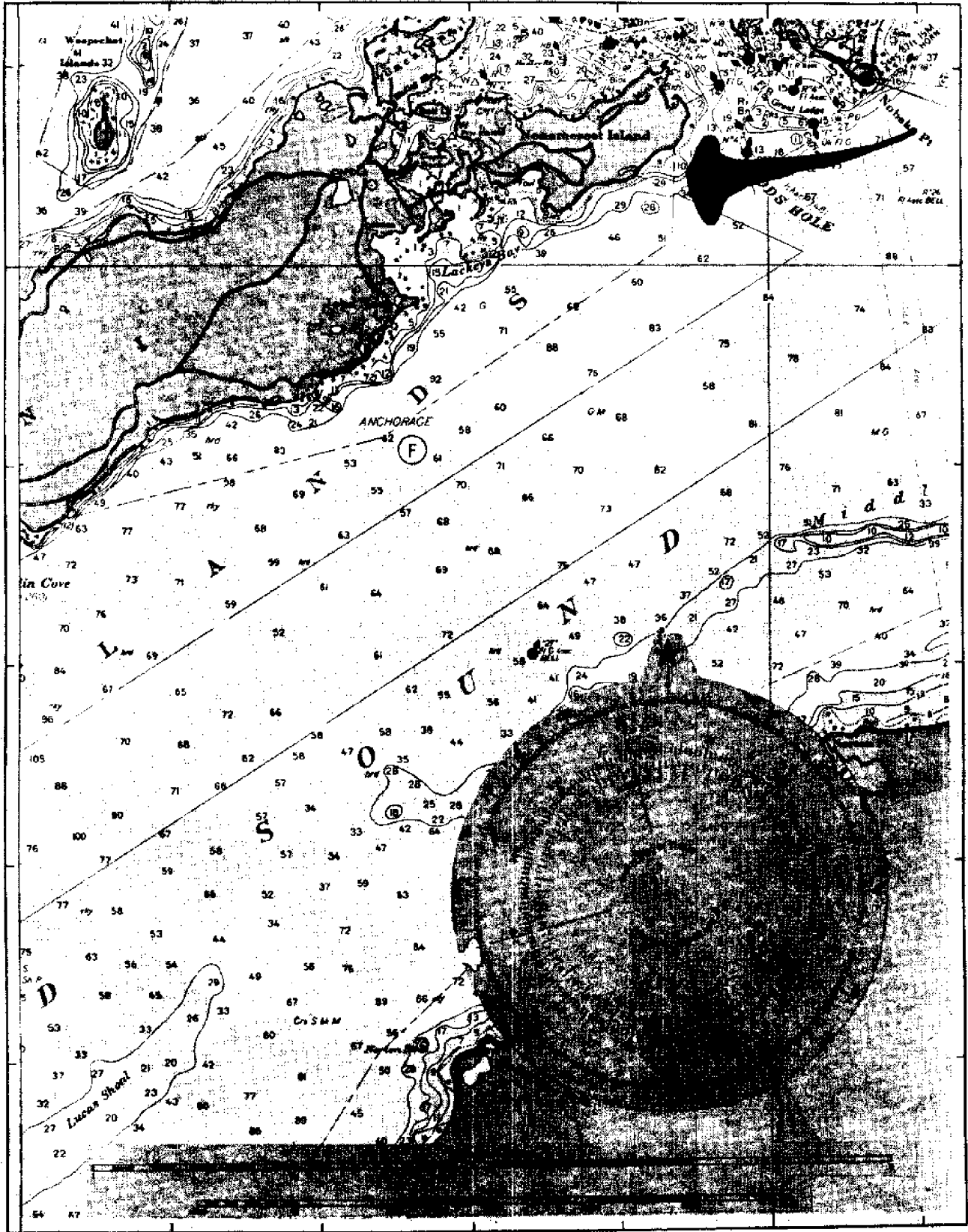
Figure 17. Westward Flow; 61 minutes after dye release



Figure 18. Westward Flow; 69 minutes after dye release

45° W

70° 40'



41° 30'

26° N

Figure 19. Westward Flow Distribution; 69 minutes after dye release



Figure 20. Westward Flow; 85 minutes after dye release



Figure 21. Westward Flow; 88 minutes after dye release

45' W

70° 40'

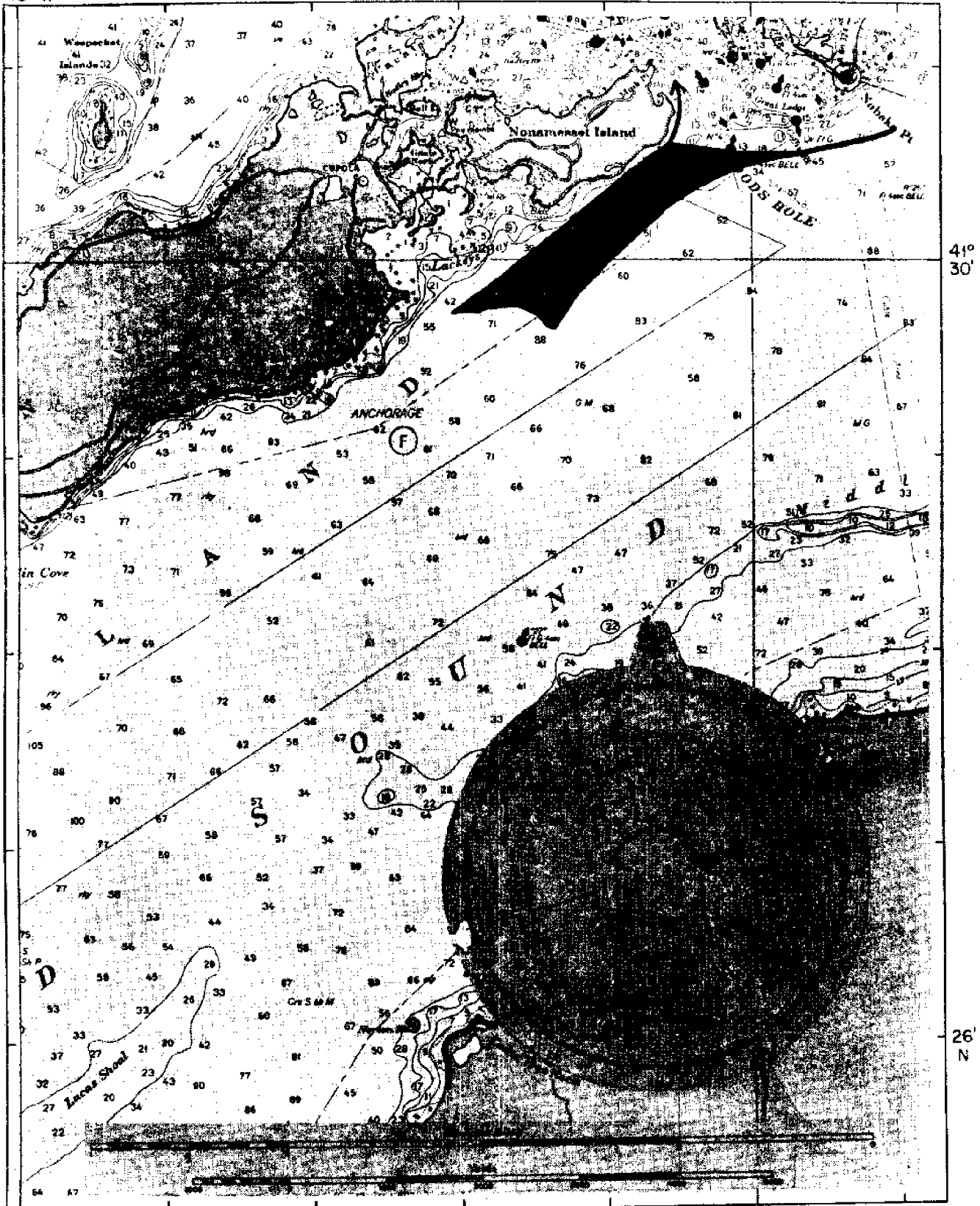


Figure 22. Overall Westward Flow Distribution

distance and direction measured on the chart, the velocity was obtained. The velocity, time, and position of the drogues are shown for the westward flow in Figure 23 and the eastward flow in Figure 10.

It was found that the velocity of the drogues increased as the tide moved farther into its cycle in both flows. In the eastward flow, the velocity was greater than in the westward flow, indicating a net eastward drift. In both cases, the drogues set at the different depths of 5, 10, 15, and 20 feet moved in a fairly close group. This can be seen by Figure 23 and Figure 10, as the circles represent the spread of the drogues at the time indicated.

The water samples were analyzed using a Turner Model 110 fluorometer. The Turner primary filters #110-814 and #110-822 together with the Turner #110-819 secondary filter were used giving a sensitivity threshold under .1 ppb. These kinds of results can be obtained since Rhodamine B dye is almost unique in being excited to fluorescence by green light of 5460 angstroms. The dye is relatively insensitive to destruction by oxidation and sunlight also. Standards to calibrate the fluorometer were made by weighing an amount of solid Rhodamine B dye on a Mettler Scale and dissolving the dye in a known quantity of water. Since the dye's fluorescence varies somewhat with temperature, the samples and the standards were kept at the same temperature throughout the testing procedure. The bottle number, time the sample was taken, and concentrations in ppb are listed in Tables 1 and 3. All the background samples taken before the experiments were found to be 0 ppb. The samples taken on the beaches the day after the eastward flow shown in Figure 9 were found to be 0 ppb. The NOBSKA took samples at various locations after the dye ran out on the eastward flow. The reading, time, and location of the samples are given in Table 2.

On the eastward flow the ASTERIAS stayed on the outer edge of the dye and thus the readings listed in Table 1 were fairly constant. The plot of the sample locations and time in Figure 11 shows the outer edge of the dye patch until sample number 5 and then shows the inner edge. Figure 10 shows the drogues and the inner edge of the dye. It can be seen from this figure that the dye generally follows the deeper water, but the onshore wind does cause the surface layer to move closer to shore.

On the westward flow, besides staying on the inner edge of the dye, four runs were made across the dye as shown in Figure 24. The readings obtained from these samples are listed in Table 2. The dye concentrations across the dye are plotted in Figure 25 and the dye concentration peak values of this graph are plotted with distance eastward away from Nobska Point in Figure 26. It can be seen from these graphs the dye concentration rapidly drops off the first three miles and then drops off more slowly from there.

From Figure 23 it can also be seen that the dye generally followed the path of the drogues, but again as in the eastward flow the dye was driven closer to shore probably by the wind.

45° W

70° 40'

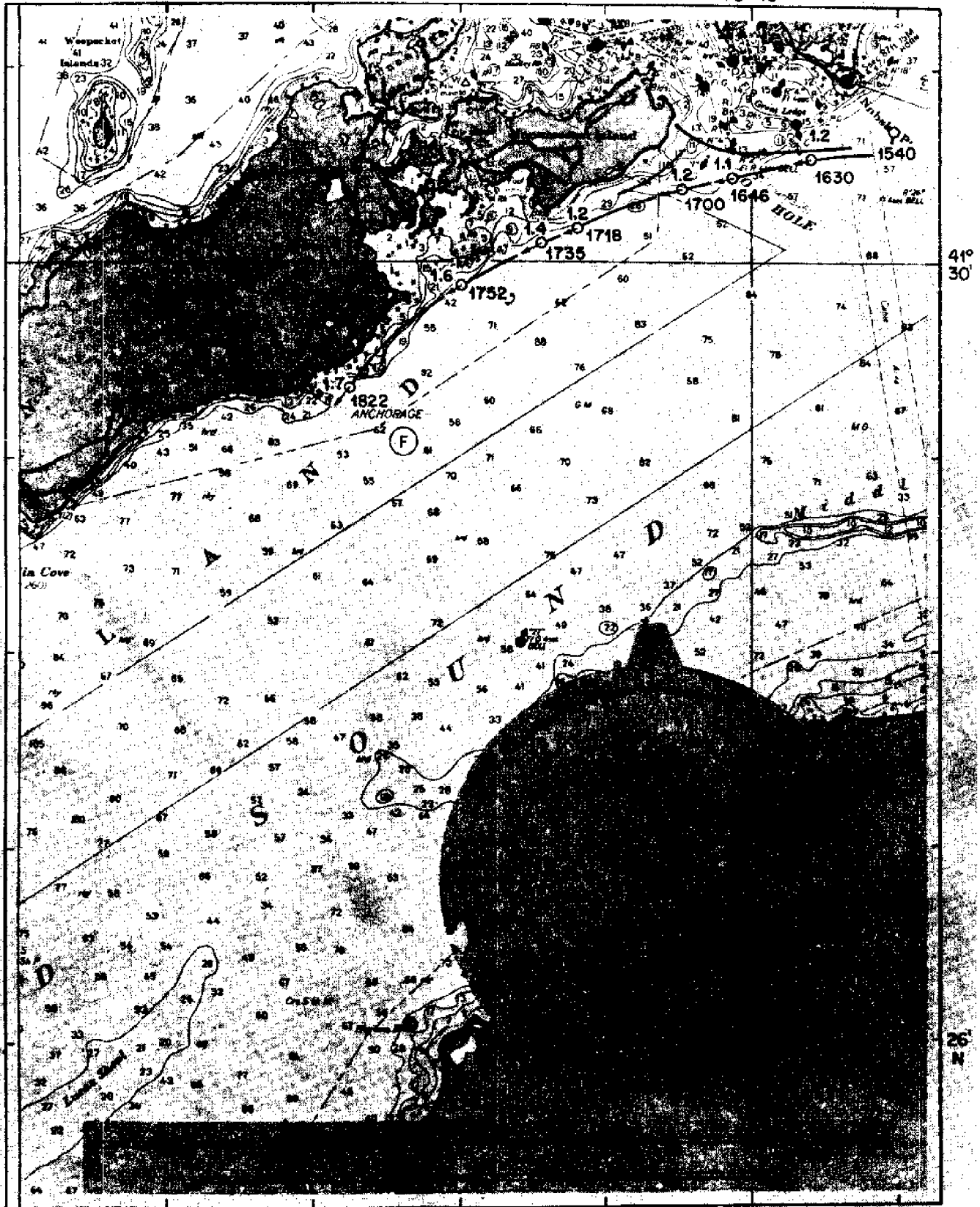


Figure 23. Westward Flow Dye

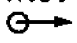
Kts.
 Drogues 
 Time

TABLE 1

Readings Obtained from Water Samples Taken by ASTERIAS on the
Eastward Flow

Time	Bottle Number	Parts Per Billion
0817	1	.2
0825	2	.4
0835	3	0
0845	4	1.1
0855	5	1.1
0905	6	1.2
0915	7	.5
0920	8	.3
0935	9	0
0945	10	.1
0955	11	0
1005	12	.4
1015	13	.8
1025	14	.3
1035	15	.1
1045	16	.4
1105	17	.1
1110	18	0
1120	19	.5
1130	20	.7
1140	21	.1
1150	22	.2

TABLE 2

Readings Obtained from Water Samples Taken by NOBSKA on the
Eastward Flow

Time	Location	Parts Per Billion
0856	At Outfall Site	0
0921	At Outfall Site	0
0923	At Outfall Site	.2
0933	At Outfall Site	1.8
0956	Buoy Red and Black Nun	0
1011	Buoy C "17"	0
1022	Buoy Bell "16"	0
1026	Falmouth Harbor Entrance	0
1034	Great Pond Entrance	0
1037	Green Pond Entrance	0
1125	Buoy FG "5"	0
1056	Buoy Bell "16"	.3
1104	Buoy Red and Black Nun	0
1115	Buoy Bell "26"	0

TABLE 2, continued:

Time	Bottle Number	Parts Per Billion
	139	0
	140	.2
	141	.5
	142	.1
	143	0
	144	0
	145	0
Run #3	146	0
	147	0
	148	0
	149	0
	150	.2
	151	0
	152	.2
	153	0
1815	154	0
	155	0
	156	.3
	157	0
	158	0
	159	0
	160	0
	161	.2
	162	0
	163	0
1829	164	0

TABLE 3

Readings Obtained from Water Samples Taken by ASTERIAS on the
Westward Flow

Time	Bottle Number	Parts Per Billion
1600	100	.2
1605	101	0
1613	102	over 12.6
1620	103	.2
	104	.4
	105	2.5
	106	1.5
Run #1	107	over 12.6
	108	over 12.6
	109	11.1
	110	over 12.6
1623	113	0
1645	114	2.0
1648	115	1.0
1655	116	.1
1740	117	0
1743	118	.2
1749	119	.2
1752	120	1.1
1755	121	0
1759	122	.3
1802	123	0
	124	.2
	125	.4
	126	1.1
	127	0
	128	.4
	129	.4
Run #2	130	.6
	131	.4
	132	.8
	133	.4
	134	.5
	135	.5
	136	.8
	137	.7
1807	138	.1

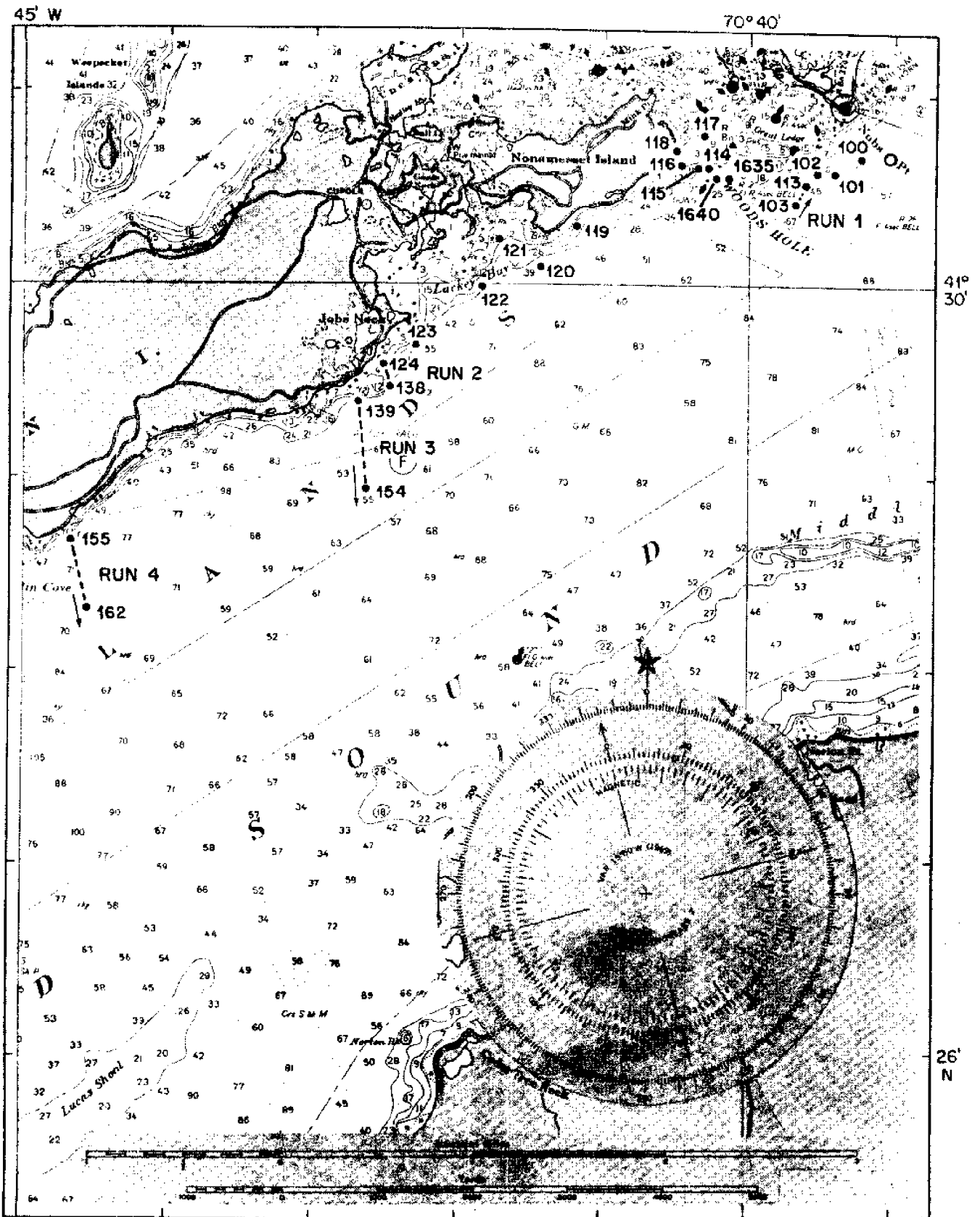


Figure 24. Westward Flow "Asterias" Water Sampling Points

Bottle No. ●

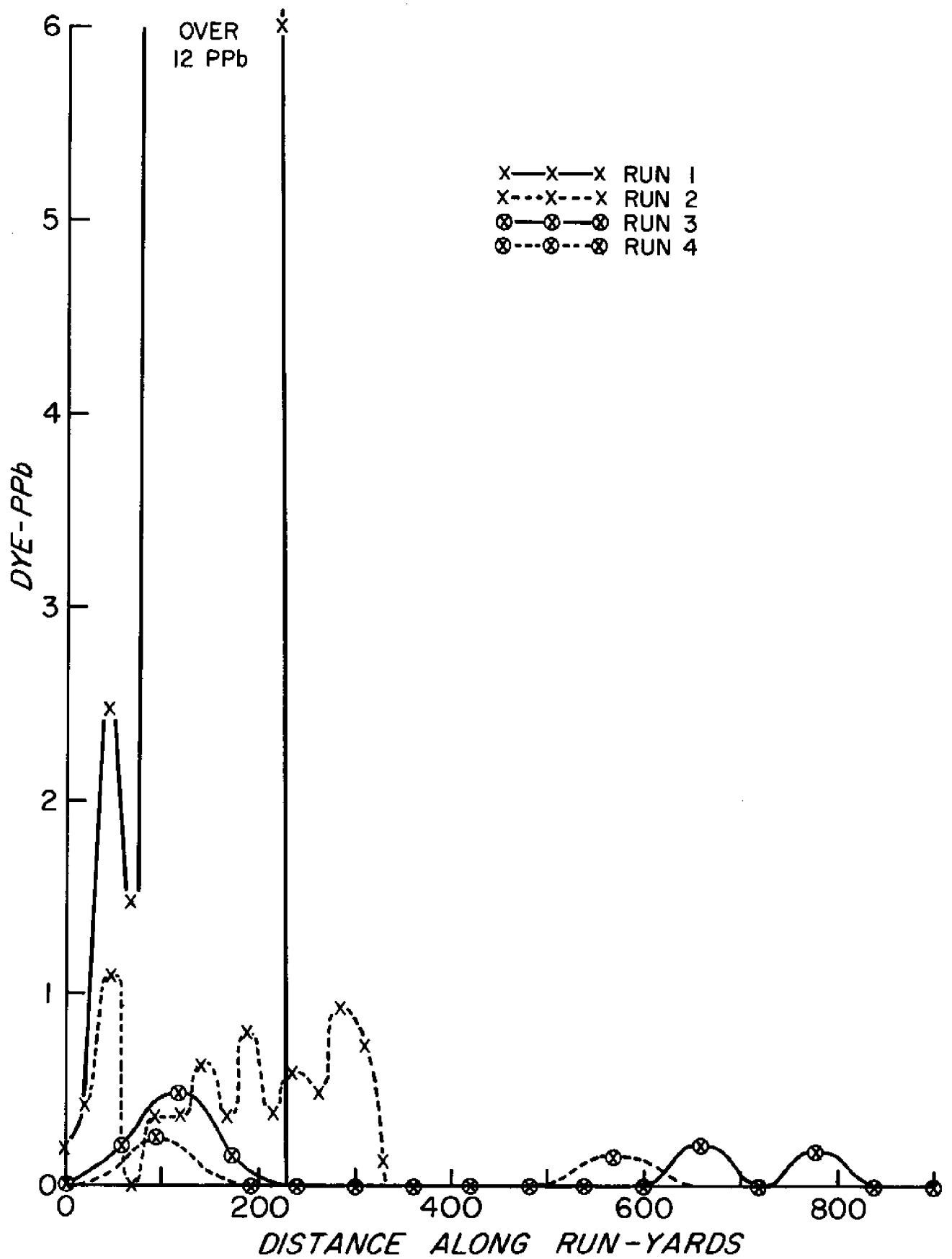


Figure 25. Dye Concentration (PPb) vs. Distance (yards) Along Run

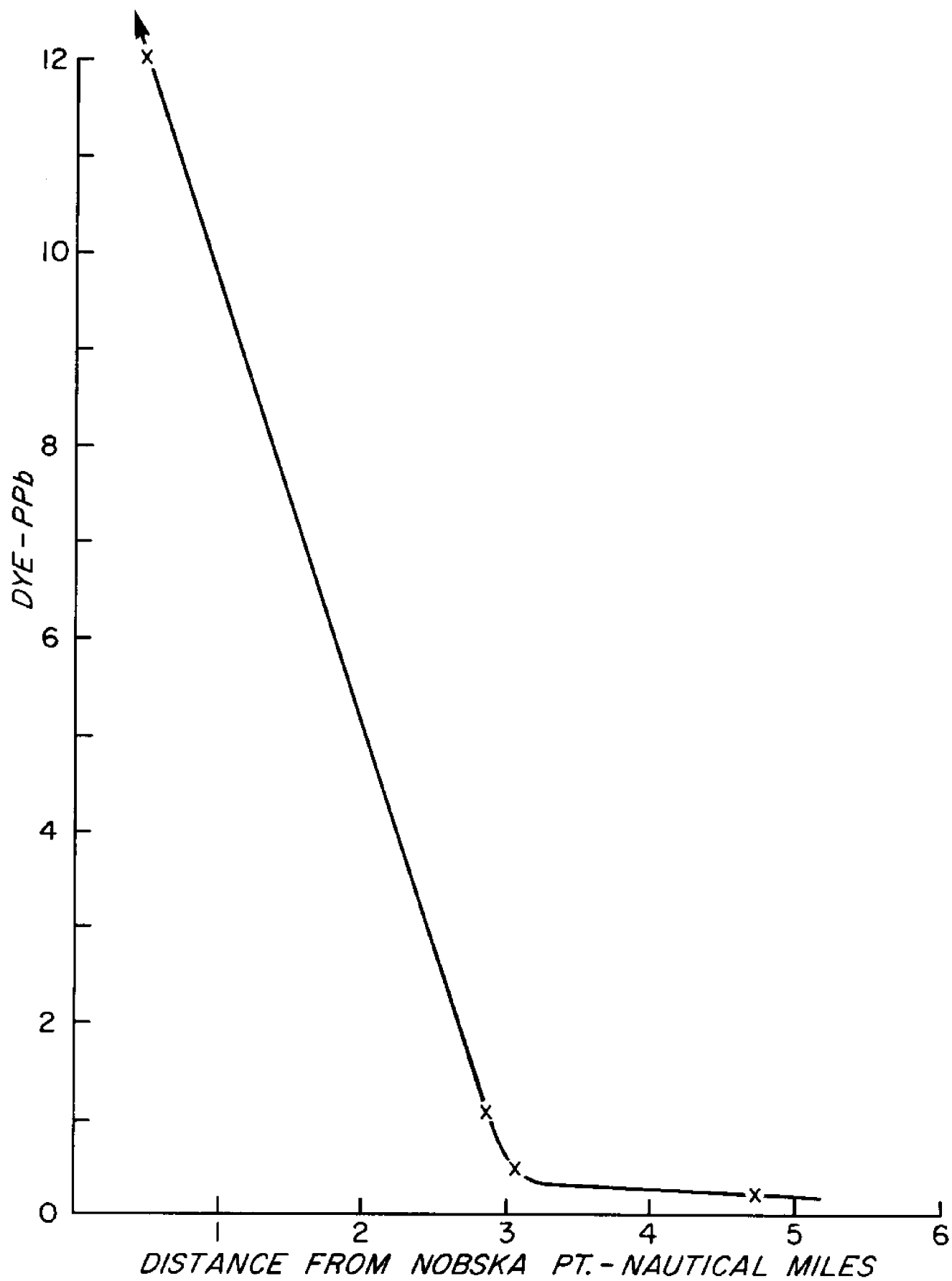


Figure 26. Dye Concentration (PPb) vs. Distance (Naut. miles) from Nobska Point

V. RESULTS

From the drogue sampling plots and the aerial photographs, it was found that the dye followed the general flow pattern of the drogues. However, on the eastward flow the dye split into two parts with most of it following the drogues while a smaller part came closer to shore. Generally, the surface water layers came closer to shore than did the deeper layers, which was probably caused by the on-shore wind. The closest the dye came to shore during the eastward flow was 0.7 nautical miles at the entrance to Falmouth Harbor. Since the drogues remained in a fairly tight group throughout the eastward flow, it can be said that the sub-surface water travels through Vineyard Sound essentially en masse in the area under study.

On the westward flow, portions of the dye moved closer to shore than did the drogues. A small section of the dye did in fact wash up on Nonamisset Island. The wind again was on-shore and probably was the cause of the surface layer moving in a different flow pattern from the sub-surface layers. An eddy current near Sheep Pen Harbor going back into Great Harbor was also observed from the plane.

VI. RECOMMENDATIONS

This project was intended to model surface water transport off Nobska Point and to obtain a correlation between surface flow and the flow of water down to a depth of 20 feet. It was not intended to indicate where sewage effluent will move en masse from an outfall off Nobska Point. It is recognized that the effluent plumes of some sewer outfalls reach the surface in significant concentrations, while the plumes of others do not by means of elaborate and costly diffusers at the discharge pipe. If the plume of the proposed Falmouth outfall were to reach the surface, our project shows where the water transporting the effluent would go under similar environmental conditions.

With this in mind, further dye studies could be made which would yield valuable information concerning the advisability of installing a sewer outfall off Nobska Point.

The dye could be released at various depths and a three dimensional profile of dye concentration could be made using a portable flow-through fluorometer and a tube taking in water at various depths. This could give a measure of the amount and extent of vertical mixing.

The dye could be prepared to match the effluent's expected density and temperature and then be pumped down and released at the 90 foot depth of the ocean outfall. Again a three dimensional profile of the dye's movement and dispersion could be obtained.

The dye could be released at the water's surface under adverse weather conditions, e.g. strong on-shore winds. The dye could be released at different times of the year during which the water transport might vary.

In all of the above, large scale releases involving several hundred gallons of dye instead of 22 gallons of dye would give a better simulation of an outfall which is expected to have a peak summertime discharge rate of 3.7 millions of gallons daily. In addition, dye could be released intermittently to produce point sources which would facilitate dispersion analysis.

REFERENCES

1. Bumpus, Dean F., Wright, W. Redwood, and Vaccaro, Ralph F. (1969), Considerations on a Sewer Outfall off Nobska Point, Woods Hole Oceanographic Institution Reference No. 69-87, December 1969.
2. Whitman and Howard, Inc., Engineers and Architects (1968), Report on Proposed Sewerage System for the Town of Falmouth, Mass., 89 Broad Street, Boston, Mass. 02110, December 1968.
3. Carter, H. H., Okubo, Akira (1965), A Study of the Physical Processes of Movement and Dispersion in the Cape Kennedy Area, Chesapeake Bay Institute Reference No. 65-2, March 1965.
4. Lamont Geological Observatory of Columbia University (1965) Symposium on Diffusion in Oceans and Fresh Waters, December 1965.
5. Costin, M., Davis, P., Gerard, R., Katz, B. (1963), Dye Diffusion Experiments in the New York Bight, Lamont Geological Observatory, Tech. Report No. CU-2-63, to the A.E.C., February 1963.

DETECTION OF SALT FINGERS
BY ECLIPSED SCHLIEREN TECHNIQUE

By

Carl S. Albro

T. Gray Curtis, Jr.

Ocean Engineering

W.H.O.I./M.I.T. Joint Program

Woods Hole Oceanographic Institution
Woods Hole, Massachusetts
September 4, 1970

ABSTRACT

Laboratory experiments were conducted to verify the feasibility of using a modified Schlieren refraction technique to detect salt fingers in the ocean. Light from a laser was expanded and passed through two Ronchi rulings and a tank of water between them. When there were sugar-salt fingers in the tank and they were translated across the laser beam, refraction within the fluid permitted light to pass the downstream ruling and register as a fluctuating intensity on a photoconductivity cell and subsequently as a fluctuating voltage record on a paper chart. When sugar-salt fingers were not present, the downstream ruling nearly eclipsed the light passed by the upstream ruling and no fluctuations were evident. Signal fluctuations apparently depend upon regions of short range alignment (coherence). Experimental results bear out the feasibility of the technique.

PREFACE

Salt fingers were investigated by the authors in an attempt to demonstrate the feasibility of development of an instrument to detect salt fingers in the ocean. The study was carried out to fulfill the summer studies requirements of the joint oceanographic engineering program which the Woods Hole Oceanographic Institution has with the Massachusetts Institute of Technology.

ACKNOWLEDGEMENT

The work done this summer was accomplished under the guidance of Dr. Albert J. Williams, 3rd and with the helpful suggestions of Dr. J. Stewart Turner, both of whom the authors would like to recognize at this point. The aid of Dr. William S. von Arx and A. T. Spencer is greatly appreciated in providing the necessary apparatus. To our fellow students we would like to extend thanks for useful criticism and suggestions.

TABLE OF CONTENTS

	Page
ABSTRACT	47
PREFACE	48
ACKNOWLEDGEMENT	49
TABLE OF CONTENTS	50
LIST OF ILLUSTRATIONS	51
1. INTRODUCTION	52
1.1 Background	52
1.2 Approach	53
2. EXPERIMENTAL INVESTIGATION	54
2.1 Salt Finger Model	54
2.2 Apparatus	54
2.2.1 Optical Subsystem	54
2.2.2 Electronic Subsystem	55
2.2.3 Mechanical Subsystem	55
2.3 Analysis	56
2.3.1 Signal	56
2.3.2 Sources of Error	58
2.4 Procedure	58
2.4.1 Alignment	58
2.4.2 Eclipsing Procedure	58
2.4.3 Sugar-Salt Finger Production	60
2.4.4 Tank Movement	60
2.5 Experiments and Results	61
3. CONCLUSIONS AND RECOMMENDATIONS	62
BIBLIOGRAPHY	64

LIST OF ILLUSTRATIONS

		Page
Figure 1	Shadowgraph View of Salt Fingers	52a
Figure 2	Density Interface	52b
Figure 3	Salt Fingers in Plan View	52c
Figure 4	Simplistic View of Salt Fingers	52d
Figure 5	Characteristics of Sea Water	53a
Figure 6	Schematic of Multi-slit Schlieren	53b
Figure 7	Optical Subsystem	54a
Figure 8	Ronchi Ruling	55a
Figure 9	Electronic Subsystem	55b
Figure 10	Photoconductivity Cell	55c
Figure 11	Schematic of Sensor Circuit	55d
Figure 12	Sanborn Recorder	55e
Figure 13	Mechanical Subsystem	55f
Figure 14	Signal Modulation by Coherence	57a
Figure 15	Transition from Fresnel to Fraunhofer Diffraction Patterns with Parallel Incident Light	58a
Figure 16	Knife Edge Diffraction	58b
Figure 17	Beam Expander	59a
Figure 18	Eclipsed Rulings	60a
Figure 19	Pouring Board	60b
Figure 20	Persistence of Sugar-Salt Fingers Arrays	61a
Figure 21	Typical Example of a Recorded Run	61b
Figure 22	Age of Sugar-Salt Fingers Versus Distance Travelled per Cycle	61c
Figure 23	Voltage Record of 103 Hours Old Sugar-Salt Fingers	61d
Figure 24	Array of Photoconductivity Cells	63a
Table 1	Subsystems and Components	56
Table 2	Tabulation of Age of Sugar-Salt Fingers Versus Distance Travelled per Cycle	62

1. INTRODUCTION

1.1 Background

Salt fingers are cells of convecting water. Adjacent cells carry fluid in alternate vertical directions. To date, salt fingers have not been detected in the ocean. Figure 1 is an elevation shadowgraph view of salt fingers in a small tank in Dr. Turner's laboratory.

Generation of cells of convection results from a force imbalance produced by variations in density induced by diffusion of heat in the moving fluid. Consider a layer of water of temperature T and salinity S which is overlain by a hotter and more saline layer of temperature $T+\Delta T$ and salinity $S+\Delta S$. The original layers are stable because the density of the upper layer, ρ , is less than that of the lower layer, $\rho + \Delta\rho$. See Figure 2.

If a particle of water mass is advected vertically, it warms (or cools) isentropically and consequently becomes less (or more) dense. The temperature diffuses faster than the salt by several orders of magnitude and it is therefore possible for a moving particle to find itself in a destabilizing neighborhood. A descending particle from the top layer will cool and being more saline will be denser than its surroundings and continue descending. According to Dr. Melvin Stern, horizontal shear above and below the salt fingers will control the height to which they can rise. Besides the height, the spatial configuration appears to be controlled by the circulation above and below salt fingers. Paul Linden contributed Figure 3 which shows salt fingers in plan view subjected to varying shear stress in the horizontal plane across the page. View (a) indicates what a salt finger pattern looks like without a horizontal shear. Dr. Stern's analysis assumes a sinusoidal variation of vertical velocity, salinity, and temperature in the horizontal plane. View (b) is a plan view of salt fingers in transition to view (c) under a relatively high shear. Salt fingers apparently are transformed from a columnar lattice to a plate-like structure. In any case there appear to be regions of considerable coherence.

If salt fingers exist in the ocean they would serve as a fundamental mechanism by which salt is convected vertically. For this reason detection of their presence is of great interest to the physical oceanographers. The size of salt fingers and the scale of the vertical velocity is diminutive; this complicates the problem of detection and makes measurements of the associated velocity field presently unattainable. Detection of a phenomena requires instrumentation several orders of magnitude less sophisticated than measuring equipment.

Just how large are salt fingers? Consider the simplistic view of salt fingers in Figure 4. There appears to be a uniform temperature gradient across the developing interface between the two layers of fluid. The change in salinity appears to occur directly above and below the salt fingers, but not in them. Dr. Turner has experimentally determined that the ratio of fluxes of heat to salinity $F_H/F_S \sim 0.5$. If we assume a change in density due to salinity $\Delta S \sim 0.10\%$, then the change in density due to temperature is given by $\Delta\rho_T \sim \frac{1}{2}(\Delta S)$.

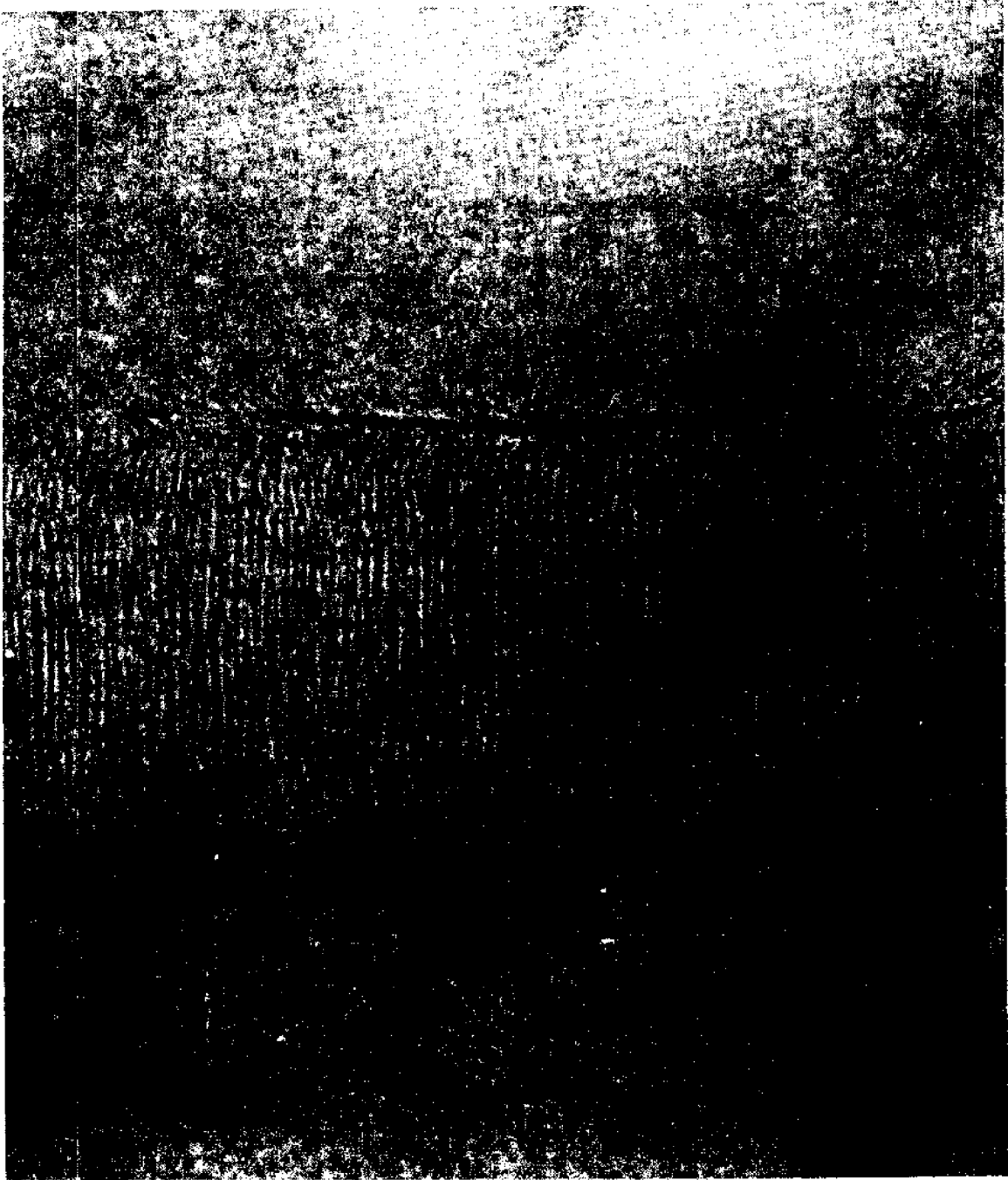


Figure 1. Shadowgraph View of Salt Fingers

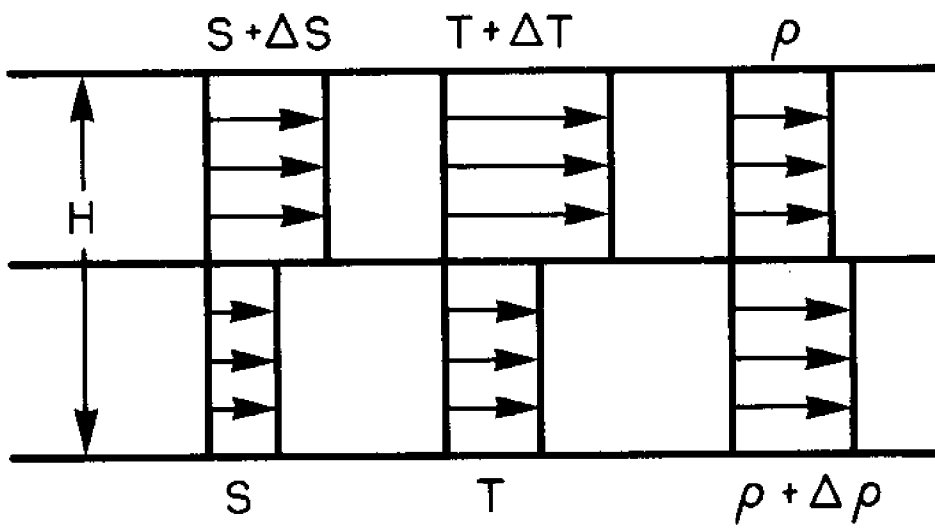
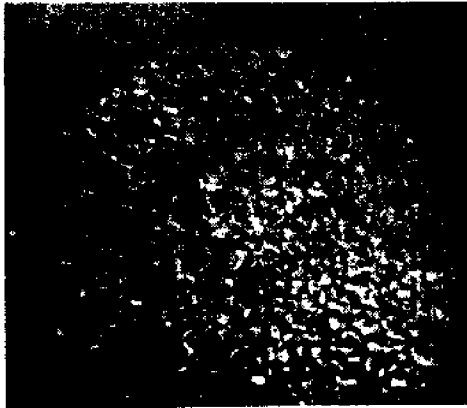
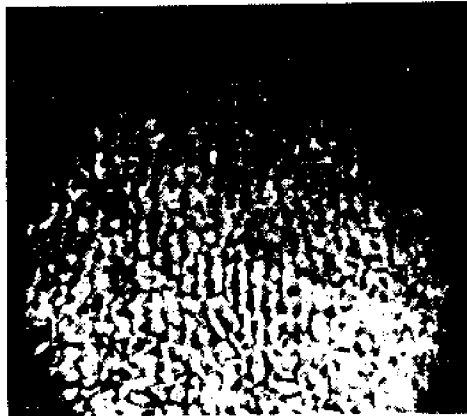


Figure 2. Density Interface



a. NO SHEAR
FLOW



b. SLIGHT SHEAR
FLOW



c. STRONG
SHEAR
FLOW

Figure 3. Salt Fingers (In plain view) A. No Shear Flow
B. Slight Shear Flow C. Strong Shear Flow

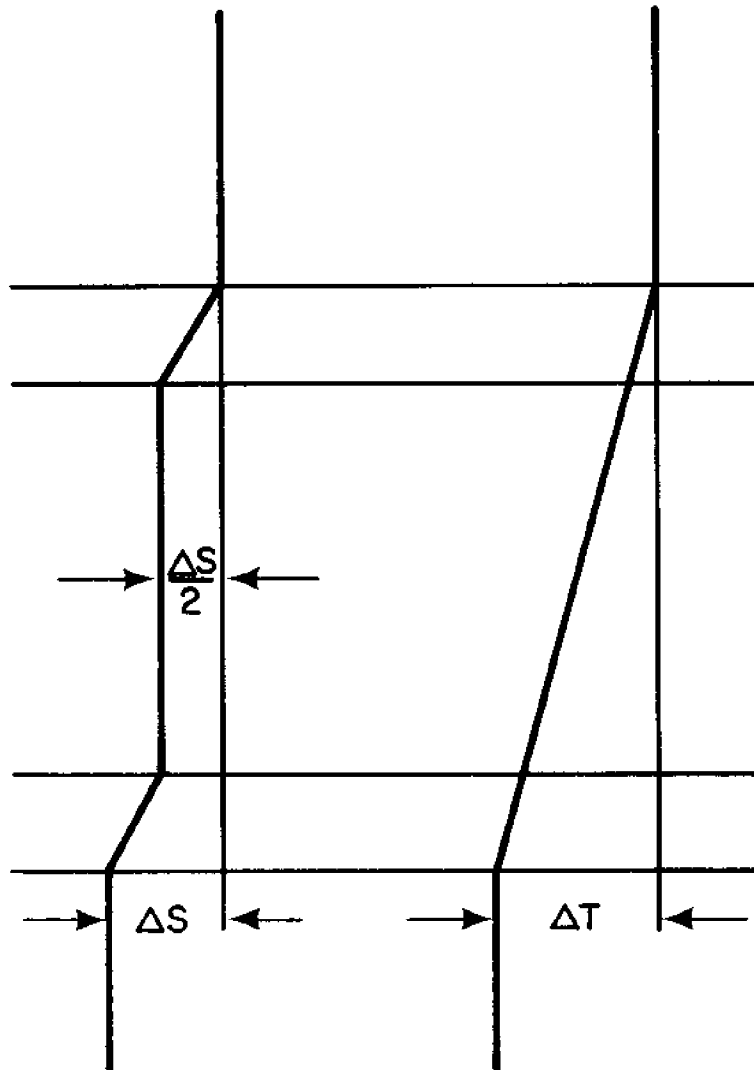


Figure 4. Simplistic View of Salt Fingers

The change in density due to salinity across the salt fingers is only $\frac{1}{2}$ the total change. Therefore, $\Delta\rho \sim \frac{1}{2}(0.05) = 0.025\%$

converting to change of temperature in degrees Centigrade, $\Delta T_e \sim 10^4 \Delta\rho$ or $\Delta T_e \sim 0.25^\circ\text{C}$. An estimate can be made of the order of magnitude of the vertical velocity in salt fingers which might be present in the ocean. Dr. Turner believes that velocity $\sim 10^{-4}$ meter per second. This would correspond to a salt finger cell one centimeter on an edge and roughly one meter high.

1.2 Approach

The detection of salt fingers depends upon the reception of a signal modified by some phenomenological process indicative of salt fingers. It has been shown that the direct parameters: salinity, temperature and velocity are quite small. Alternative approaches to detection would rely upon the effect of changes in the indirect parameters, such as: speed of energy propagation, electrical conductivity, refractive indices, and polarization. To illustrate, according to Wilson the speed of sound, c , is given in meters per second by

$$c = 1410 + 4.21T = 0.037T^2 + 1.14A + 0.018D$$

where T is temperature in centigrade
 S is salinity in parts per thousand
and D is depth in meters.

The variation of c with variations of both T and S are positive for reasonable temperatures. $\Delta c = \frac{\partial c}{\partial T} \Delta T + \frac{\partial c}{\partial S} \Delta S$

For $T=15^\circ\text{C}$, $\Delta T=.25^\circ\text{C}$, $\Delta S=.10\%$

$$\frac{\partial c}{\partial T} \Delta T = (4.21 - 0.074T) \Delta T \sim 3.1 \text{ ft/sec}$$

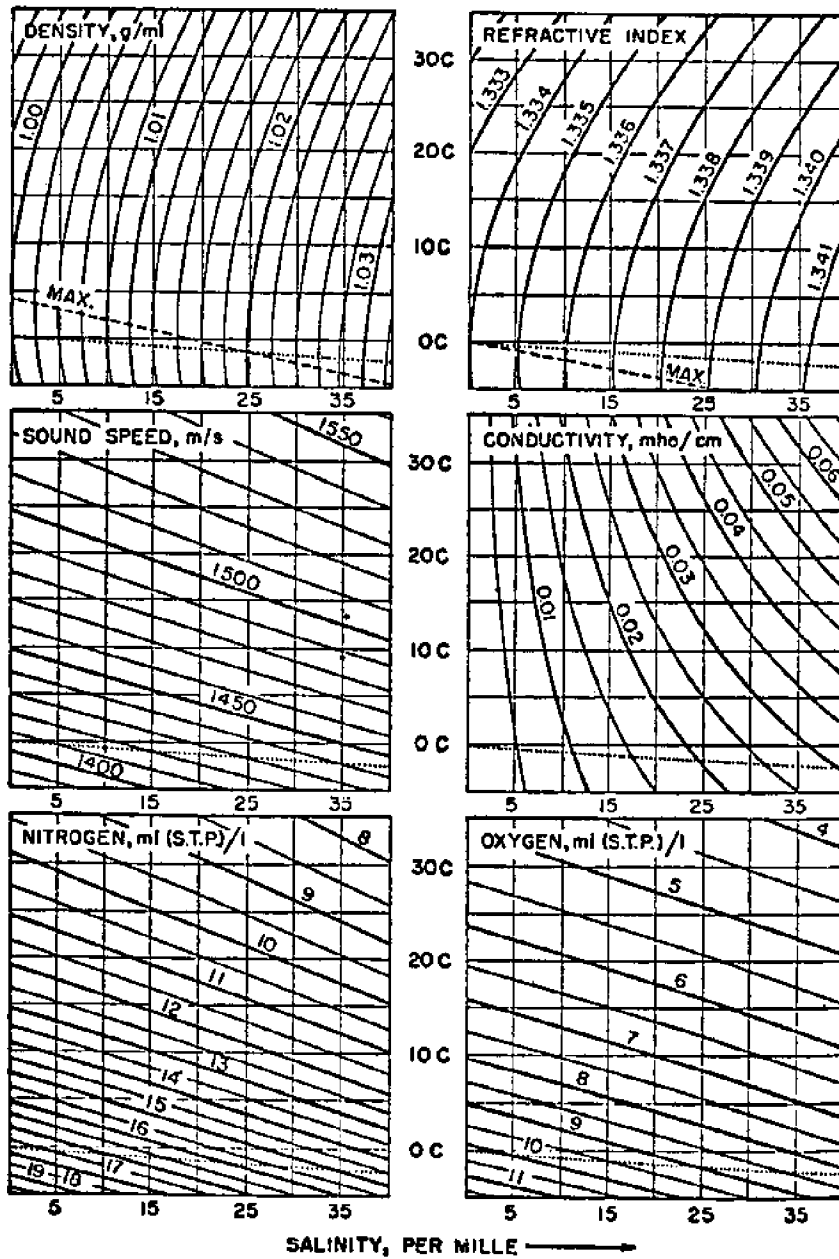
$$\frac{\partial c}{\partial S} \Delta S = 1.14 \Delta S \sim 0.3 \text{ ft/sec}$$

$$\Delta c \sim 3.4 \text{ ft/sec}$$

The variation of refractive index, n , increases with S and decreases with T as indicated in Figure 5. For the values given above when computing variation in speed of sound, $\Delta n \sim 5 \times 10^{-6}$. Such small variations in both direct and indirect parameters suggests that individual salt fingers will be difficult to measure, however, their coherent nature can be utilized to insure detection.

Salt fingers are assumed to be coherent and symmetrical at least in the short range. Energy radiated horizontally through salt fingers will therefore be diffracted, refracted and scattered in a plane normal to the axis of the salt fingers. Over a large region of salt fingers this will result in a stochastic fluctuation of signal which will be statistically detectable. Acoustic and optical forms were considered. It is believed that acoustic waves of the appropriate wavelength will be diffracted and produce an acoustic form of x-ray powder pattern. An optical detection system was investigated because of the relative ease of experimental verification of coherency and signal within the time limits.

A variant form of Schlieren was used. Collimated light was passed through a Ronchi Ruling, the image of which was eclipsed by a second ruling. When salt fingers were present between the two rulings the image from the first ruling was refracted and not totally eclipsed by the second ruling. The passed signal was received on a photoconductive cell and amplified and recorded on a Sanborn paper chart recorder. This technique is illustrated schematically in Figure 6.



(From the Am. Inst. of Physics Handbook)

Figure 5. Characteristics of Sea Water

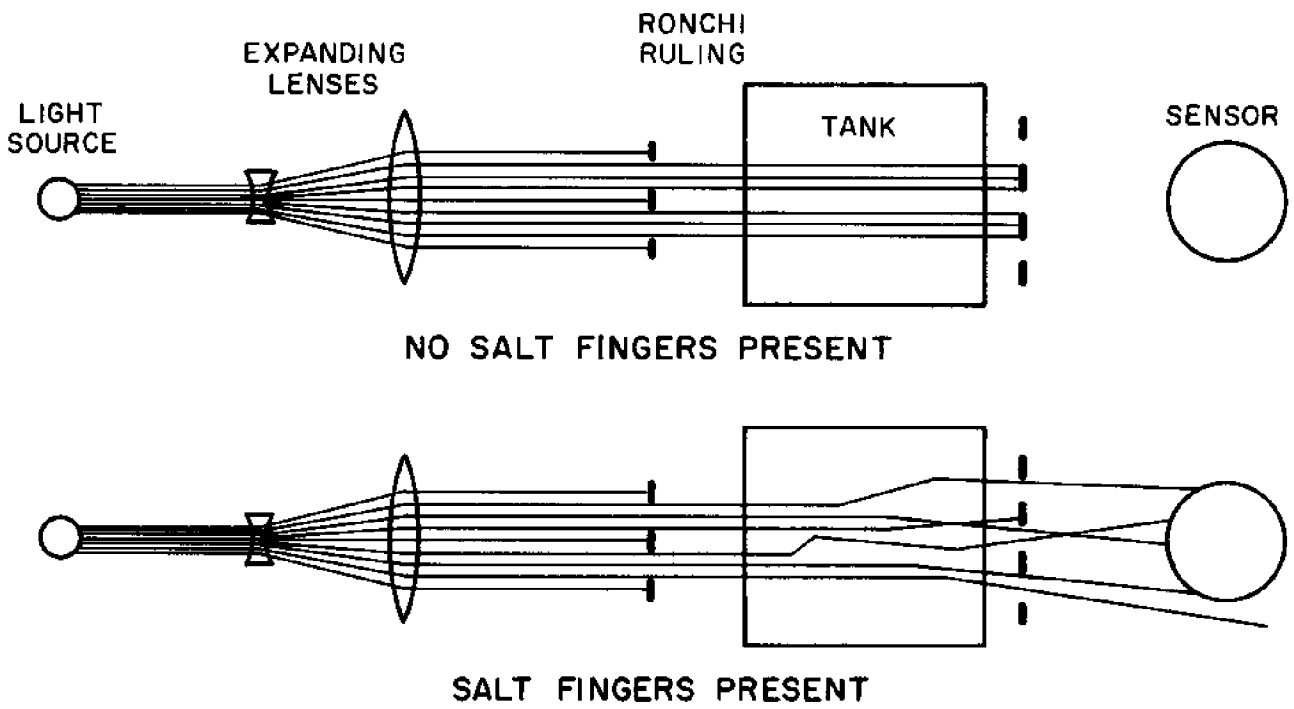


Figure 6. Schematic of Multislit Schlieren

2. EXPERIMENTAL INVESTIGATION

2.1 Salt Finger Model

Although salt fingers can be produced in the laboratory, their lifetime is limited by their fragile nature. Perturbing laboratory conditions such as evaporation and differential heating and cooling tends to establish circulations which disrupt the delicate imbalance of salt finger stratifications. Therefore different solutions are used to simulate the cellular convection of salt fingers.

The diffusivity of sugar ($D=0.5 \cdot 10^{-5} \text{cm}^2/\text{sec.}$) is sufficiently weaker than that of salt ($D=1.5 \cdot 10^{-5} \text{cm}^2/\text{sec.}$) that the hydrodynamics of salt fingers can be modeled by a saline solution overlain by a sugar solution of appropriate density. There are three basic advantages of sugar-salt fingers. 1.) Because the ratio of diffusivities of sugar to salt is 1/3 and not 1/100, the ratio of diffusivity of salt to heat, the time scale of sugar-salt finger development is much larger than that of salt finger aging. 2.) Whereas salt fingers are sensitive to cooling at the tank walls and at the surface and are readily destroyed by thermal effects, sugar-salt fingers are not greatly influenced by them. 3.) A wide range of solution densities can be accurately produced, and consequently, stratification and stability can be readily controlled. As the sugar-salt fingers mature, the transport drives the stratification towards a weaker gradient and causes the fingers to grow in height and increase in cross-sectional area in a manner similar to heat-salt fingers.

2.2 Apparatus

The laboratory apparatus is a bread-board version of that which might be used in the sea. It consists of three fundamental subsystems:

- 1). Optical Subsystem - The optical subsystem controls the visible electro-magnetic radiation.
- 2). Electronic Subsystem - The electronic subsystem transduces and records the modulated signal.
- 3). Mechanical Subsystem - The mechanical subsystem translates the tank of salt fingers and thereby provides the mechanism by which various regions of water are examined.

Table I lists the various components of the different subsystems.

2.2.1 Optical Subsystem (Refer to Figure 7)

The optical subsystem produces monochromatic light with a helium-neon gas laser ($\lambda=6328 \text{ \AA}$). The laser beam is diffused with a beam expander consisting of a double concave and double convex lens. The beam is directed along an optical bench holding two eclipsing Ronchi rulings. Holders for most of the lighter weight components were threaded aluminum posts equipped with retaining nuts for adjustment of vertical position. One of the Ronchi rulings was mounted in a microscope stage secured to the optical bench. The microscope stage permits accurate translation and rotation of one ruling relative to the other, and therefore, eclipsing of one ruling image by the other ruling.

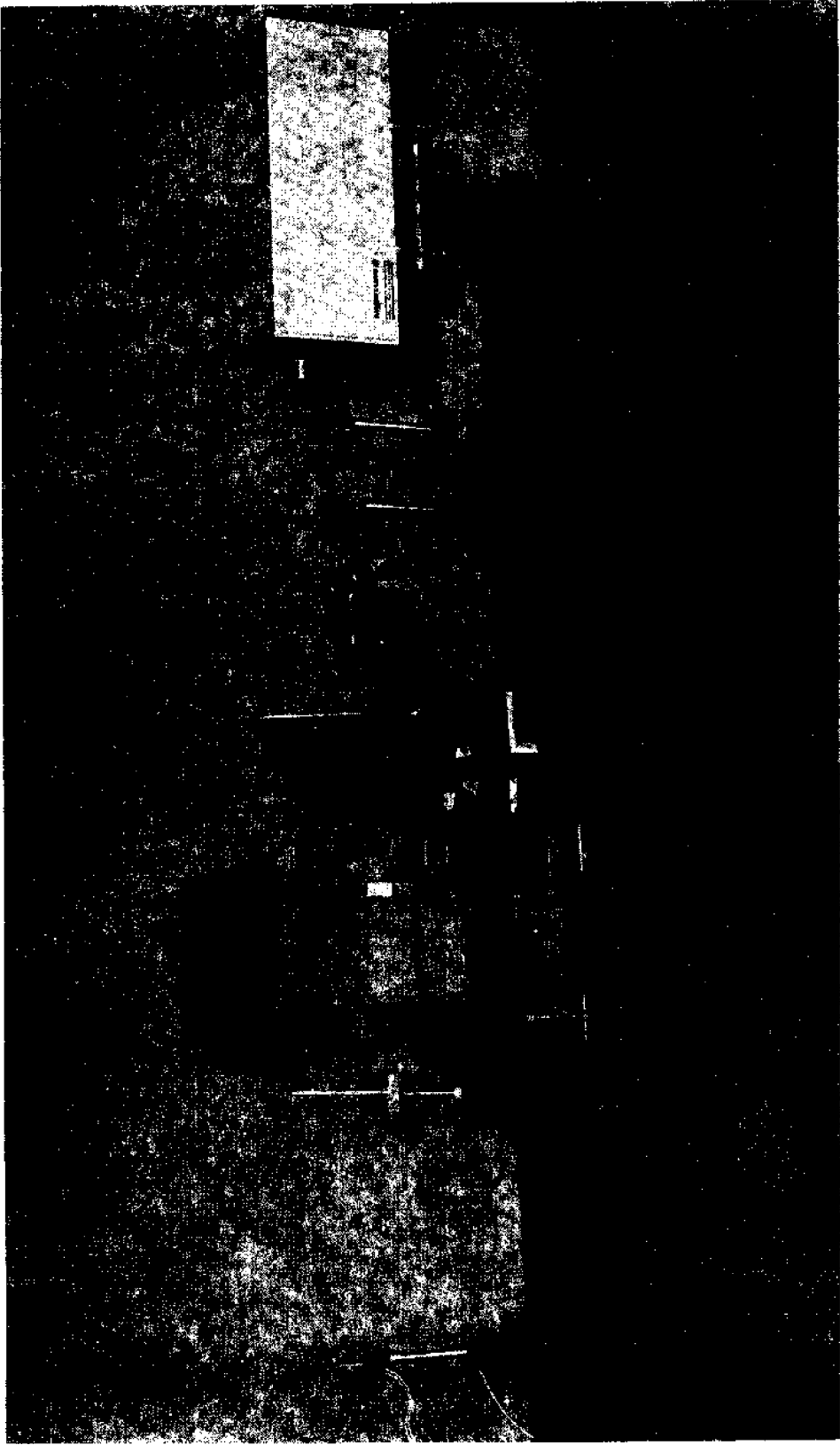


Figure 7. Optical Subsystem

The Ronchi rulings were constructed from a negative and a contact positive transparency of an inked drawing of 20 lines, each $\frac{1}{2}$ inch wide by ten inches long and separated one from another by $\frac{1}{2}$ inch. In the photographic processing, the rulings were reduced to a 2"x2" image of ten lines per inch, each line being reduced to 0.05 inch width. The transparencies were mounted between lantern slide glass and secured in a thin aluminum frame. Refer to Figure 8.

2.2.2 Electronic Subsystem (Refer to Figure 9)

The light intensity incident upon the photoconductivity cell, shown in Figure 10, must be transduced into an appropriate electrical signal. In order to minimize the fluctuations in the ambient background signal, it was decided to conduct investigations in a darkened room. The photoconductivity cell resistance varied over a wide range; in a darkened room the cell used had a resistance on the order of megohms. The circuit design, indicated schematically in Figure 11, attempts to maximize the sensitivity of the recorder voltage to changes in light intensity at the photoconductivity cell and filter out 60 Hz alternating current fluctuations which occur in the laser beam. Appendix A presents the circuit design calculations. The sensor circuit increased the signal gain from the photoconductivity cell so that it could be recorded on a Sanborn, hot pen, paper chart, recorder. The recorder is shown in Figure 12.

If the instrument is to be developed for use in the ocean, an ambient light intensity sensor should be included in the sensor circuit design. The resistance of such a sensor, used as R_1 , would maximize the sensitivity of the circuit.

2.2.3 Mechanical Subsystem (Refer to Figure 13)

Salt finger detection is contingent upon the spatial regularity of the fingers and the consequent regularity in variation of signal strength. A mechanism or method must be employed to translate the laser beam through the salt fingers. In the laboratory, this function was achieved by moving the tank of salt fingers by placing them on a lathe table which could be advanced by a feed screw driven by a variable speed DC motor. In the ocean, it is assumed that the instrument would gradually rise or sink. Unable to remain absolutely stationary, the beam may naturally move through various regions of salt fingers. If this assumption is not appropriate, a method for instrument movement will have to be incorporated into the instrument design.

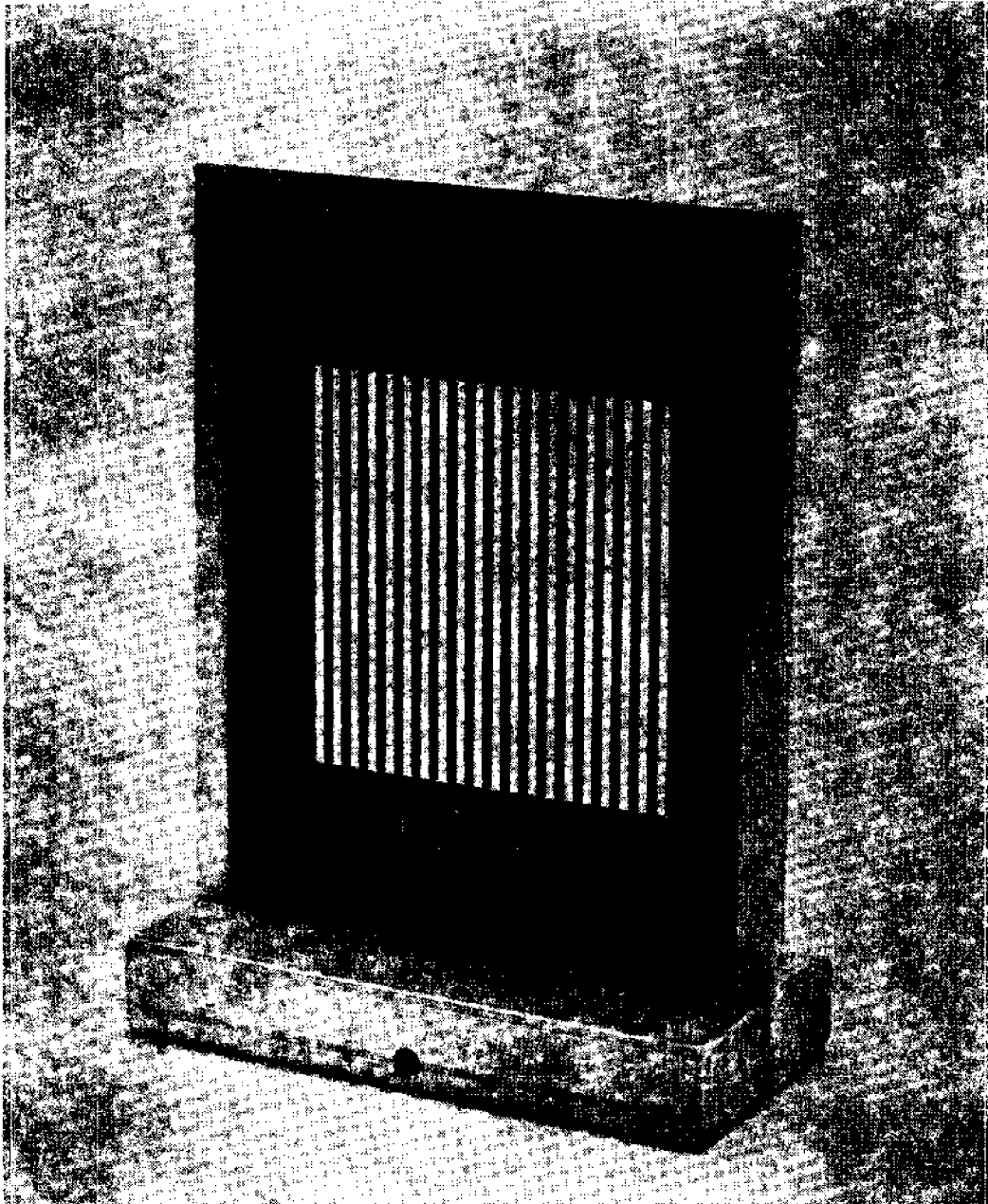


Figure 8. Ronchi Ruling

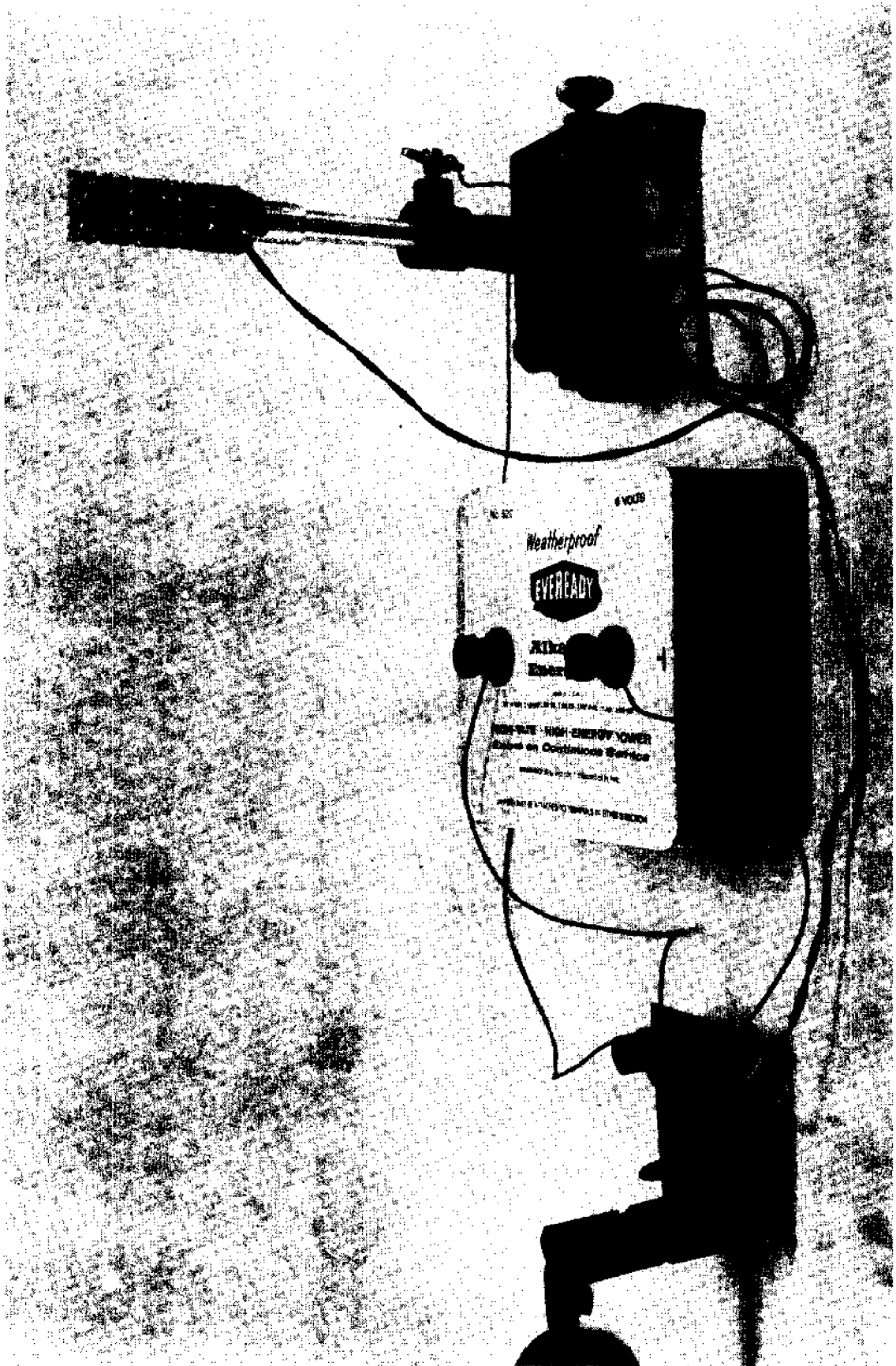


Figure 9. Electronic Subsystem

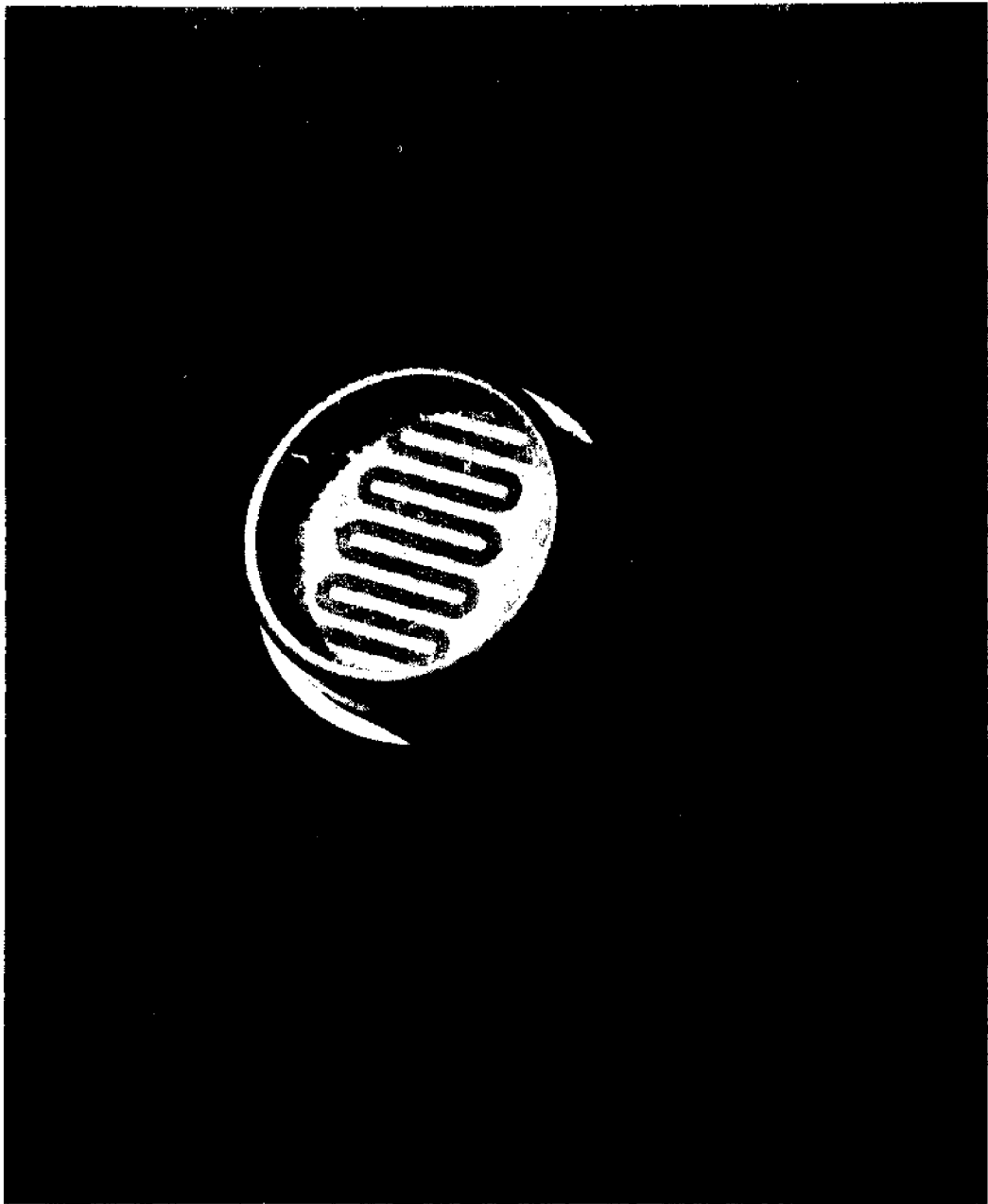


Figure 10. Photoconductivity Cell

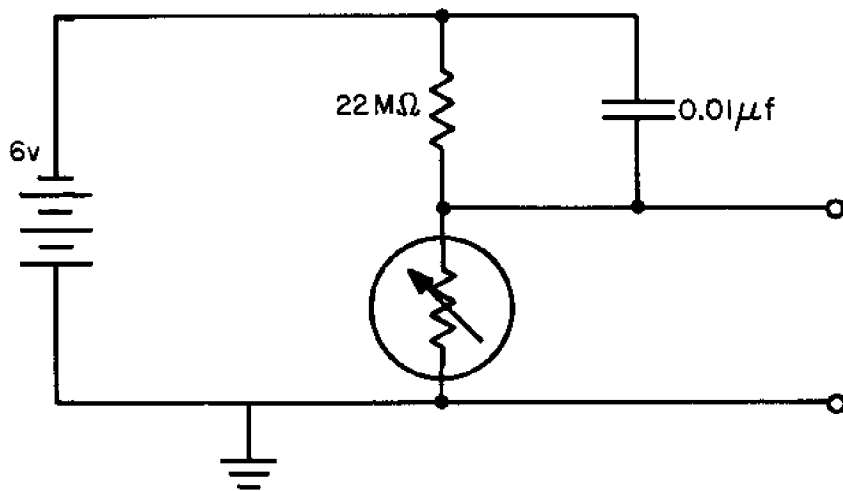


Figure 11. Schematic of Sensor Circuit

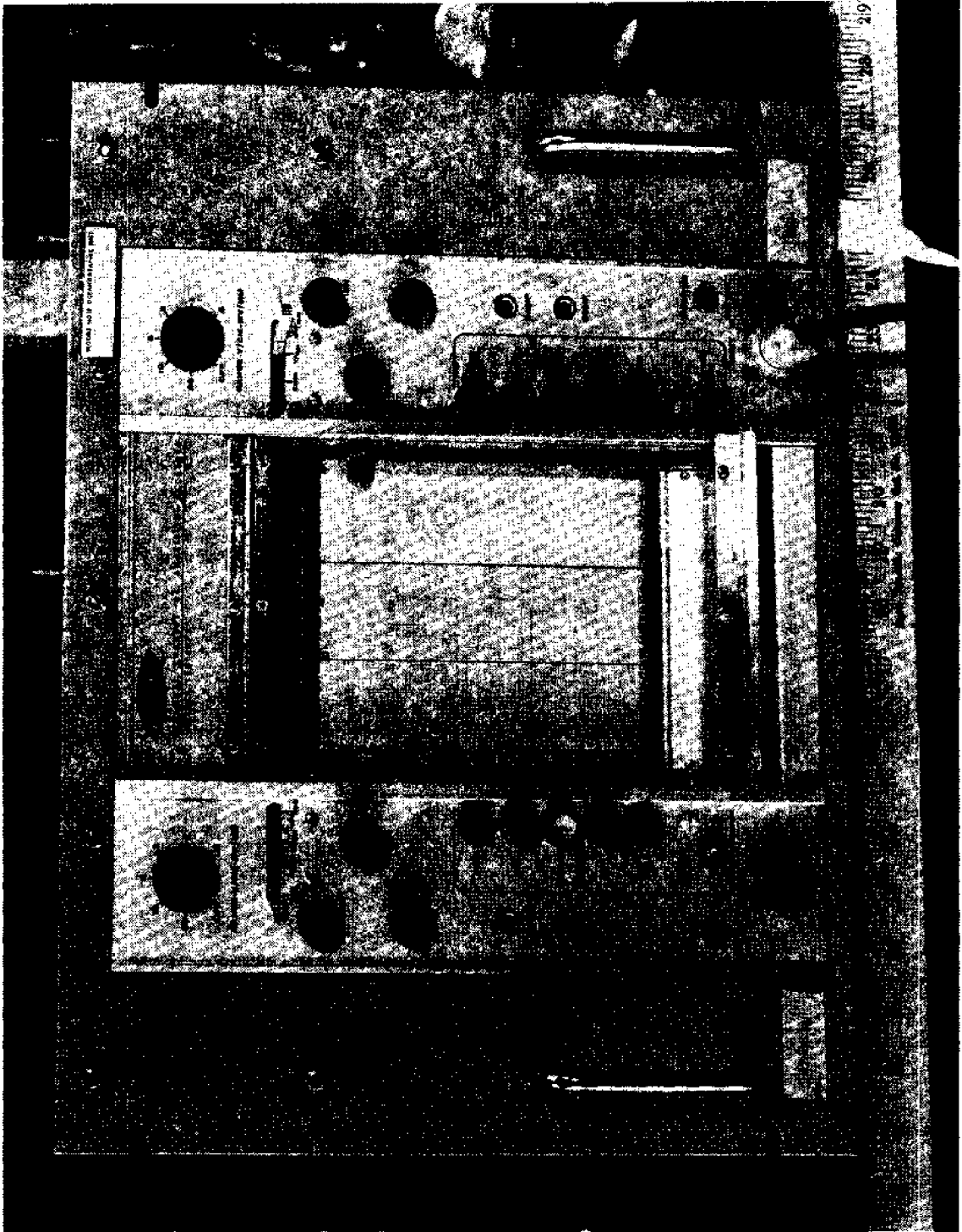


Figure 12. Sanborn Recorder

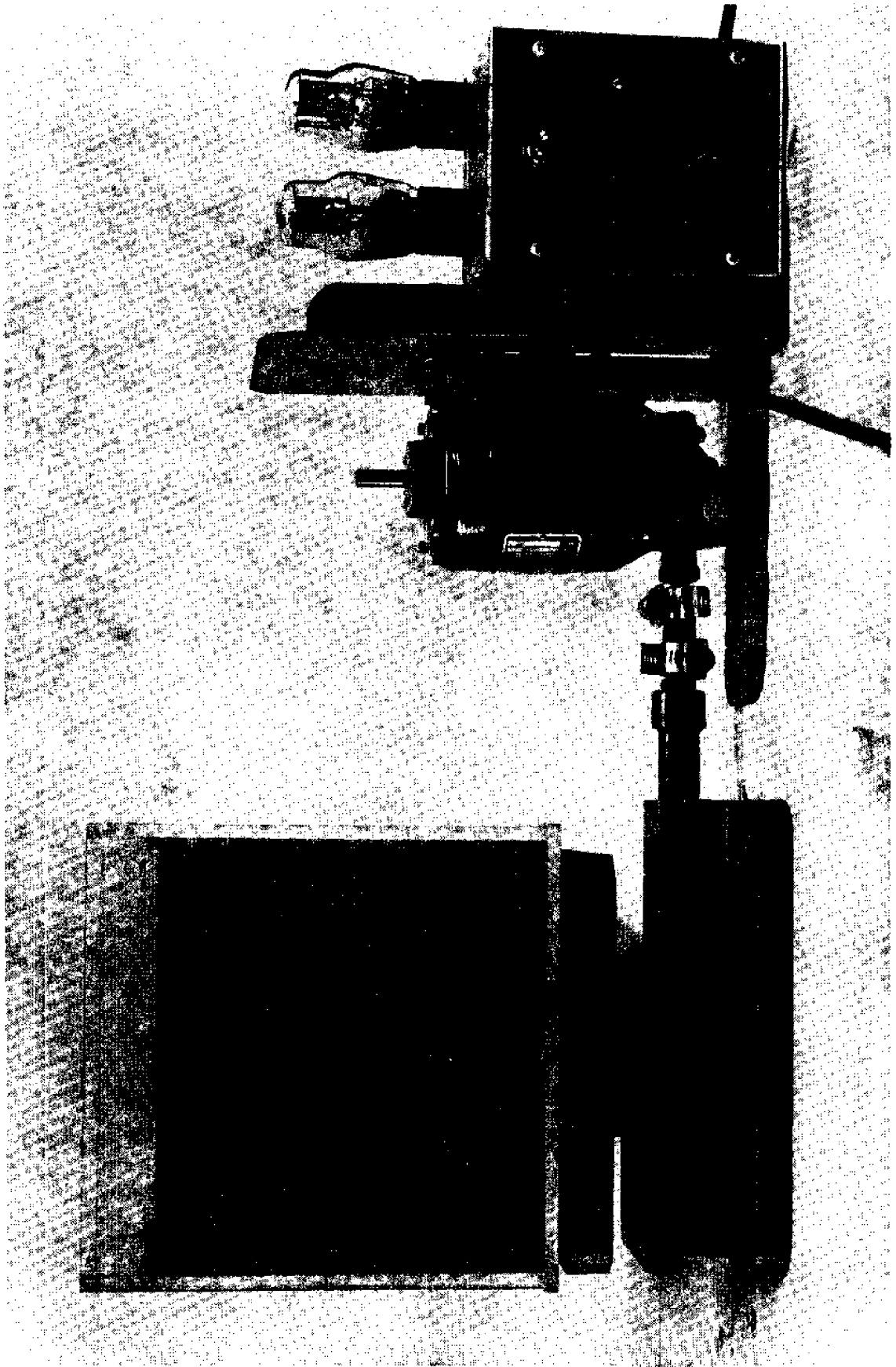


Figure 13. Mechanical Subsystem

TABLE I
SUBSYSTEMS AND COMPONENTS

I. Optical Subsystem

- 1a. Laser - Bausch & Lomb He=Ne gas (=6328Å) Model #41.17.50
- 1b. Optical bench
- 1c. Double Convex Lens 51 mm diam. 88 mm f.l.
- 1d. Double Concave Lens 9 mm diam. - 8.5 mm f.l.
- 1e. Ronchi Ruling (2) 2"x2" 10 lines per inch
- 1f. Holder, Microscope Mount
- 1g. Holder, Aluminum Post

II. Electronic Subsystem

- 2a. Photoconductivity cell, Clairex Model #CL5M7 CdS (6150Å peak response)
- 2b. Resistor 22 M 10%
- 2c. Capacitor 0.01 μf
- 2d. Battery Eveready 6v DC
- 2e. Recorder 230 Dual Channel DC Amplifier-Recorder by Sanborn

III. Mechanical Subsystem

- 3a. X-Y Table
- 3b. Variable Speed Motor Bodine 3.5 in-lb 1/70 hp.
- 3c. Speed Controller G. K. Heller Motor Controller 2T 60
- 3d. Tank 6"x8"x4" ¼" plexiglas wall

IV. Procedural Apparatus

- 4a. Hydrometer 1.000 to 1.220 Fisher Scientific Cat.No.11-520A
- 4b. Graduated Cylinder 100 ml.
- 4c. Tubing, 1/16 inch, flexible
- 4d. Mixing Buckets (2) 1 gal.

2.3 Analysis

2.3.1 Signal

The intensity of light incident upon the sensor is the sum of a steady background signal and an unsteady fluctuating signal due to translation of water with differing indices of refraction across the path of the laser beam. It is the regular variation of signal with translation, indicative of the coherence among groups of salt fingers, which is relied upon

for evidence of detection. The magnitude of the background voltage is only of concern when it is of such magnitude that it obscures the signal, the fluctuating voltage. Anomalies in signal due to singular fluctuations in index of refraction are similarly of little consequence.

A multi-slit Schlieren refraction technique is desirable because coherent regions of large angle refraction having the same spatial periodicity of the multiple slits enhance the signal measured at the photoconductivity cell. Each ruling edge acts as a knife edge and so, if there are N edges, there are N knife edge Schlieren experiments in progress at a given time. The sensor sums these N experiments. Random events give a signal which sums as

$$I_{\text{noise}} = i_{\text{noise}} \sqrt{N} \quad \text{for large } N$$

where I_{noise} is the intensity of noise at the sensor, i_{noise} is the intensity of noise at each knife edge, and N is the number of knife edges. Coherent regions with the same spatial periodicity as the slits give a signal which sums as

$$I_{\text{signal}} = i_{\text{signal}} N$$

where I_{signal} is the intensity due to coherent refraction at the sensor, i_{signal} is the intensity due to coherent refraction at each knife edge, and N is as before.

$$\begin{aligned} \text{The signal to noise ratio } \frac{I_{\text{signal}}}{I_{\text{noise}}} &= \frac{i_{\text{signal}} N}{i_{\text{noise}} \sqrt{N}} \\ &= \frac{i_{\text{signal}}}{i_{\text{noise}}} \sqrt{N} \end{aligned}$$

Thus the signal to noise ratio increases as the square root of the number of slits. If the periodicity of the coherent regions of refraction is not the same as the slits, the signal does not add. This would suggest a strong signal response when the ruling spacing was equal to the spacing between salt fingers. Sizes of salt fingers may be determined therefore, by changing the ruling spacing until the maximum signal response is achieved.

If sugar-salt fingers are coherent, at least on the small scale, (presumably heat-salt fingers are as well) then it is also reasonable to expect the signal to be modulated, perhaps by a sinusoid to appear roughly similar to the wave of Figure 14. The signal voltage might resemble such a curve because it could be expected to increase and decrease as the beam of light passes through more or less of a region of salt finger coherence. A light beam intercepting a large region of salt fingers will be more effectively refracted as the optical path in the region increases.

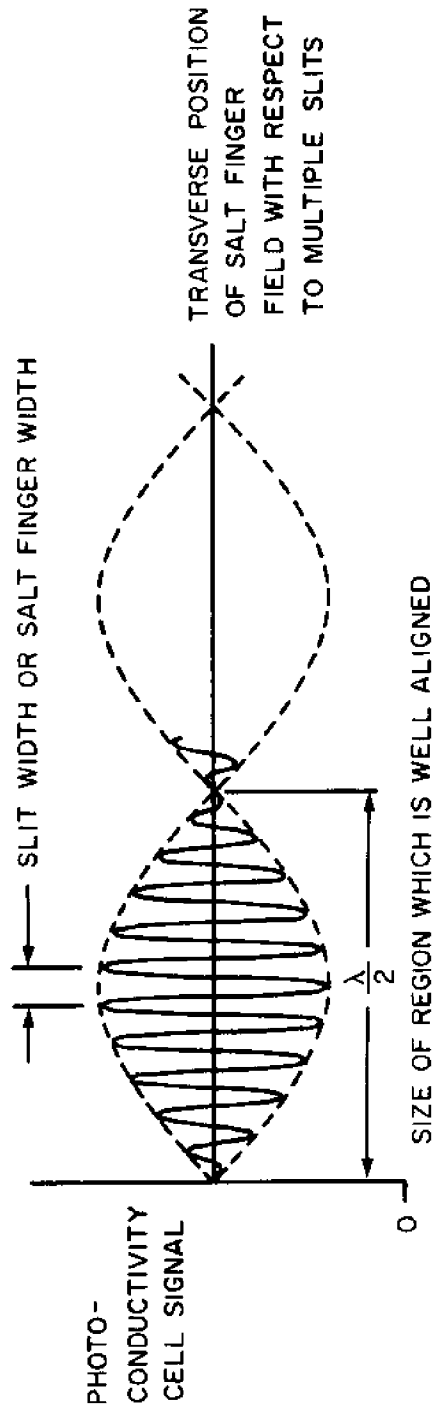


Figure 14. Signal Modulation by Coherency

2.3.2 Sources of Error

The optical signal of interest is that which is refracted through the second Ronchi ruling by salt fingers and is incident upon the sensor. Detection can only occur when the fluctuating intensity at the sensor is sufficiently great so that the fluctuating voltage can be resolved above the steady background signal resulting from leakage due to improper or poor alignment and diffraction.

Leakage of light to the sensor is predominantly the result of a non-collimated light beam. If not precisely located, the elements of a beam expander will not be able to produce parallel rays and leakage results.

No matter how parallel the rays from a monochromatic laser, light will reach the photoconductivity cell by diffraction. Although not as grave an error as misalignment, diffraction places a lower bound upon noise. Each ruling acts as a knife edge, at its borders, and produces different visible patterns downstream at different distances. The change from the near field pattern to that of the far field is indicated in Figure 15 taken from John Strong's book, Concepts of Classical Optics. The experiments were conducted in the far near field and consequently leakage due to diffraction was not appreciable. The rise in intensity in the "shade" of one Ronchi ruling edge, for the apparatus used, is indicated in the graph of Figure 16. The area under the curve indicates the linear power density. Approximately 1/25th of the incident light is diffracted through the second ruling. The refracted light must be at least 1/25th of the incident light intensity in order to equal the diffracted noise. Resolution and detection require levels of refraction higher than 1/25I.

A major cause for concern is the refraction at the boundaries of the tank induced by experimental conditions which do not represent the state of the ocean. Spurious signals must be eliminated or identified as such. The tank wall, for example, is planar and probably the site of considerable salt finger coherence which would lead to unnaturally large refraction and signal amplitude. This influence can be minimized by making investigations in a large tank with turbulence induced locally at the wall. Bubbles at the wall and the plexiglas walls themselves may be the source of error. The plexiglas may cause bending of light and shift of path sufficient to alter the intensity at the sensor. This will happen if the tank walls are not parallel to the advancing wave front and cannot cause periodic fluctuations, and is therefore of little concern. Air bubbles on the wall can produce a fluctuating refraction of light similar to the effect of salt fingers and therefore should be removed from the tank prior to making meaningful runs.

2.4 Procedure

In conducting the experiments, the setup had to be done correctly in order to get any meaningful results.

2.4.1 Alignment

All alignments were conducted in the dark because the intensity of

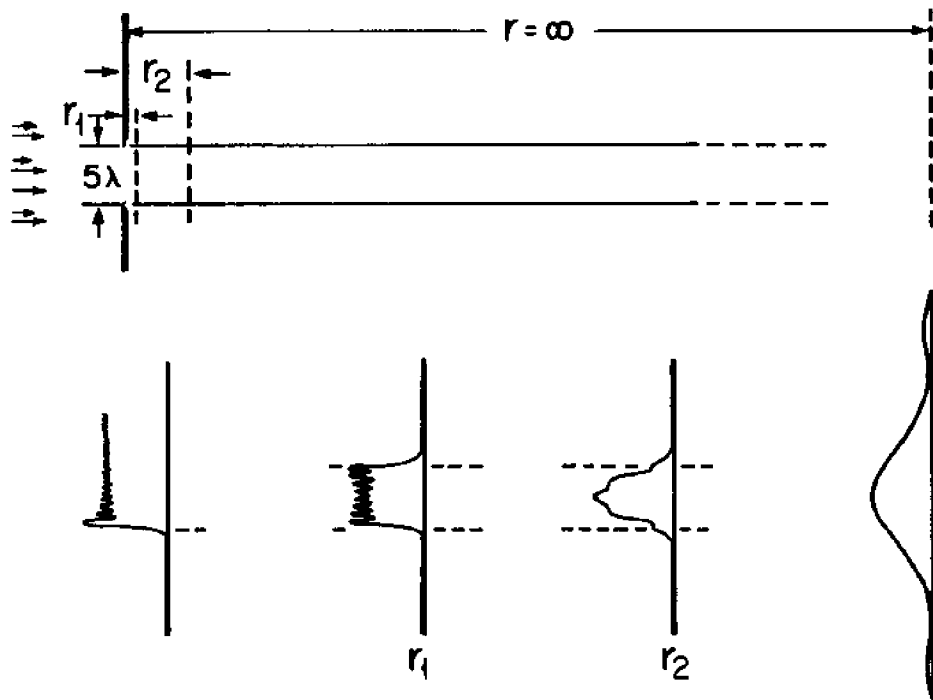


Figure 15. Transition from Fresnel to Fraunhofer diffraction patterns with parallel incident light. (Redrawn from Slater's *Introduction to Theoretical Physics*.)

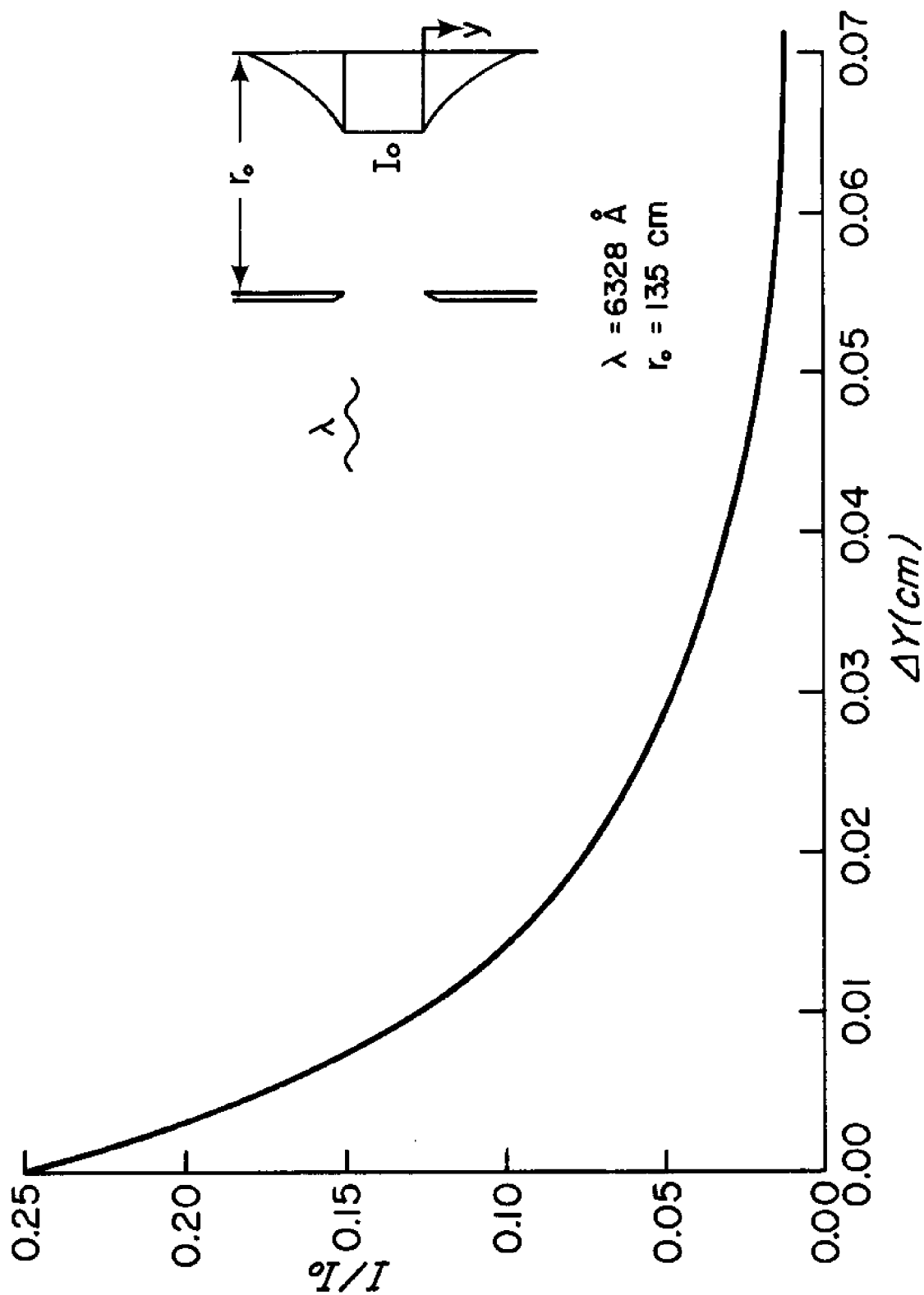


Figure 16. Knife Edge Diffraction

the laser beam became weaker each time the beam passed through an object such as the Ronchi rulings and the lenses. The laser beam was adjusted so that it was parallel to the optical bench and remained at the same distance above the track of the optical bench over its entire length. To check the beam image location, a white card was moved longitudinally along the optical bench so that the beam image fell on it.

The effect of each optical component on the beam was checked. The white card was set at the end of the optical bench opposite the laser. A small point was marked on the card at the center of the beam image. Each time a lens or a Ronchi ruling was set in the path of the laser beam, it could be seen if the beam was deflected. If the beam was deflected, the object was adjusted until the beam image was again centered on the dot.

To illuminate a large enough region of salt fingers, it was necessary to expand the laser beam from its original diameter of two (2) millimeters to 20 millimeters. Another reason for expanding the laser beam was that the Ronchi ruling spacing was of the same order of magnitude as the unexpanded beam. To expand the beam, two lenses were used - one double concave and the other double convex (see Figure 17). The double concave lens was centered on the laser beam. The lens was set close to the laser because of the limited space on the optical bench. Being larger than the laser beam, it diverted the entire beam. The double convex lens was also centered on the laser beam, and it was positioned along the optical bench so that its focal point coincided with that of the double concave lens. Had the laser beam been collimated before passing through the two lenses, the expanded beam would also be collimated providing the two focal points coincided.

2.4.2 Eclipsing Procedure

In order to insure the maximum change in signal strength, the change in light intensity incident upon the photoconductivity cell was maximized. This was done by conducting the experiments in a darkened room and by eclipsing the undisturbed image of the first ruling with the second ruling. A microscope stand was clamped onto the optical bench so that it would not move with respect to the optical bench and the first Ronchi ruling was attached to the slide base of the microscope stand. The ruling was adjusted until it was in the laser beam and perpendicular to it. The second Ronchi ruling was attached to a rigid stand at the same level as the first ruling, perpendicular to the laser beam, and 13.5 inches beyond the first ruling along the optical bench. The spacing of the two rulings was influenced by two factors. One, the closer the two rulings were to each other the greater was the change from dim to bright. Second, enough space had to be allowed for the movable table and tank to be set between the two rulings. The first ruling was rotated until the image of its lines was parallel to the lines of the second ruling. Any slight angle of the two rulings relative to one another prevented the rulings from eclipsing perfectly.

In order to eclipse the two rulings, the spacing of the first ruling's image had to be the same as the second ruling. When adjusting the collimation, a check was made to see if the rulings could be eclipsed. When the beam was not collimated, a moving fringe pattern was observed as the first ruling was moved back and forth in a direction perpendicular to the beam. The fringe pattern was due to the difference in the spacing

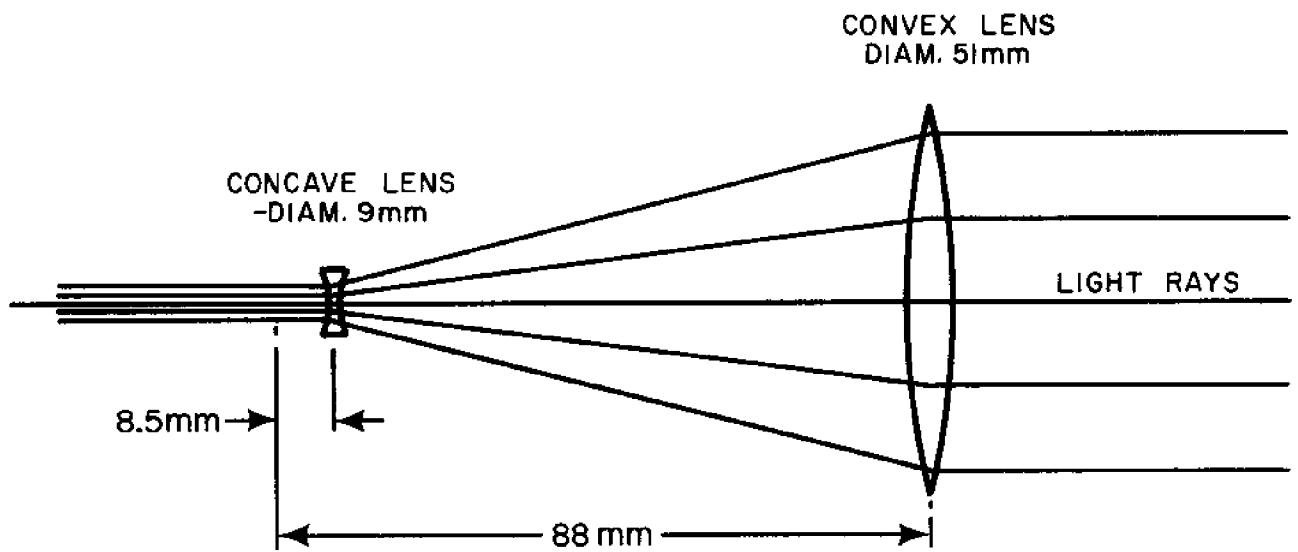


Figure 17. Beam Expander

between the image of the first ruling and the second ruling. When the fringe pattern moved in the same direction as the first ruling, the two expanding lenses were moved closer together. When the fringe pattern and ruling moved in opposite directions, the two lenses were moved further apart. When the fringe pattern disappeared, the beam was considered collimated and the two rulings could be eclipsed. The two rulings, when eclipsed behaved as shown in Figure 18. The eclipsing was not total, but was sufficient to produce large changes in intensity as the beam was refracted by sugar-salt fingers and was deflected past the second ruling.

2.4.3 Sugar-Salt Finger Production

Sugar-salt fingers are possible when an aqueous sugar solution overlies an aqueous salt solution. The density of the aqueous sugar solution has to be less than that of the aqueous salt solution. The specific gravity was determined with a hydrometer. For the aqueous salt solution, sea water was used. If it was desired to have a higher density, rock salt was added to fresh water until the desired density was obtained. For the aqueous sugar solution, sugar was added to fresh water until the desired difference in density was obtained. It was discovered during initial experiments that bubbles would form on the walls of the tank. To prevent the bubbles from forming, the aqueous solutions were heated to drive out the oxygen. The solutions were allowed to return to room temperature before they were poured into the tank.

Placing the solutions in the tank had to be done with care so that stratifications could be produced and mixing minimized. After the two solutions cooled to equilibrium and the density was checked, the salt solution was poured into the tank set between the two rulings. The level of the salt solution was set at the lower limit of the laser beam so that the sugar-salt fingers would be in the beam as the fingers grew. They grow relatively rapidly upward from the interface. A wooden board with holes in it (see Figure 19) was set on the salt solution to suppress the mixing between the solutions as the sugar solution was being siphoned into the tank. When the sugar solution was near the top of the tank the board was removed and a cover was put on the tank to prevent evaporation from establishing a disruptive circulation.

2.4.4 Tank Movement

During the initial experiments the tank was motionless with respect to the laser beam, but an inadvertent perturbation of the apparatus by one of the investigators elbows resulted in a periodic signal response. It was suggested by Dr. Turner that more meaningful results would be obtained by moving the laser beam horizontally through the tank so that the beam would pass through different sets of fingers. Instead of moving the laser, which would have required moving the entire optical bench, it was decided to move the tank, giving the same relative motion. To move the tank, one direction of an x-y table was used. The table was attached directly to the optical bench and it was moved back and forth perpendicular to the beam by a feed screw driven by a variable speed DC motor.

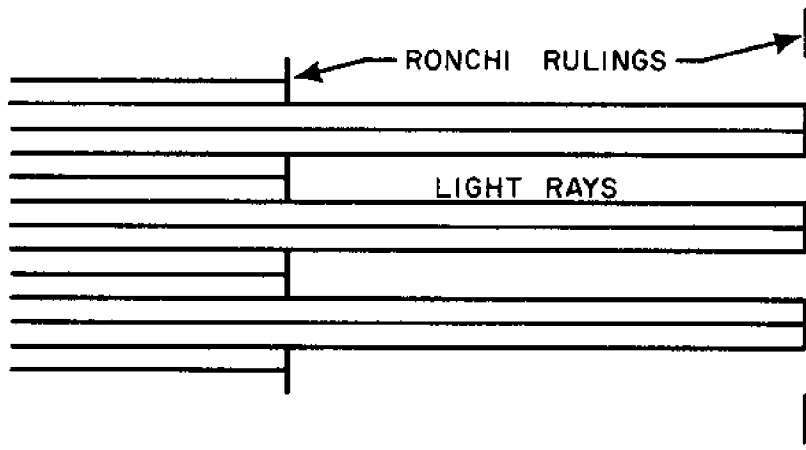


Figure 18. Eclipsed Rulings

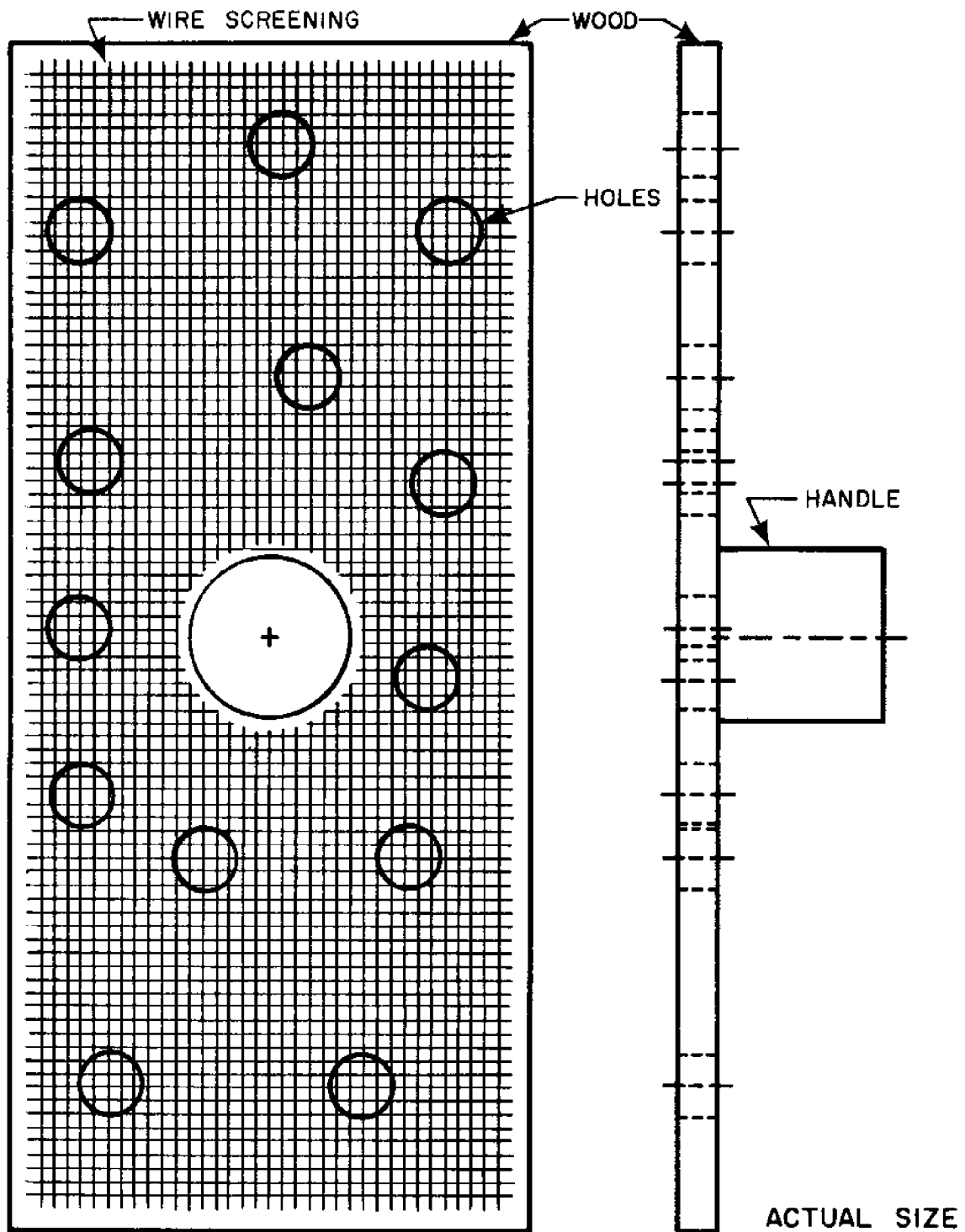


Figure 19. Pouring Board

2.5 Experiments and Results

A series of tests were conducted to determine the effect of various experimental sources of error. The tank was translated across the beam while empty and again while filled with turbulent sea water. Neither test produced any significant signal response. Bubbles on the wall of the tank were detected during an early run, when the tank was translated, therefore later experiments were conducted in the absence of bubbles.

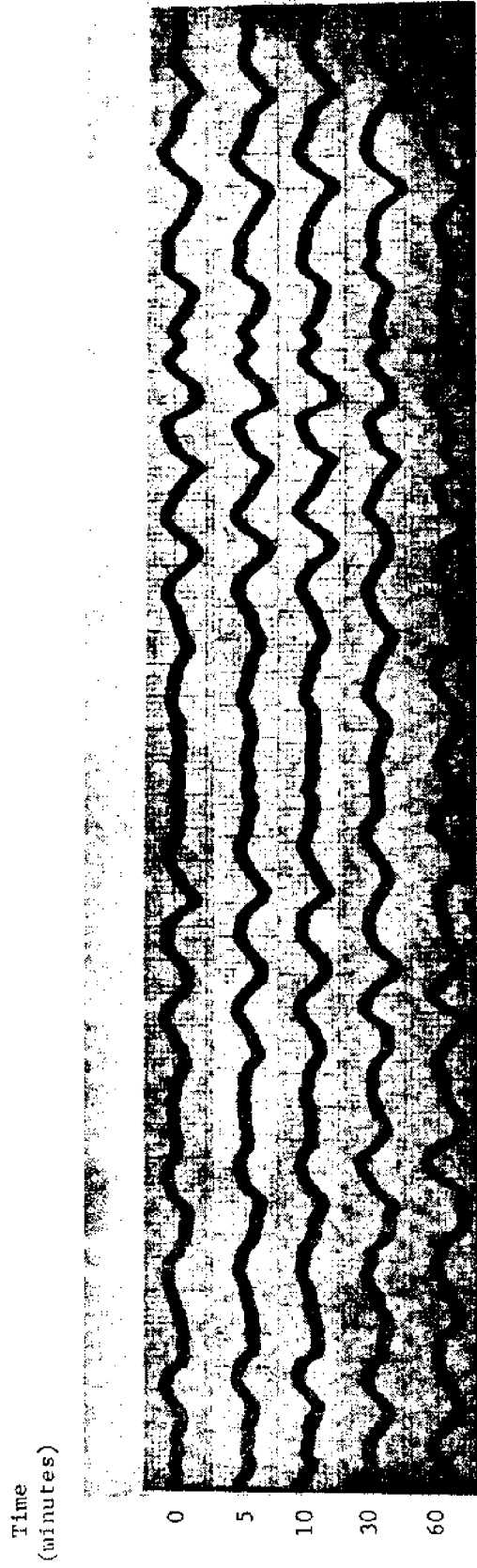
In the initial experiments, regular sea water was used which had a specific gravity of about 1.023. The specific gravity of the sugar solution was set about five per mill less than the sea water density. This density difference was too small; the sugar-salt fingers did not survive the rough laboratory conditions and broke up relatively rapidly. In later experiments, the specific gravities and the differences in density were increased to increase the stability and life of the sugar-salt fingers.

An experiment was conducted to determine the persistence of sugar-salt fingers arrays. Persistence was indicated by the correlation between subsequent signals. For each run, the tank was started in the same position and moved at the same constant speed. The runs were made every five minutes for the first 20 minutes and every 10 minutes for the next 40 minutes. A record of five of the runs is shown in Figure 20. A study of the runs shows that slow changes are taking place. New peaks are forming and old peaks are dying. The change seems to indicate activity similar to grain growth in metal.

Since the sugar-salt fingers change with age, data was recorded periodically with time. The experiment was conducted for 105.25 hours. The speed at which the tank was moved was .035 inch per second. The sensitivity used on the recorder was .5 millivolt per millimeter. The chart speed was usually five millimeters per second. After five hours the sugar-salt fingers were readily detected. Figure 21 is a typical example of a recorded run.

It was decided to determine how far the tank traveled per cycle as a function of the age of the sugar-salt fingers. A cycle is the periodic change from dimness to brightness back to dimness. The distance traveled by the tank per cycle was irregular, therefore the minimum, average and maximum distances traveled per cycle (DT/C) were determined. To determine the average DT/C, the number of cycles were counted on the charts over as large a time period as possible. Sometimes it is difficult to tell each of the cycles, therefore there could be at times an error of ± 2 cycles over any time period. The above information gives us the cycles per second while inches per cycle is desired. To get inches per cycle, the speed of the moving tank was multiplied by seconds per cycle. To determine the minimum and maximum DT/C the individual cycles were checked. Table 2 shows the tabulation of this data and Figure 22 is a plot of this data. Also in Table 2 the maximum amplitude of each run is shown. This data was not plotted because it was not certain that it was reliable since it seems that the intensity of the laser beam became dimmer as the experiment proceeded.

Figure 23 indicates a voltage record taken after 103 hours. At this stage of development (old age) the concentration gradients are sufficiently weak that the regions of coherency, those regions where salt fingers are aligned in a lattice pattern, could be quite large. Although the variation of index of



Total time span that is shown of each run is 45.4 sec.
Distance that tank travelled is 1.59 inches.

Figure 20. Persistence of Sugar-Salt Finger Arrays

3:42 P.M.

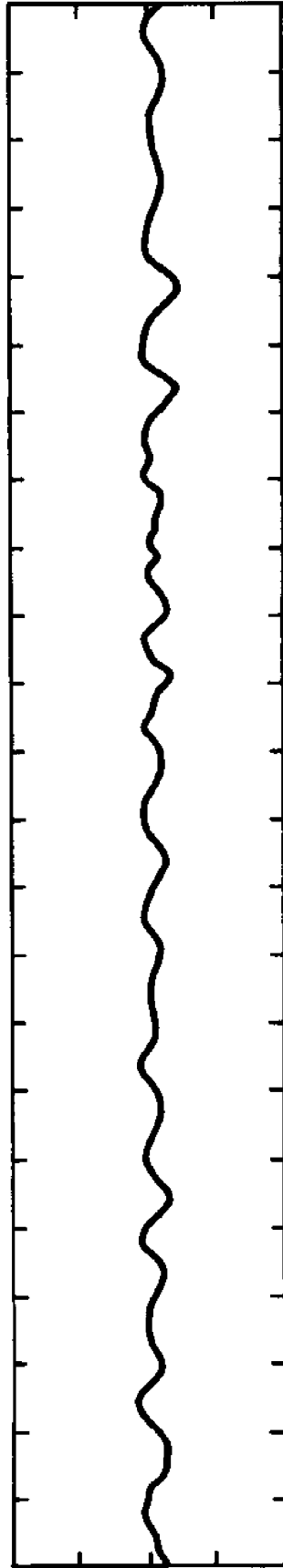


Figure 21. Typical Example of a Recorded Run.

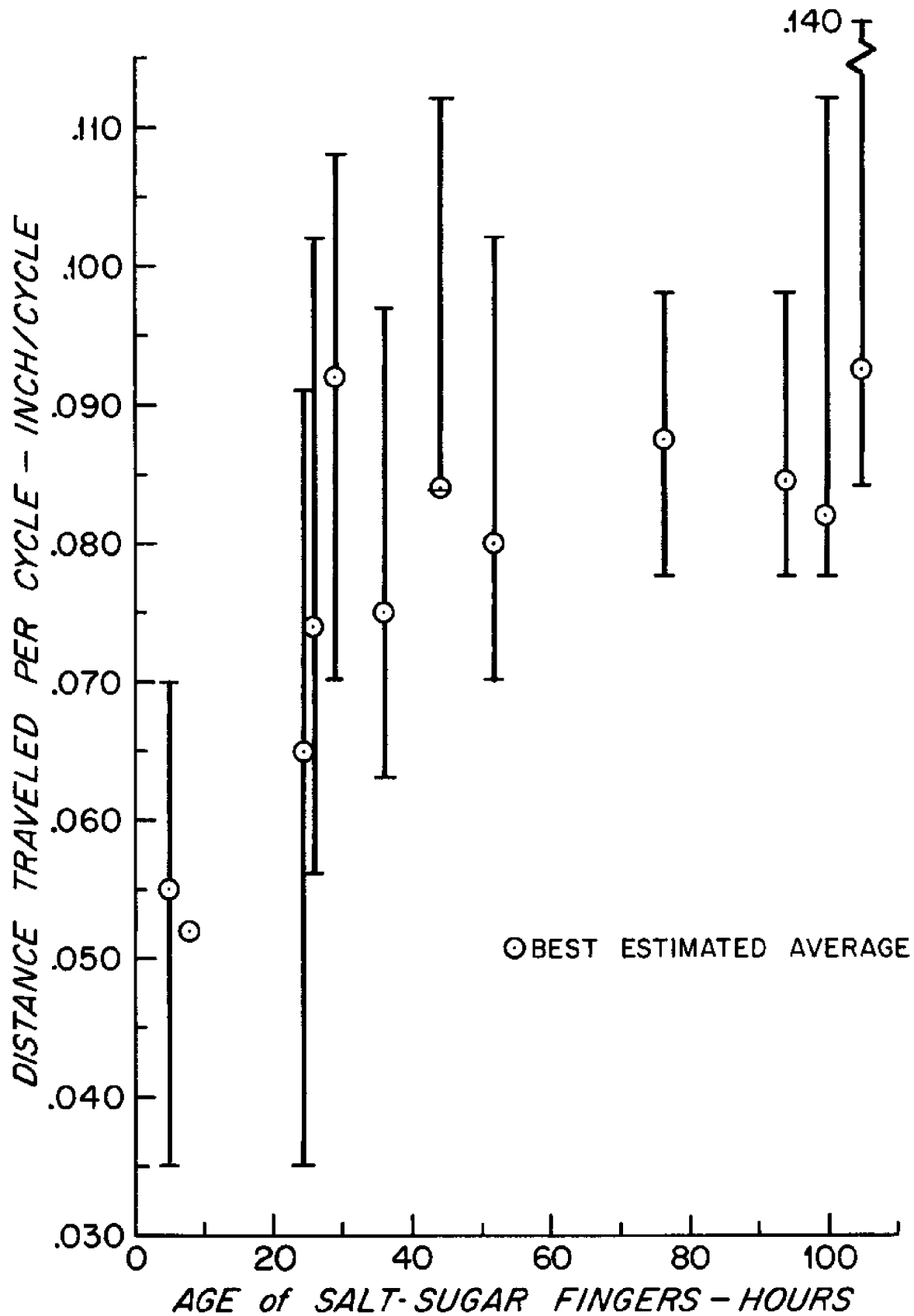


Figure 22. Age of Sugar-Salt Fingers versus Distance Traveled per Cycle

5:05 P.M.
8/31

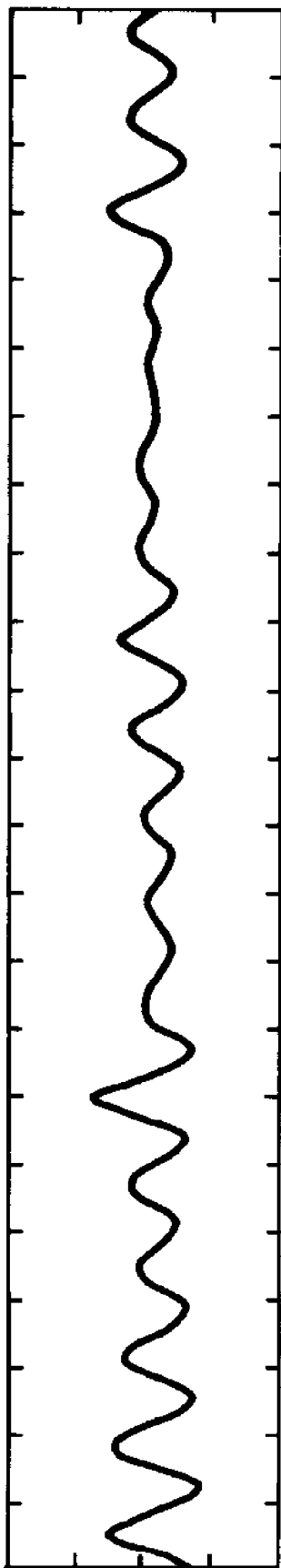


Figure 23. Voltage Record of 103 Hours Old Sugar-Salt Fingers

refraction across one salt finger is decreased, the increase in net refractive path is increased with coherency. The increase in magnitude of the voltage envelope is perhaps indicative that the optical beam passes through larger regions of coherency.

At the start of the previously mentioned experiment, the specific gravities were 1.107 for the salt solution and 1.091 for the sugar solution. When the experiment was terminated, the specific gravity of the lower, middle, and upper regions were 1.109, 1.099, and 1.085, respectively. This is what was expected. 1.099 is the average of 1.107 and 1.091, the starting densities.

TABLE 2

Tabulation of Age of Sugar-Salt Fingers versus Distance Traveled per Cycle

Age of Sugar-Salt Fingers (hours)	Distance Traveled per Cycle			Maximum Amplitude (millivolts)
	Minimum	Average	Maximum	
	(inch/cycle)			
5.	0.035	0.055	0.070	1.5
8.	*	0.052	*	2.5
24.5	0.035	0.065	0.091	5.0
26.	0.056	0.074	0.102	5.0
29.	0.070	0.092	0.108	3.0
36.	0.630	0.075	0.098	4.0
44.25	0.084	0.084	0.112	2.0
51.75	0.070	0.080	0.102	5.0
76.5	0.077	0.0875	0.098	13.0
94.	0.077	0.0845	0.098	3.0
99.75	0.077	0.082	0.112	6.5
105.25	0.084	0.093	0.140	9.0

*The chart speed used at this time was too slow to measure single cycles.

3. CONCLUSIONS AND RECOMMENDATIONS

An instrument for detection of salt fingers in the sea appears feasible. Investigation of sugar-salt fingers in the laboratory seems to indicate that salt fingers are coherent in the small scale and that these regions of coherency are arranged similar to crystallographic grains of nickel. The investigation was conducted under laboratory conditions, and although the basic feasibility seems to exist, further investigations are recommended before an ocean going prototype is constructed.

Future laboratory investigations should be conducted first with sugar-salt fingers and then with heat-salt fingers. The correlation between finger spacing and ruling spacing, as indicated by signal magnitudes, may indicate when they are nearly equal. A large tank should be used in future tests so that the wall effects can be minimized; solutions near the wall might be kept in agitation to prohibit the abnormal development of large regions of coherent salt fingers on the planar boundaries. Other methods of detecting salt fingers should be investigated. One method is to study the temporal fluctuations at various locations which may indicate the presence of fingers as the

spatial fluctuations do in the present work. A laser beam would be directed through a large region of salt fingers, and the temporal fluctuations would be sensed by photoconductivity cells which might be mounted in an array as shown in Figure 24. This proposed method would not require the same precise alignment, and it would cause less disturbance of the salt fingers since the distance between the laser and photoconductivity cells can be greater than the distance between the two rulings of the present method. If further work warrants, experiments should also be conducted with heat-salt fingers. After the laboratory work has provided an appropriate detection system, a prototype ocean instrument should be constructed, tested in the laboratory on heat-salt fingers, and then given a sea trial.

The ocean going version of the salt finger detector might resemble, at least generically, the laboratory modified multislit Schlieren system developed this summer. If such is the case, the very real problem of optical bench alignment must be surmounted. In the sea, the optical bench must be very rigid. Rigidity can be achieved by placing most of the components in rigid circular cylinders and allowing a sufficient water path for the salt fingers. The price of rigidity cannot be paid at the expense of perturbing the flow and destroying the salt fingers. An instrument could quite profitably be rigged for use on an Autoprobe. As the instrument rose and fell it would sample various regions of the salt fingers and might not need a device for additional translation of the optical bench.

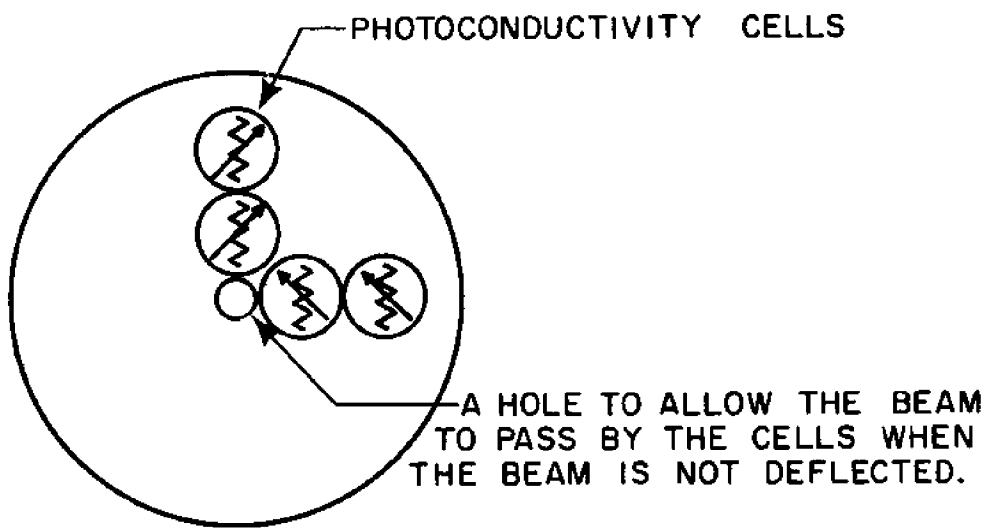


Figure 24. Array of Photoconductivity Cells

BIBLIOGRAPHY

- Gray, Dwight E., Institute of Physics Handbook,
McGraw-Hill, New York 1963, p. 2-126.
- Stern, Melvin E., "Collective Instability of Salt
Fingers", Journal of Fluid Mechanics, 1969,
vol. 35, part 2, pp. 209-218.
- Strong, John, Concepts of Classical Optics,
W. H. Freeman, San Francisco 1958, pp. 192-200
- Turner, "The Behavior of a Stable Salinity Gradient
Heated From Below", Journal of Fluid Mechanics,
1968, vol. 33, part 1, pp. 183-200.

APPENDIX A

SENSOR CIRCUIT DESIGN

The photoconductivity cell is a semiconductor in which the charge carriers are generated by photons. Its conductivity is approximately proportional to the photon flux incident upon it. Photoconductivity cells require a power supply. We chose a series resistor to measure the conductivity of the cell. Care must be taken to insure that too much power is not dissipated by the cell.

Selection of the photoconductivity cell is based on compatibility with the light source used and in turn governs the design of the supporting circuitry. Because the light source was a 6328 Å Helium-Neon gas laser, a cell was chosen which had a peak spectral response at 6150 Å, Clairex No. CL5M7 CdS. The maximum power and voltage were therefore set at 500 mw and 250 mv.

The circuit shown in Figure A-1 does not permit too much power or too high a voltage to pass through the cell, if E is small. This can be represented by the equivalent circuit shown in Figure A-2.

By a little algebra we can see that

since $Z_2 = S/I$ where S is the cell sensitivity and I the light intensity,

and $Z_1 = \frac{R_1 X_c}{R_1 + X_c}$, where $X_c = \frac{1}{i\omega C}$,

$$Z_1 = \frac{R_1 / i\omega C}{R_1 + 1/i\omega C} = \frac{R_1}{i\omega C R_1 + 1}$$

so that $V = E \left(\frac{Z_2}{Z_1 + Z_2} \right)$

or

$$V = \frac{E S (i\omega R_1 C + 1)}{R_1 I + S (i\omega R_1 C + 1)}$$

In order to maximize the change in recorder voltage, V, with changes in incident intensity upon the photoconductivity cell,

$$\frac{d^2 V}{dI dR_1} = 0$$

$$\frac{dV}{dI} = - \frac{E S (i\omega R_1 C + 1) R}{[R_1 I + S (i\omega R_1 C + 1)]^2}$$

and

$$\frac{d^2 V}{dI dR} = - \frac{E S (2 i\omega R_1 C + 1)}{[R_1 I + S (i\omega R_1 C + 1)]^2} + \frac{2 E S (i\omega R_1^2 C + R_1) (I + S i\omega C)}{[R_1 I + S (i\omega R_1 C + 1)]^3} = 0$$

which simplifies to $R_1 = \frac{1}{I/s + i\omega C}$.

For DC signals, $\omega=0$ and $R_1 = S/I$.

In order to maximize the sensitivity of the recorder to changes in light intensity, I , R_1 should be of the order of the resistance of the photoconductivity cell at working light levels. The impedance Z_2 varies considerably with light intensity, from 500Ω in daylight to megohms in a darkened room. Since experiments were to be conducted in darkness, R_1 was selected as $22M\Omega$.

For convenience, a six (6) volt battery was used as the power supply. Peak power dissipation in the photoconductivity cell occurs when its impedance is equal to that in the rest of the series circuit, $22M\Omega$. Then half the voltage appears on it and the power dissipated in it is found from

$$P = \frac{V^2}{R_1} = \frac{(3v)^2}{22 \cdot 10^6 \Omega} = 4 \cdot 10^{-7} \text{ watts.}$$

This is negligible.

The quantity RC has the dimensions of time and is called the capacitive time constant of the circuit. It is the time at which the charge on the capacitor has increased to within a factor of $(1 - e^{-1}) \sim 63\%$ of its equilibrium value. To filter out the noise due to 60 Hz oscillations of the laser beam, a capacitor with a time constant greater than the period of the noise was needed.

$$T = \frac{2\pi}{f} = 0.105 \text{ sec.}$$

If $R_1 = 22M\Omega$ and $C = 0.01 \mu f$, then $RC = 0.22$ second and $RC > T$.

$C = 0.01 \mu f$ was acceptable.

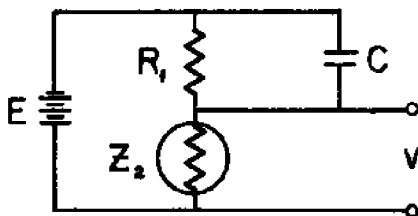


Figure A-1

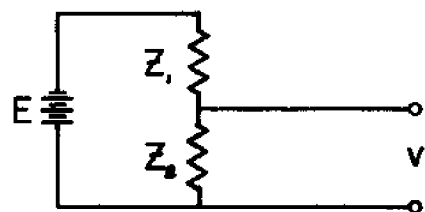


Figure A-2

Woods Hole Oceanographic Institution
Reference No. 71-5

REPORT OF THE OCEANOGRAPHIC ENGINEERING SUMMER PROJECT by
Scott C. Daubin, A. J. Williams, III, Ronald C. Gularte,
Peter F. Poranski, Daniel P. Charnews, Richard J. Jaffee,
Carl S. Albro and T. Gray Curtis, Jr. January 1971.
Sea Grant No. GH-104.

The syllabus of Oceanographic Systems, a summer course in oceanographic engineering, is presented with suggested student projects. Six students participated in the course and in three projects. These project reports are here presented.

An in situ surface film detector was constructed which monitored and recorded the presence of hydrocarbons on its surface. The design and testing of this field instrument is reported here.

Aerial photographs of dye released into Vineyard Sound over a proposed sewer outfall site allowed the surface flow to be mapped. This information, which is presented here, may aid planners of the sewer system.

A laboratory study of a salt-finger detection scheme is reported on. It was found that optical effects were enhanced by the regular alignment of the fingers.

1. In Situ Surface Film Detector

- Water Transport off Nobska Point by Dye Tracing
- Detection of Salt Fingers by Eclipsed Schlieren Technique.

I. Daubin, Scott C.

II. Williams, A. J.

III. Gularte, Ronald C.

IV. Poranski, Peter F.

V. Charnews, Daniel P.

VI. Jaffee, Richard J.

VII. Albro, Carl S.

VIII. Curtis, T. Gray

IX. GH-104

This card is UNCLASSIFIED

Woods Hole Oceanographic Institution
Reference No. 71-5

REPORT OF THE OCEANOGRAPHIC ENGINEERING SUMMER PROJECT by
Scott C. Daubin, A. J. Williams, III, Ronald C. Gularte,
Peter F. Poranski, Daniel P. Charnews, Richard J. Jaffee,
Carl S. Albro and T. Gray Curtis, Jr. January 1971.
Sea Grant No. GH-104.

The syllabus of Oceanographic Systems, a summer course in oceanographic engineering, is presented with suggested student projects. Six students participated in the course and in three projects. These project reports are here presented.

An in situ surface film detector was constructed which monitored and recorded the presence of hydrocarbons on its surface. The design and testing of this field instrument is reported here.

Aerial photographs of dye released into Vineyard Sound over a proposed sewer outfall site allowed the surface flow to be mapped. This information, which is presented here, may aid planners of the sewer system.

A laboratory study of a salt-finger detection scheme is reported on. It was found that optical effects were enhanced by the regular alignment of the fingers.

Woods Hole Oceanographic Institution
Reference No. 71-5

REPORT OF THE OCEANOGRAPHIC ENGINEERING SUMMER PROJECT by
Scott C. Daubin, A. J. Williams, III, Ronald C. Gularte,
Peter F. Poranski, Daniel P. Charnews, Richard J. Jaffee,
Carl S. Albro and T. Gray Curtis, Jr. January 1971.
Sea Grant No. GH-104.

The syllabus of Oceanographic Systems, a summer course in oceanographic engineering, is presented with suggested student projects. Six students participated in the course and in three projects. These project reports are here presented.

An in situ surface film detector was constructed which monitored and recorded the presence of hydrocarbons on its surface. The design and testing of this field instrument is reported here.

Aerial photographs of dye released into Vineyard Sound over a proposed sewer outfall site allowed the surface flow to be mapped. This information, which is presented here, may aid planners of the sewer system.

A laboratory study of a salt-finger detection scheme is reported on. It was found that optical effects were enhanced by the regular alignment of the fingers.

1. In Situ Surface Film Detector

- Water Transport off Nobska Point by Dye Tracing
- Detection of Salt Fingers by Eclipsed Schlieren Technique.

I. Daubin, Scott C.

II. Williams, A. J.

III. Gularte, Ronald C.

IV. Poranski, Peter F.

V. Charnews, Daniel P.

VI. Jaffee, Richard J.

VII. Albro, Carl S.

VIII. Curtis, T. Gray

IX. GH-104

This card is UNCLASSIFIED

1. In Situ Surface Film Detector

- Water Transport off Nobska Point by Dye Tracing
- Detection of Salt Fingers by Eclipsed Schlieren Technique.

I. Daubin, Scott C.

II. Williams, A. J.

III. Gularte, Ronald C.

IV. Poranski, Peter F.

V. Charnews, Daniel P.

VI. Jaffee, Richard J.

VII. Albro, Carl S.

VIII. Curtis, T. Gray

IX. GH-104

This card is UNCLASSIFIED

1. In Situ Surface Film Detector

- Water Transport off Nobska Point by Dye Tracing
- Detection of Salt Fingers by Eclipsed Schlieren Technique.

I. Daubin, Scott C.

II. Williams, A. J.

III. Gularte, Ronald C.

IV. Poranski, Peter F.

V. Charnews, Daniel P.

VI. Jaffee, Richard J.

VII. Albro, Carl S.

VIII. Curtis, T. Gray

IX. GH-104

This card is UNCLASSIFIED